Universität Potsdam

Institut für Ernährungswissenschaft

Lehrstuhl für Lebensmittelchemie

Toxic or beneficial? What is the role of food-relevant selenium species selenoneine?

Monograph dissertation
to obtain the academic degree
"Doctor rerum naturalium" (Dr. rer. nat.)
in the scientific discipline
"Food Chemistry"

submitted to the
Faculty of Mathematics and Natural Sciences
University of Potsdam

Evgenii Drobyshev

Date of disputation
30.11.2022

Dean: Professor Dr. Helmut Elsenbeer
First Supervisor: Professor Dr. Tanja Schwerdtle
Second Supervisor: Professor Dr. Burkhard Kleuser
Reviewer: PD Dr. Frank Neuschäfer-Rube
Reviewer: Prof. Dr. Melanie Esselen

Published online on the
Publication Server of the University of Potsdam:
https://doi.org/10.25932/publishup-57379
https://nbn-resolving.org/urn:nbn:de:kobv:517-opus4-573794

Table of Contents

List of figures

Figure 25. Induction of RONS in Caco-2 cells by 150 µM TBHP after pre-incubation with 200 nM of Se species or ET for 3-72 hours. Untreated control is marked as "C-". Positive control cells treated with TBHP only are marked as "C+". Results are presented as % of fluorescence of positive control cells. Shown are mean values + SD of at least two independent experiments with six replicates each. Statistically significant difference was calculated in relation to the positive control using one-way ANOVA followed by Dunnett's test, * $P < 0.05$, *** $P < 0.001$

Figure 26. Viability of the Caco-2 cells determined by neutral red uptake after 72-hour preincubation with 100 nM of Se species or ET and subsequent 24-hour treatment with indicated TBHP concentrations. Positive control cells treated with TBHP only are marked as "C+". Shown are mean values ± SD, expressed as % of the untreated control value, calculated from three independent experiments with six replicates each.

Figure 27. Viability of Caco-2 cells determined by Hoechst staining after 72-hour preincubation with 100 nM of Se species or ET and subsequent 24-hour treatment with indicated TBHP concentrations. Positive control cells treated with TBHP only are marked as "C+". Shown are mean values ± SD, expressed as % of the untreated control value, calculated from three independent experiments with six replicates each.

Figure 28. Effect of selenite (A), SeMet (B), SeN (C), and ET (C) on the GPx activity in Caco-2 cells after 72-hour incubation. Shown are mean values + SD, expressed as % of the control value, calculated from three independent experiments with two replicates each. Statistically significant difference was calculated in relation to the control value using one-way ANOVA followed by Dunnett's test, ** $P < 0.01$, *** $P < 0.001$

Figure 29. Selenium concentration in Caco-2 cells after 72-hour incubation with selenite, SeMet, SeN and ET. Shown are mean values + SD, calculated from four independent experiments. Statistically significant difference was calculated in relation to the control value using one-way ANOVA followed by Dunnett's test, *$P < 0.05$, ** $P < 0.01$, *** $P < 0.001$

Figure 30. SelenoP concentration in the culture medium of Caco-2 cells after 72-hour incubation with selenite, SeMet, SeN, and ET. Shown are mean values + SD, calculated from four independent experiments. Statistically significant difference was calculated in relation to the control value using one-way ANOVA followed by Dunnett's test, ** $P < 0.01$, *** $P < 0.001$

List of tables

List of abbreviations

Aβ	Amyloid-β
ABC	ATP-binding cassette
AD	Alzheimer's disease
AdoSeHCys	Se-Adenosylhomoselenocysteine
AdoSeMet	Se-Adenosylselenomethioneine
AHCY	Adenosylhomocysteinase
ALS	Amyotrophic lateral sclerosis
ASCT1	Alanine, serine, cysteine, and threonine transporter 1
ASCT2	Alanine, serine, cysteine, and threonine transporter 2
ATP	Adenosine triphosphate
BBB	Blood-brain barrier
BCSFB	Blood-cerebrospinal fluid barrier
BSA	Bovine serum albumin
Carboxy-DCF	Carboxy-dichlorofluorescein
Carboxy-H2DCF	Carboxy-dihydrodichlorofluorescein
Carboxy-H2DCFDA	5(6)-Carboxy-2',7'-dichlorodihydrofluorescein diacetate
CBS	Cystathionine beta-synthase
CNS	Central nervous system
CPE	Constant phase element
CSF	Cerebrospinal fluid
DIO	Deiodinase

DMSO	Dimethyl sulfoxide
DOC	Deoxycholic acid sodium salt
DPPH	1-Diphenyl-2-picrylhydrazyl
EDTA	Ethylenediaminetetraacetate
EFSec	Selenocysteine specific elongation factor
ESI	Electrospray ionization
ET	Ergothioneine
GNMT	Glycine-N-methyltransferase
GSH	Glutathione reduced
GPx	Glutathione peroxidase
GR	Glutathione reductase
GSSG	Glutathione oxidized
NADH	Nicotinamide adenine dinucleotide
NADPH	Nicotinamide adenine dinucleotide phosphate
HNMT	Histamine-N-methyltransferase
HPLC	High performance liquid chromatography
ICP-MS	Inductively coupled plasma mass spectrometry
LC	Liquid chromatography
LRP2	Low-density lipoprotein receptor-related protein 2
LRP8	Low-density lipoprotein receptor-related protein 8
MAT	Methionine adenosyltransferase
MeHg	Methylmercury
MEM	Eagle's minimal essential medium

MeSeCys	Se-Methylselenocysteine
MeSeH	Methylselenide
MeSeN	Se-Methylselenoneine
MS	Mass spectrometry
Met	Methionine
NEA	Non-essential amino acids
NMDA	N-Methyl-D-aspartate
NNMT	Nicotinamide-N-methyltransferase
NP	Nanoparticle
NVU	Neurovascular unit
OCTN1	Organic cation transporter 1
PBCEC	Porcine brain capillary endothelial cells
PD	Parkinson disease
PSer-tRNA$^{[Ser]Sec}$	Phosphoseryl-tRNA
PSTK	Phosphoseryl-tRNA$^{[Ser]Sec}$ kinase
RBC	Red blood cells
RNA	Ribonucleic acid
RONS	Reactive oxygen and nitrogen species
RTC	Rat tail collagen
Scly	Selenocysteine β-lyase
Se	Selenium
Sec	Selenocysteine
Sec-tRNA$^{[Ser]Sec}$	Selenocysteinyl-tRNA

SECIS	Selenocysteine-insertion sequence
SecS	Selenocysteine synthase
SeCysta	Selenocystathionine
SeHCys	Selenohomocysteine
SelenoP	Selenoprotein P
SeN	Selenoneine
SeMet	Selenomethionine
SEPHS2	Selenophosphate synthetase 2
Ser	Serine
SerS	Serine-tRNA ligase
Ser-tRNA$^{[Ser]Sec}$	Seryl-tRNA
SPB2	Selenocysteine-insertion sequence binding protein 2
T_3	3,5,3'-Triiodothyronine
T_4	Thyroxine
TBHP	*tert*-Butyl hydroperoxide
TEER	Transendothelial electrical resistance
TJ	Tight junction
TMH	Trimethylhystidine
TMSe	Trimethylselenonium ion
tRNA	transfer ribonucleic acid
tRNA$^{[Ser]Sec}$	Selenocysteine tRNA
TCEP	*tris*(2-Carboxyethyl)phosphine
TrxR	Thioredoxin reductase

Explanations

- References in the text given as a number in square brackets. Complete bibliographical information for certain references indicated in section 9 “References”.

- Due to the complex structure of substances described in the current work, they are not named in accordance with IUPAC nomenclature, but with common and trivial names used in literature.

- The mass concentrations used in this work refer to the mass of elemental selenium, and not to the mass of the whole compound unless otherwise stated.

- Products named by legally protected trademark or registered name are marked with the addition of “™” or “®” signs.

Statement of authorship

I, Evgenii Drobyshev, hereby declare that the present dissertation, entitled

"**Toxic or beneficial? What is the role of food-relevant selenium species?**"

has been written independently, that I have not used other than the declared sources, and that I have explicitly marked as references all material that has been quoted either literally or by content from the used sources.

I also declare that the present dissertation was not submitted as graded academic work for examination procedure in any other organization, neither in the same nor another form.

_____

Evgenii Drobyshev

1. Abstract

Selenium (Se) is an essential trace element that is ubiquitously present in the environment in small concentrations. Essential functions of Se in the human body are manifested through the wide range of proteins, containing selenocysteine as their active center. Such proteins are called selenoproteins which are found in multiple physiological processes like antioxidative defense and the regulation of thyroid hormone functions. Therefore, Se deficiency is known to cause a broad spectrum of physiological impairments, especially in endemic regions with low Se content. Nevertheless, being an essential trace element, Se could exhibit toxic effects, if its intake exceeds tolerable levels. Accordingly, this range between deficiency and overexposure represents optimal Se supply. However, this range was found to be narrower than for any other essential trace element. Together with significantly varying Se concentrations in soil and the presence of specific bioaccumulation factors, this represents a noticeable difficulty in the assessment of Se epidemiological status. While Se is acting in the body through multiple selenoproteins, its intake occurs mainly in form of small organic or inorganic molecular mass species. Thus, Se exposure not only depends on daily intake but also on the respective chemical form, in which it is present.

The essential functions of selenium have been known for a long time and its primary forms in different food sources have been described. Nevertheless, analytical capabilities for a comprehensive investigation of Se species and their derivatives have been introduced only in the last decades. A new Se compound was identified in 2010 in the blood and tissues of bluefin tuna. It was called selenoneine (SeN) since it is an isologue of naturally occurring antioxidant ergothioneine (ET), where Se replaces sulfur. In the following years, SeN was identified in a number of edible fish species and attracted attention as a new dietary Se source and potentially strong antioxidant. Studies in populations whose diet largely relies on fish revealed that SeN represents the main non-protein bound Se pool in their blood. First studies, conducted with enriched fish extracts, already demonstrated the high antioxidative potential of SeN and its possible function in the detoxification of methylmercury in fish. Cell culture studies demonstrated, that SeN can utilize the same transporter as ergothioneine, and SeN metabolite was found in human urine.

Until recently, studies on SeN properties were severely limited due to the lack of ways to obtain the pure compound. As a predisposition to this work was firstly a successful approach to SeN synthesis in the University of Graz, utilizing genetically modified yeasts. In the current study, by use of HepG2 liver carcinoma cells, it was demonstrated, that SeN does not cause toxic effects up to 100 µM concentration in hepatocytes. Uptake experiments showed that SeN is not bioavailable to the used liver cells.

In the next part a blood-brain barrier (BBB) model, based on capillary endothelial cells from the porcine brain, was used to describe the possible transfer of SeN into the central nervous system (CNS). The assessment of toxicity markers in these endothelial cells and monitoring of barrier conditions during transfer experiments demonstrated the absence of toxic effects from SeN on the BBB endothelium up to 100 µM concentration. Transfer data for SeN showed slow but

substantial transfer. A statistically significant increase was observed after 48 hours following SeN incubation from the blood-facing side of the barrier. However, an increase in Se content was clearly visible already after 6 hours of incubation with 1 µM of SeN. While the transfer rate of SeN after application of 0.1 µM dose was very close to that for 1 µM, incubation with 10 µM of SeN resulted in a significantly decreased transfer rate. Double-sided application of SeN caused no side-specific transfer of SeN, thus suggesting a passive diffusion mechanism of SeN across the BBB. This data is in accordance with animal studies, where ET accumulation was observed in the rat brain, even though rat BBB does not have the primary ET transporter – OCTN1. Investigation of capillary endothelial cell monolayers after incubation with SeN and reference selenium compounds showed no significant increase of intracellular selenium concentration. Species-specific Se measurements in medium samples from apical and basolateral compartments, as good as in cell lysates, showed no SeN metabolization. Therefore, it can be concluded that SeN may reach the brain without significant transformation.

As the third part of this work, the assessment of SeN antioxidant properties was performed in Caco-2 human colorectal adenocarcinoma cells. Previous studies demonstrated that the intestinal epithelium is able to actively transport SeN from the intestinal lumen to the blood side and accumulate SeN. Further investigation within current work showed a much higher antioxidant potential of SeN compared to ET. The radical scavenging activity after incubation with SeN was close to the one observed for selenite and selenomethionine. However, the SeN effect on the viability of intestinal cells under oxidative conditions was close to the one caused by ET. To answer the question if SeN is able to be used as a dietary Se source and induce the activity of selenoproteins, the activity of glutathione peroxidase (GPx) and the secretion of selenoprotein P (SelenoP) were measured in Caco-2 cells, additionally. As expected, reference selenium compounds selenite and selenomethionine caused efficient induction of GPx activity. In contrast to those SeN had no effect on GPx activity. To examine the possibility of SeN being embedded into the selenoproteome, SelenoP was measured in a culture medium. Even though Caco-2 cells effectively take up SeN in quantities much higher than selenite or selenomethionine, no secretion of SelenoP was observed after SeN incubation.

Summarizing, we can conclude that SeN can hardly serve as a Se source for selenoprotein synthesis. However, SeN exhibit strong antioxidative properties, which appear when sulfur in ET is exchanged by Se. Therefore, SeN is of particular interest for research not as part of Se metabolism, but important endemic dietary antioxidant.

2. Background

Among the essential trace elements, the metalloid selenium (Se) takes a very special place. Being discovered in the year 1817 it was firstly solely recognized as a toxic substance. Only in 1957 Se was found to be essential for mammals. From this moment on, investigations of Se's biological properties took a much larger scale. Already in 1973 Se was found to be a constituent of such an important enzyme as glutathione peroxidase (GPx) and presented there in form of selenoamino acid selenocysteine (Sec). Consequently, the biological functions of Se began to attract more and more attention. Just in 8 years, Sec was discovered to be encoded by the UGA codon. Its insertion into proteins occurs when the UGA codon, usually identified as a stop codon, is translated in the presence of a specific RNA element, changing its functions for Sec insertion. The overall complexity and high energy demand of such a process clearly indicated the exceptional importance of selenoproteins for the body. Later studies demonstrated that Se distribution in the human body follows a hierarchical structure. Under adequate Se intake, all organs receive Se in form of selenoprotein P (SelenoP), which is synthesized in the liver. However, Se homeostasis in the brain differs from other tissues. Although the brain has far not the highest Se content, under Se deficiency the brain becomes a primary target for Se delivery. The importance of Se for brain functions is also expressed in constant Se level, which is kept even when other tissues demonstrate significant deficiency. Overall, selenoproteins were shown to take part in multiple physiological processes like thyroid hormone metabolism, immune functions, antioxidant defense, and much more.

However, being firstly identified as a toxic substance, Se can be a source of harmful effects. As good as Se deficiency cause myodegenerative diseases, cardiovascular impairments, and cognitive decline, overexposure to Se is equally problematic. Since nutrition is a primary source of Se, it mostly depends on regional Se content in soil and nutritional habits. Therefore, it is very hard to exclude Se overexposure in endemic regions with elevated environmental Se background. For example, amyotrophic lateral sclerosis is known to correlate with elevated Se consumption, as well as some other neurodegenerative diseases. The assessment of risks associated with sub-chronic Se overexposure is also complicated by the presence of various Se species, which have different metabolic and toxicological profiles. Such a two-faced nature of Se leads to the very narrow optimal uptake range. Epidemiological studies are still providing controversial information about correlations between Se intake and risk of diabetes, cancer, and cardiovascular diseases. At the moment it is known that around 1 µg/kg bw/day of Se is necessary for adults to maintain the selenoproteins activity at a stable level. And daily intake of 300 µg of Se or more already leads to undesirable sub-toxic effects.

As it becomes clear, assessing the role of separate Se species present in food is a complex task. This requires the investigation of their own toxicity, bioavailability, and effects on induction of selenoproteins synthesis. Despite the close attention to Se for over 60 years, one of the Se-containing amino acid derivatives common in fish was discovered recently. Selenoneine (SeN) firstly identified in the blood and tissues of the bluefin tuna was found to be the Se isologue of a

naturally occurring compound with strong antioxidative properties – ergothioneine (ET). Further studies demonstrated that SeN is presented in plenty of edible fish species and is actively consumed by populations with a significant part of fish products in their diet. Moreover, these populations exhibit high SeN content in their blood, indicating the bioavailability of SeN for humans. The difficulty with the investigation of SeN properties was associated with the absence of methods for its laboratory production. The successful development of synthetic and biosynthetic approaches in the last years has made it possible to obtain pure SeN. Thus, as a Se species widely present in food, SeN should be comprehensively described from the points of toxicological safety and its relevance for human Se metabolism.

3. Introduction

3.1 Selenium

3.1.1 Chemical occurrence

Selenium (Se, atomic number 34), as a chemical element, is a metalloid and a member of the chalcogen group. Correspondingly, Se is closely related in its chemical and physical properties to sulfur and tellurium [1]. Selenium is a rare element with an average content in the Earth's crust around 0.3-0.5 μg/kg [2]. Due to the close chemical properties of sulfur, selenium is often accompanying sulfur minerals in combination with heavy metals [2]. As a material for industrial use, selenium is mostly utilized for pigments and glass production.

Despite its low content in the soil, selenium's wide distribution leads to its accumulation in many plant species [3]. Concentration in plants depends not only on the selenium content in soil but also on its chemical form, in which selenium is presented. In some plants, growing on the Se-rich soils, accumulation of selenium occurs in form of non-proteinogenic selenoamino acids, thus ensuring detoxification processes [4].

3.1.2 Epidemiological status

Being a rare element in the Earth's crust and not essential for plants, selenium is a constituent of multiple enzymes in animals and is of great importance for all living organisms [5]. Diet is a primary route of Se intake for most individuals [6]. Due to the different levels of selenium in soil and local nutritional habits, Se intake among humans differs from 30 to 200 μg/day [7]. In extreme cases daily Se uptake can reach 5000 μg/day and lead to a strong chronic intoxication [8]. Normally, the required amounts of Se are received with cereals and meat in form of selenoamino acids [9].

Since Se has several essential functions in the body, the assessment of selenium exposure is conducted through the assessment of dietary intake or the expression of certain biomarkers [10]. The importance of the epidemiological studies on selenium status in different populations is associated with its bipolar effect on human health. On the one hand, Se is an essential trace element and its deficiency leads to the detrimental effects on the body [9, 11]. On the other hand, most of the selenium species exhibit significant toxicity to humans and are still being discussed as potential carcinogens [12]. Recommended daily selenium intake is in the range between 40 to 70 μg/day [13]. Intake of more than 400 μg/day can already lead to the manifestation of adverse selenosis [14].

3.1.3 Importance for human health

Selenoproteins were found in eukaryotes, bacteria, and even archaea, indicating that the formation of selenoproteins occurred before the separation of evolutionary lines. Genes

encoding the synthesis of selenoproteins are found in all mammals [15]. Despite the fact that selenoproteins have also been found in prokaryotic cells, their selenoproteome does not coincide with eukaryotic cells. While eukaryotic selenoproteins serve for antioxidant and anabolic processes, in prokaryotes they promote various redox reactions [16]. Disruption of selenoproteins encoding genes in eukaryotes lead to death at the embryonic state [17].

Se is known to take part in multiple vital physiological processes in all mammalians [18, 19]. The most important among them are antioxidant defense, thyroid hormone metabolism, immune response, and fertility [20-23]. Structural and enzymatic functions of Se in humans are manifested mainly through 25 selenoproteins [24-26]. Lack of adequate Se consumption has been recognized to induce severe pathophysiological conditions like cardiovascular system diseases [27], infertility [28, 29], myodegenerative diseases [30], cognitive decline [31], and anxiety [32]. The role of Se supplementations and selenoproteins in cancer [33], HIV [34], and diabetes [22] progression is still being discussed and could make a positive contribution to treatment development.

The biological functions of selenoproteins are connected with the presence of selenocysteine (Sec), the 21st proteinogenic amino acid [35], which is cotranslationally incorporated into proteins. When Sec is unspecifically replacing usual cysteine in proteins they are called selenium-containing proteins. When Sec act as an active enzymatic center such proteins are called selenoproteins. This distinguishes selenium from other essential elements, since, unlike most of the active sites of metalloenzymes where the active metal center is only coordinated to proteins, selenium is covalently bound to the protein structure. Even though sulfur and selenium have quite similar chemical properties, a slight difference in redox abilities leads to significant shifts in biochemical behavior. The selenol group of selenocysteine is a better electron donor than its sulfur analog in cysteine and consequently is ionized much easier at physiological conditions [36, 37]. Due to the same difference in electronic structure, Se has a lower reduction potential than sulfur in cysteine [38]. Thereby, compared to sulfur-containing cysteine, the presence of Sec in selenoproteins drastically increases their activity by orders of magnitude [36, 39].

It has been shown, that Sec acts as an active center of selenoproteins and functions as a redox center. For example, thioredoxin reductase (TrxR) is the only enzyme able to reduce thioredoxin due to the presence of a redox-active disulfide bond, and hence it is a crucial component for the proper function of the thioredoxin system [40]. Together with thioredoxin, quenching of active peroxide radicals is one of the most abundant functions of selenoproteins and, thus, protecting biomolecules such as lipids and cell membranes from oxidative damage [41]. This process is promoted by a family of different glutathione peroxidases (GPx). In particular, GPx1 and GPx4 are indispensable for healthy development and their absence leads to cardiac dysfunction [42] and disturbs the ferroptosis process [43]. Another example of the indispensability of selenium is the family of iodothyronine deiodinases (DIO), which are responsible for the activation of thyroxine (T_4) to 3,5,3'-triiodothyronine (T_3) [44]. Therefore, the whole thyroid hormone system relies on the Se-dependent enzyme. As selenium enters the body with food, which is dependent on plants and soil selenium content, human Se-deficiency diseases like Keshan disease [45],

Kashin-Beck disease [46], endemic arthritis [47], or cardiomyopathy [48] have been recognized in different regions all over the world.

Not only acute selenium deficiency critically affects human health. Subchronic selenium deficiency has impairing effects on the immune system [49]. In such cases, supplementation with selenium leads to immunostimulation and enhanced lymphocytes and T-cell response [50]. Selenium is needful for the expression of interleukin-2 on the surface of activated lymphocytes [50] and also necessary for the expansion of cytotoxic T-cells since they are characterized by elevated selenophosphate synthetase activity [51]. Another manifestation of suboptimal selenium intake is decreased spermatozoa activity [52], which positively correlates with selenium content in seminal plasma. Most probably this occurs due to the crucial role of GPx4 in the protection of developing sperm from oxidative damage [53]. The decline in GPx activity, even when serum Se levels stay in the adequate range, is associated with intractable seizures [54] and can be treated by selenium supplementation [55]. In more severe cases, selenium depletion causes a higher rate of cardiovascular mortality [56]. Less obvious, yet not less important are consequences of selenium deficiency like depression, anxiety, and more hostile behavior [57, 58].

The first identified selenoprotein was an enzyme belonging to the GPx family, namely GPx1 [59]. Strong interest in these enzymes comes from the variety of their functions and high importance for human health [60-63]. The main function of all GPx is to neutralize endogenously generated hydrogen peroxide and other RONS. If the activity of GPx is decreased due to a low selenium status or due to diseases, more peroxides accumulate in cells leading to tissue damage and inflammation [64, 65]. As GPx utilizes glutathione (GSH) as a reducing substrate, its functions depend on the glutathione reductase (GR) activity, which provides constant GSH supply. GPx family includes 4 enzymes, which differ in their localization [63, 66-68]. GPx1 is a cytosolic enzyme, that was initially called cGPx [69] and ranked quite low in the selenoproteins hierarchy. Mice with GPx1 knockout demonstrate normal development, thus indicating that the lack of GPx1 activity can be substituted by other enzymes and maintain normal redox status [70, 71]. However, mice with GPx1 knockout phenotype were not able to survive paraquat-induced acute oxidative stress irrespective of their selenium status, whereas wild-type animals were not affected so severely [72]. GPx2, also called gastrointestinal GPx, has around 60% similarity in amino acid and nucleotide sequence with GPx1 [73]. As in the GPx1 case, GPx2 knockout mice do not develop any different phenotype [74] but seem to be susceptible to allergic inflammation [75]. The absence of GPx2 significantly increases the number of apoptotic cells in mice colonic crypts [76], which demonstrates a unique intestinal role of this GPx. The third member of this family, GPx3, was firstly found in blood plasma and considered to be “leaked” GPx1 from the liver. But later it was shown, that GPx3 does not react with GPx1 antibodies [77]. Although GPx3 was firstly identified in plasma and purified from it, the primary location of GPx3 in the human body is the kidney proximal tubes epithelium [78]. Other organs, like lungs, gastrointestinal epithelium, and thyroid gland also contribute to GPx3 production [79-81]. Interestingly, GPx3 requires lower GSH concentrations for its activity and it can utilize TrxR as the electron donor in humans, suggesting its potential role in the regulation of thyroid function [82]. The last identified GPx – GPx4 significantly differs from other family members. Unlike GPx1-3, having tetrameric

structures, GPx4 is a single protein [83]. It is also able to react with phospholipid hydroperoxides, while other GPx not. At all, GPx4 has a wider range of possible substrates, as good as electron donors, due to its monomeric structure [84, 85]. Many impairments caused by Se-deficiency are associated with strong oxidative damage, thus being attributed to deficient GPx activity [86]. At the moment new GPx5-8 are identified and it is proven, that the functions of GPx are not solely limited to antioxidative protection [69].

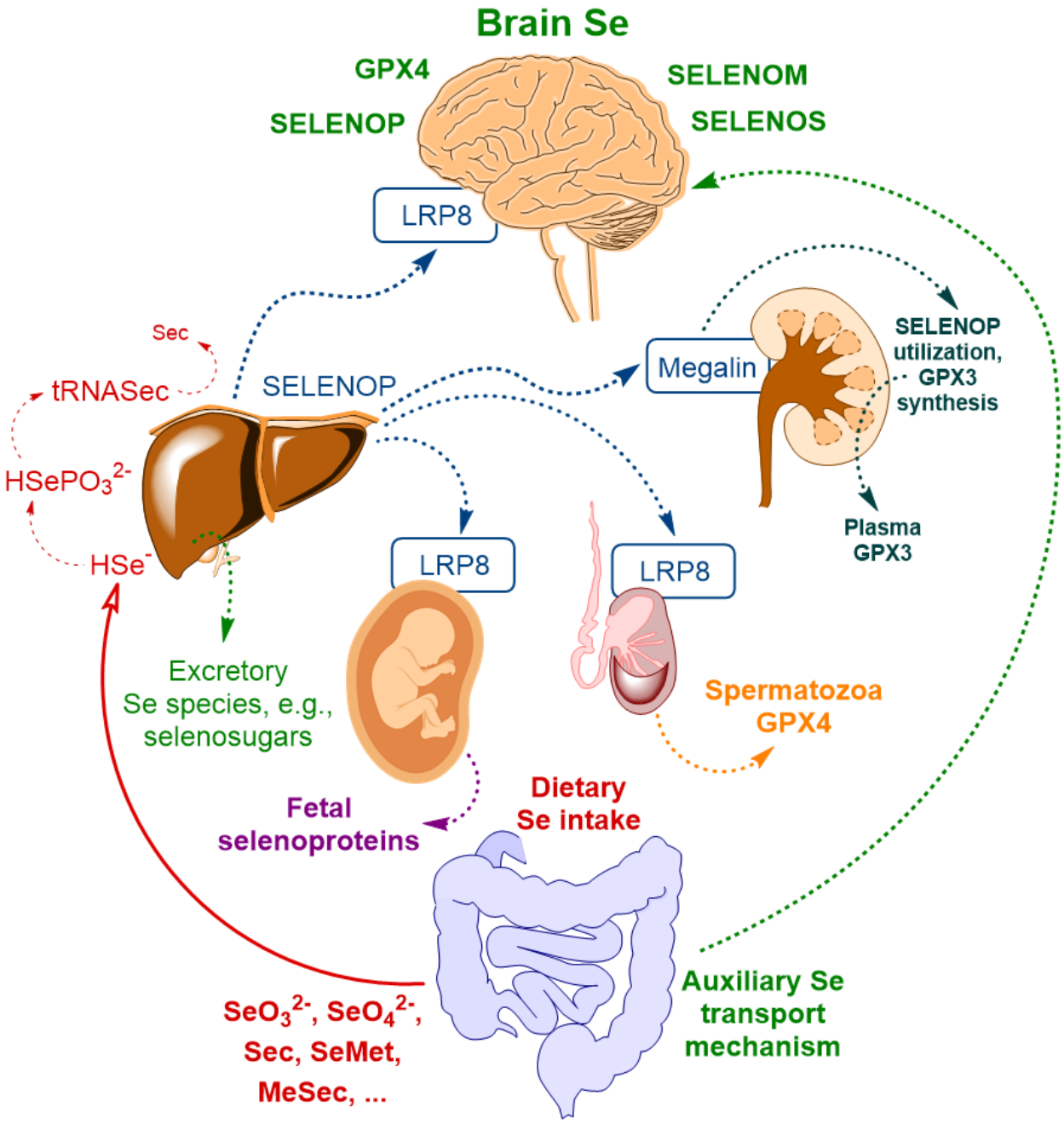

Figure 1. Basic transport concept of Se in human body [87].

All organs in the human body receive selenium in form of selenoprotein P (SelenoP) after ingestion and its synthesis in the liver (Fig. 1). The most dependent organ on selenium status is the brain. Homeostasis of selenium in the brain shows significant differences from other tissues

[88]. Although the brain has a relatively low selenium content under sufficient selenium supply, it shows the highest priority in selenium uptake when a deficiency occurs. Studies in rats with ^{75}Se-labeled SelenoP demonstrate a much higher accumulation of Se in the brain of Se-depleted animals compared to the Se-sufficient control [89]. At the same time, all other organs and tissues were not different in ^{75}Se activity between deficient and control groups. The brain also shows the most stable Se status in the body and tends to keep a nearly constant level of Se content under low supply [90]. Such hierarchy and privileged position of the brain in it shows the extreme importance of Se for maintenance of brain functions. Moreover, under restricted selenium supply, different selenoproteins also demonstrate different expression priorities. As well as the brain, the enzymes GPx2, GPx4, and DIO1-3 are substantially insensitive to Se restriction [91, 92]. Whereas some other enzymes like GPx1, SelenoP, and SelenoW are highly dependent on selenium intake.

The role of selenium in the pathology of neurodegenerative diseases is extensively discussed [93-95]. Such neurodegenerative impairments as Alzheimer's disease (AD), Parkinson's [96] disease (PD), or amyotrophic lateral sclerosis (ALS) are always reported to be connected with elevated oxidative stress [97], which cause significant secondary neuronal damage [98-100]. As a significant part of selenoproteins serve for antioxidant defensive functions their role in such diseases is undeniable, as the brain is highly exposed to RONS formation due to the great oxygen consumption. Selenium deficiency showed a pernicious effect on the area of amyloid-β plaques (Aβ) in Se-deficient transgenic mice [101], while selenium supplementation decreases cognitive disturbance and morphological changes in the rat AD model [102]. Reliable investigation of selenium's role in neurodegenerative pathology is complicated since the direct sampling of tissues is not possible and *in vitro* studies cannot provide unambiguous results. However, *post-mortem* studies indicate co-localization of Aβ with SelenoP and direct interaction between SelenoP and AD-specific molecules [103, 104]. PD pathology is known to affect dopaminergic neurons in substantia nigra, which have the highest selenium concentrations among brain tissues. A possible role of GPx in PD development was reported [96]. The same as in the AD studies, experiments in animal models show increased damage to dopaminergic neurons under selenium deficiency [105]. Co-localization of SelenoP with Lewy bodies in substantia nigra was also reported in a *post-mortem* study [106]. In contrast to AD and PD, selenium seems to play a negative role in ALS development, as an increased risk of ALS development was reported in seleniferous areas [107, 108]. However, while elevated levels of selenium consumption are associated with a higher risk of ALS, predominantly to the pro-oxidant action [109], higher SelenoP content in CSF was found to lower the risk of ALS.

3.1.4 Human selenium metabolism

The commonly accepted concept of Se metabolism is centered around one process similar to all dietary assimilated selenium species. Regardless of the type of consumed selenium form, all these species are firstly reduced to hydrogenselenide (HSe^-) which serves as a universal starting point for further selenoproteins synthesis (Fig. 2) and also as intermediate between excretory pathways and reductive transformation of Se conjugate with GSH. In the case of inorganic Se

compounds, like selenite, the most likely way of their conversion to HSe^- is GSH-mediated reduction [110] with the formation of GSH-HSe^- conjugate. This conjugate is further reduced by cleavage of HSe^- in a dependent from glutathione reductase (GR) activity and NADPH level [111] manner. For selenoamino acids, another route is proposed, which is similar to the trans-sulfuration pathway [112]. Similar to regular methionine (Met), selenomethionine (SeMet) firstly gets conjugated with adenosine by methionine adenosyltransferase (MAT) [113]. Resulting Se-adenosylselenomethioneine (AdoSeMet) then demethylated to Se-adenosylhomoselenocysteine (AdoSeHCys) [114] by the set of three demethylases: histamine-, glycine- and nicotinamide-N-methyltransferases (HNMT, GNMT, NNMT). After demethylation, this adenosyl conjugate is hydrolyzed by adenosylhomocysteinase (AHCY) [115]. The obtained selenohomocysteine (SeHCys) reacts with serine (Ser) and converts to selenocystathionine (SeCysta) under the action of cystathionine beta-synthase (CBS). The final step is taking place under the action of cystathionine gamma-lyase (CTH) which produces Sec from SeCysta. Despite the fact, that Sec is the active center of selenoenzymes, obtained on this stage Sec or readily ingested still has to be transformed.

For further biosynthesis of Se-dependent enzymes, hydrogenselenide should be converted to selenophosphate by selenophosphate synthetase 2 (SEPHS2) (Fig. 2). Selenophosphate acts as an activated form of hydrogenselenide and plays a central role in the formation of the active center of future enzymes. This process starts from the unique transfer ribonucleic acid (tRNA) which refers as $tRNA^{[Ser]Sec}$ and acts as specific Sec tRNA. Firstly, serine (Ser) connected to $tRNA^{[Ser]Sec}$ by serine-tRNA ligase (SerS) forming seryl-tRNA (Ser-$tRNA^{[Ser]Sec}$) [116] which then is phosphorylated by phosphoseryl-$tRNA^{[Ser]Sec}$ kinase (PSTK) and turns into phosphoseryl-tRNA (PSer-$tRNA^{[Ser]Sec}$) [117]. From this point phosphorylated tRNA enters the crossroad and will be utilized not only for *de novo* synthesis of cysteine (Cys) tRNA but also can be transformed to Sec-$tRNA^{[Ser]Sec}$. Formation of desired selenocysteine goes from the abovementioned selenophosphate on PSer-$tRNA^{[Ser]Sec}$ under the action selenocysteine synthase (SecS) [116]. After the described process, Sec is ready for incorporation into selenoproteins as their active center. Thereby, Sec is recognized as the 21^{st} proteinogenic amino acid, because its synthesis is encoded in the ribosome machinery.

Features of selenium metabolism and selenoprotein synthesis are not limited to the above-described sequence of direct selenocysteine synthesis on its tRNA, which differs from usual for other amino acids synthesis before aminoacetylation to the corresponding tRNA. It becomes even more pronounced when taking a look at the process of Sec incorporation into selenoproteins. Insertion of Sec into proteins encoded by the UGA codon, which normally works as a “stop” codon in genetic code [118]. To make Sec incorporation possible, also special selenocysteine-insertion sequence (SECIS) RNA element is required [119]. This is a key factor for selenoproteins synthesis since SECIS signalizes the cells to translate “stop” UGA codon as Sec insertion point. Other elements, required for this unconventional interpretation of a standard piece of genetic code, are SECIS-binding protein 2 (SPB2) [120], elongation factor EFSec [121, 122], few other proteins like SEC43p [122, 123], L30 [124], and presumably more [118]. This is a necessary set of elements to make Sec insertion into selenoproteins possible.

The process of selenoproteins synthesis consists not only in their generation in specific tissues, but also plays a transport function. This function is carried out by SelenoP, which is further delivered to the target organs. Uptake of SelenoP is accomplished by low-density lipoprotein receptor-related proteins 2 and 8 (LRP2 and LRP8 accordingly). LRP2, also known as the megalin receptor, mainly responsible for SelenoP uptake by kidneys (Fig. 1). Other tissues rely on the LRP8 receptor, which is highly expressed in the most Se-dependent organs like the brain and testis [125, 126].

Returning to hydrogenselenide, its function is not limited only by the precursor role for selenoproteins synthesis. Hydrogenselenide also acts as an intermediate for Se excretion through the synthesis of selenosugars [127, 128]. This is the primary route for removing excessively ingested selenium when it is consumed in the required or low-toxic range [127, 129]. In case of a substantial excess of consumed selenium, it will be removed from the process of formation of reactive selenium species and reduced to methylated forms. SeMet can be directly reduced by β-lyase to methylselenide (MeSeH) [130]. In general, it was known for a long time, even before the first comprehensive concept of selenium metabolism, that an acute excess of selenium in the body is accompanied by the appearance of a strong garlic-like odor due to the excretion of dimethylselenide through the lungs via exhalation and dermally via the skin [131].

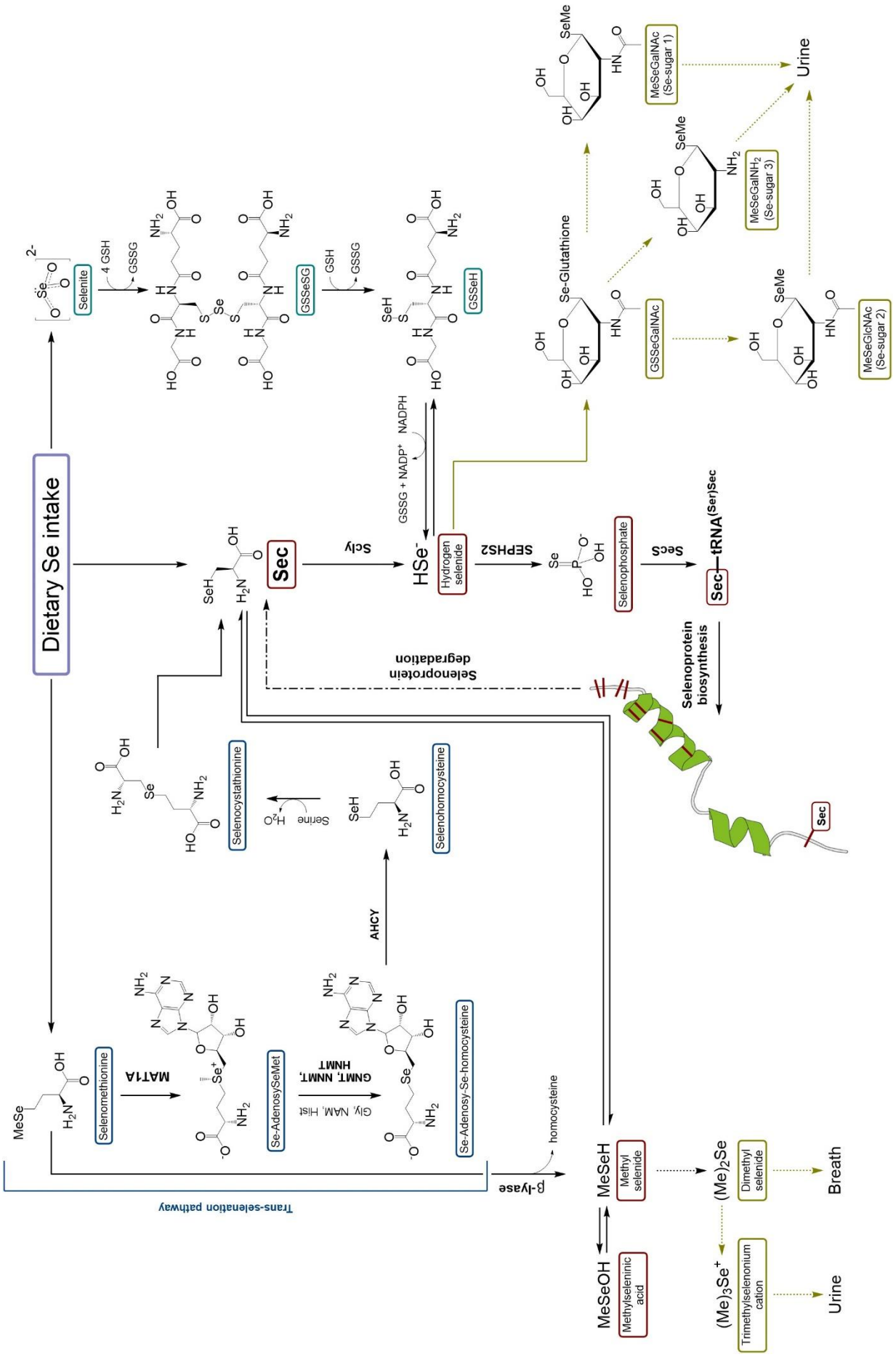

Figure 2. Possible routes of selenium metabolism and selenoprotein synthesis; modified from [87].

3.1.5 Selenium role in intestinal functions

The gastrointestinal tract is often exposed to radical inducing stimuli [132-134] and other adverse factors [135-137]. At the same time, natural processes in the gastrointestinal tract are associated with elevated RONS formation [138] and strong dependence on redox signaling [139]. Therefore, intestinal epithelium integrity is highly dependent on fast and efficient processing and elimination of RONS. Dysregulation of oxidative homeostasis is known to occur in almost all gastrointestinal diseases [140-142].

The importance of selenium for gastrointestinal functions is now beyond reasonable doubt. The condition of microbiota is known to take part in host selenium intake [143] and reversibly affects selenoprotein production [144]. Chronic intestinal Chagas disease is associated with low selenium status, even when patients living in Se-sufficient regions [145]. Studies in GPx3 knockout mice demonstrate that the absence of GPx3 leads to the increased inflammatory colonic tumorigenesis [146]. Intracellular GPx4 is also responsible for RONS scavenging in intestinal microvilli [147]. Besides the enzymes with primary antioxidative functions, SelenoP was demonstrated to be inversely correlated with the development of irritated bowel disease and colorectal cancer [148, 149]. Due to the absorptive functions of colonic epithelium, it is not clear, if selenium deficiency occurs after disease development, or serves as a predisposition factor [150]. However, the role of selenoproteins in the regulation of the RONS level and development of inflammation is evident.

3.1.6 Toxicity of selenium species

While the daily selenium intake is essential for human health, consumption above the tolerable level causes dose-dependent toxic effects. When given in excessive amounts, selenium compounds are promptly distributed to most of the tissues. Selenium species are mainly metabolized in the liver and excreted with urine as selenosugars [127, 129] and trimethylselenonium (TMSe) [151-154] (detailed description in section 3.1.4). Biotransformation to inactive forms seems to be a primary regulatory mechanism of selenium homeostasis under exceeding selenium exposure. In the case of acute intoxication with high content selenium supplements, followed by diarrhea, tremor, and abdominal pain, symptoms mostly disappear after 24 hours, while urinary selenium excretion was extremely high [155], thus reaffirming a highly effective detoxification mechanism for selenium. However, acute selenium poisoning can also be fatal [156-160], especially at doses of 10 mg/kg of body weight or higher [155]. Mainly, selenium intoxication is associated with ingestion of its inorganic forms: selenite, selenate, and selenium dioxide. Data from animal studies indicate LD_{50} for selenite around 2-5 mg/kg body weight [161]. *In vitro* studies showed that selenite causes significant cytotoxic effects in the lower micromolar range [162-165]. It is quite ironic, that selenite at high dosage promotes RONS formation, lowers GSH level, and induces apoptotic cell death [166-169]. Possible genotoxic effects of selenite are also discussed. Namely, studies on yeast demonstrate possible mutagenic effects [170], chromosomal breakage, and chromatid exchange in human lymphocytes [171] and fibroblasts [172], as well as single and double DNA strand breaks in mouse-derived cells [173].

However, no clear results about the possible genotoxic effects of selenite can be summarized. Most probably, observed effects are the consequence of elevated RONS production. The exact mechanism of selenite toxic action has not yet been established. Formation of the selenium nanoparticles (NPs) after selenite exposure has been proposed as a primary cause of selenite-induced cytotoxicity [174].

Compared to selenite, other abundant selenium compounds demonstrate lower toxicity. Selenate is less toxic than selenite because it anyway needs to be converted to selenite by TrxR at the slow rate [175]. Organic selenium compounds are also less toxic than selenite. The reason for this lies in the lower oxidation state of selenium in organic compounds and stabilizing the C-Se bond, which requires multistage metabolization of these species before they can manifest toxic effects [176]. For example, no data on acute intoxication with SeMet was reported so far. In the animal studies, it demonstrates four times higher LD_{50} than selenite after intravenous injection in mice [177]. Chronic exposure to the elevated SeMet levels also causes milder effects in pigs than the same amounts of selenium given as selenite [178]. The reason behind the low toxicity of SeMet is the unspecific incorporation of SeMet instead of Met into proteins [179-181], thus reduced amounts of SeMet are available for metabolization into active species. While excessive substitution of Met with SeMet also leads to protein aggregation and reduction of translation rates in protein synthesis [182]. In HepG2, UROtsa, and CCF-STTG1 cell culture models SeMet exhibits no or very little toxic effects at hundreds of micromolar [162, 183]. Such absence of toxicity might be explained by a lack of methionase activity, therefore SeMet is not metabolized to MeSeH and only minor amounts of ROS are generated [184]. Similar to SeMet, methylselenocysteine (MeSeCys) demonstrates the absence of genotoxic effects and very moderate toxicity *in vivo* [185], administering 11 mg/kg bw to mice.

While acute selenium intoxication is mainly associated with intended or unintended ingestion of Se-containing substances or occupational episodes, chronic intoxication is mainly caused by endemic reasons. Thus, in China exists regions with extremely high selenium content in the soil which leads to high selenium consumption through local food [186]. In some cases, weathering of coal with extremely high selenium content (> 300 μg/g) comes together with drought caused a regional outbreak of selenosis [8], due to the failure of rice crops and dietary changes to higher consumption of Se-accumulating vegetables. Chronic selenosis changed to the subacute phase and lead to the 50% morbidity during the peak in the worst affected villages.

3.2 Selenoneine

The naturally occurring Se compound selenoneine (2-selenyl-N_α,N_α,N_α-trimethyl-L-histidine, SeN, Fig. 3A) was firstly identified in blood and other tissues of the bluefin tuna (*Thunnus thynnus*) [187]. Since its discovery in 2010 SeN was also found in a number of edible fish species [188-192]. From the moment of its discovery, SeN attracted significant attention due to multiple reasons. First of all, it is related to the abovementioned reasons: being widespread in fish species, which are included in ration of people around the world, there is very limited information available

about health-related properties of SeN. Until now, it is known, that SeN is actively consumed by the people whose diet strongly relies on fish [188, 190, 193]. For such populations, SeN was found to constitute the major part of the non-protein bound Se pool in the blood [188, 190, 194]. Most of the SeN was identified in red blood cells (RBC) – around 54% of total Se content was measured in RBC [188, 195]. Also, a possible metabolite of SeN – Se-methylselenoneine (MeSeN) was identified in the RBC and showed a strong positive correlation with the SeN content. The same species, MeSeN, was detected in human urine [193, 196].

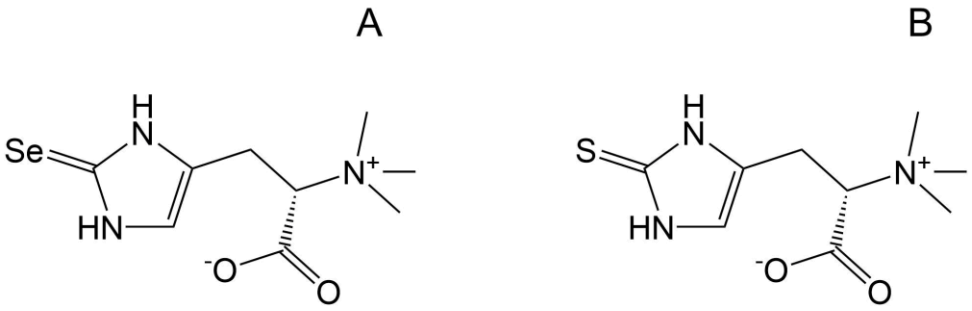

Figure 3. Chemical structures of selenoneine (A) and ergothioneine (B) [197].

The second reason for the high interest in SeN is the fact, that the basis of SeN chemical structure is the amino acid histidine. As it was described in section 3.1.4, selenium-containing amino acids can be used for the synthesis of selenoproteins or can be unspecifically incorporated into proteins. Thus, SeN is of interest to be studied as a potential Se source for the human selenoproteome.

The final reason for increasing attention to SeN is its similarity to the naturally occurring compound ergothioneine (ET, Fig. 3B). More specifically, SeN has an ET structure where sulfur is replaced by selenium. As ET is widely distributed in nature [198-200], it is synthesized by a number of fungi [201] and bacteria [202, 203] and being accumulated in a higher organism at significant level [204-207] utilizing organic cation transporter 1 (OCTN1) [208-210]. The biological functions of SeN consequently attract the focus in the Se research field. Not so much is known about SeN properties to the current moment, but available studies demonstrate similarity to ET in some properties. As mentioned above, SeN is found predominantly in erythrocytes and the same can be told about ET [206, 211]. Accordingly, it has been suggested that SeN can utilize the same transporter, and was demonstrated in zebrafish embryos and human embryonic kidney HEK239 cells, that SeN actually has a strong affinity to OCTN1 [191, 212]. Also, SeN was reported to prevent iron in erythrocytes from auto-oxidation by binding to heme proteins [191] and the same protective properties were found for ET [213, 214]. Besides, it was reported that SeN may play a role in the methylmercury detoxification process [212, 215] by enhancing the demethylation rate of MeHg.

However, sulfur to selenium substitution is known to endue amino acids with new or modified properties as described in section 3.1.3. Respectively, the antioxidant properties of SeN differ from ET. From the moment of SeN discovery it was already reported, that SeN exhibit higher *in vitro* radical scavenging activity against 1-diphenyl-2-picrylhydrazyl (DPPH) [187]. Nevertheless, these studies were conducted using not a pure SeN, but enriched extracts from fish tissues, which

makes interpretation of these results difficult. However, at the moment, biochemical [197] and fully synthetic [216] approaches are available for SeN synthesis. Higher antioxidant activity of SeN compared to ET was confirmed now using the pure compound [216]. Treatment of ET and SeN with hydrogen peroxide showed different stabilities and oxidation rates. Under these conditions, ET oxidized to the unstable sulfinic acid intermediate (Fig. A), which immediately converted further to trimethylhistidine (TMH, Fig. B) with cleavage of C-S bond or ergothioneine sulfonic acid (Fig. C). These compounds were earlier detected in biological samples [217], representing oxidative degradation of ET. At the same time, SeN demonstrates completely opposite behavior. Oxidation of SeN almost stops at the stage of seleninic acid formation (Fig. A). Subsequent formation of selenonic acid (Fig. C) and deselenation to TMH occur with marginal rate. Wherein stable SeN, seleninic acid intermediate is readily reduced in the presence of GSH and converted back to the SeN. Thereby SeN not only demonstrates higher stability compared to ET under oxidative conditions but also should exhibit stronger antioxidative activity in the cells, due to the absence of irreversible oxidative degradation. This is most probably due to the strong cyclic conjugation of the selenol group with a double bond and electronic pairs of nitrogen atoms in the imidazole ring. Therefore, better nucleophilic potential of Se cause stronger mesomeric effect, which stabilizes its oxidized seleninic acid intermediate.

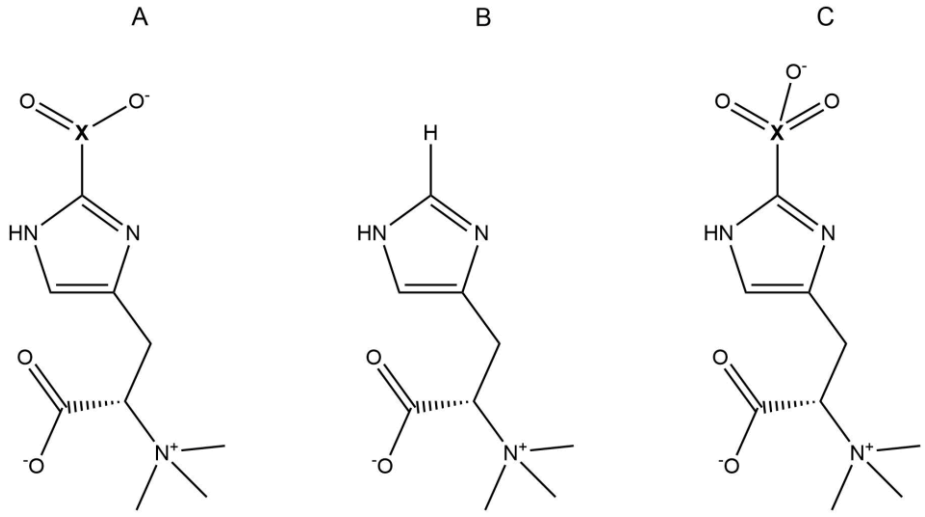

Figure 4. Chemical structures of sulfinic/seleninic acids (A), trimethylhistidine (B), and sulfonic/selenonic acids (C), where X represent sulfur for ET and selenium for SeN [216].

This also differs SeN from conventional nutrition-relevant selenium compounds. Usually, Se is presented in organic forms as a free or methylated selenol group, while SeN has tautomeric equilibrium between selenol and selenoketone groups (Fig. 5 A), due to the above-mentioned conjugation. Lower oxidation potential and stabilized electronic density also lead to the easier oxidation of SeN at normal conditions, which leads to the oxidative dimerization of SeN in contact with air (Fig. 5 B). Therefore, pure SeN under normal conditions is almost presented in the dimer state.

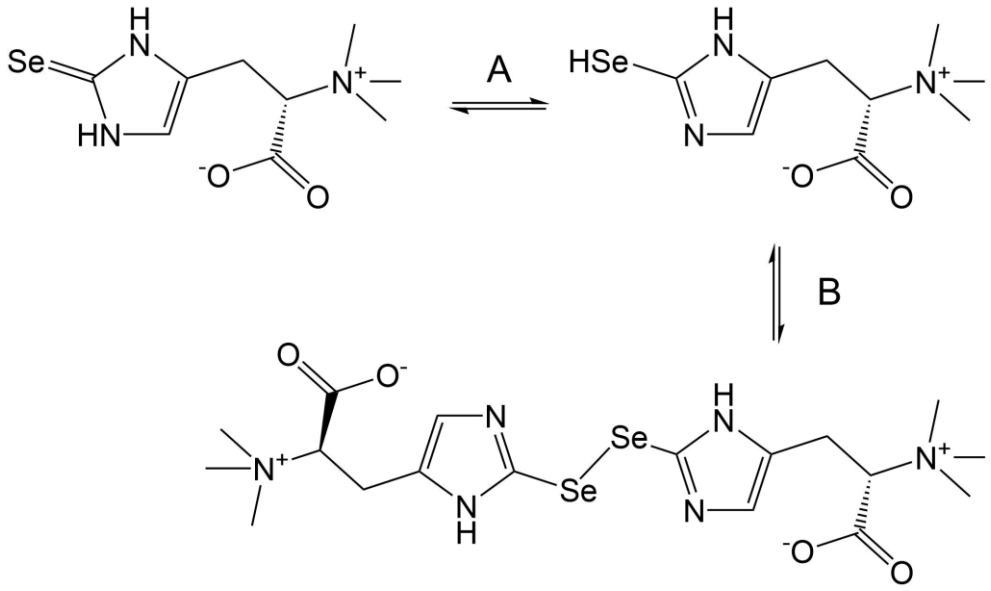

Figure 5. Tautomerization (A) and oxidative dimerization (B) of selenoneine [197].

3.3 Blood-brain barrier

The central nervous system (CNS) requires very fine regulation of nutrients uptake, microglia, and surrounding microenvironment conditions to make precise neuronal signaling and development of new neuronal cells possible [218]. There are three key components, that separate CNS from blood: blood-brain barrier (BBB), blood-cerebrospinal fluid barrier (BCSFB), and arachnoid barrier [219]. Brains of all mammals, including humans, are separated from peripheral and cardiovascular systems by the BBB, which plays a crucial role in CNS development [220]. BBB plays a major role in the separation of CNS from general circulation systems since it includes most of the brain microvessel endothelium, thus representing the largest site of blood-CNS contact [221]. The primary function of BBB is the maintenance of CNS homeostasis and regulation of nutrient, hormone, and ion transport [222]. Hence, the BBB protects the brain from toxic substances, including xenobiotics and endogenous toxins [223], regulates nutrients [224] and metabolites [225] uptake, and separates the brain from neurotransmitter pools in the peripheral nervous system. Also, the BBB maintains a privileged brain immune system [226], which is dependent on microglia [227], rather than on the general immune system compartments like the thymus [228] and bone marrow [229].

3.3.1 Structure and functions of blood-brain barrier

The main anatomic units of BBB are endothelial cells, which are mainly responsible for barrier functions [221]. Endothelial cells in the BBB are connected with each other by so-called tight junctions (TJ) [230]. These cellular junctions are formed by special proteins such as occludin, claudins and associated with their proteins of zona occludens (ZO-1, ZO-2, and ZO-3) [231], which are highly expressed in the BBB endothelium [232, 233] and plays the scaffolding role ensuring structural basis for branching multiprotein intercellular complexes [234]. Another important

function of TJs is the prevention of lateral diffusion of membrane proteins [221] and the formation of selective paracellular channels for small cations and anions [235] or water transport [236].

Endothelial cells of the BBB do not act alone or only by TJ functions [237]. The close location of neuronal axons, astrocytes, and other glial cells leads to the inevitable interactions between them and influence on each other [238-240]. The combination of such interactions forms a well-organized modular structure, ensuring the integration of endothelial cells with neuronal and microglial cells surrounding. This modular complex gave rise to a concept of BBB subunit – neurovascular unit (NVU) [241]. Astrocytes were shown to be related to endothelial cell development [242] and TJs expression [243]. Other important components of NVU are pericytes, which also affect the development of endothelial phenotype [244]. Pericytes cover the outer surface of the vascular tube and adjoin to endothelial cells. Due to the presence of similar to smooth muscles fibers and the expression of vasoactive mediators, they were hypothesized to play only a vasoregulatory function [245], like in blood vessels in other parts of the body [244]. Later studies demonstrate that pericytes cover around 60% of capillary endothelium [246] and are closely coupled with astrocytes endfeets [247]. The contact between pericytes and endothelial cells formed as peg and socket arrangements together with gap junctions [248, 249] proving their regulatory influence on barrier functions. Gap junctions allow pericytes to contact with endothelial cells by the exchange of ions and small molecules [250]. Loss or decrease in pericytes coverage is known to lead to a decrease of BBB barrier function [251], thus showing the complex involvement of pericytes into the regulation of BBB permeability. From the neuronal site, NVU can be regulated by growth factors, like the neuregulin protein family [252]. The BBB also responds to neuronal activity and its permeability can be upregulated by neurotransmitter release through glutamate-dependent NMDA receptors [253] or activate the transport of insulin-like growth factor 1 [254]. Summarizing the contribution of astrocytes, pericytes, neurons, and interactions between them on functions of BBB condition, the NVU concept represents the integral nature of maintenance of CNS homeostasis.

The BBB has very limited capabilities for passive transport of not only toxic or harmful compounds but also essential nutrients required by nervous tissues [255, 256]. While small lipophilic molecules and oxygen can diffuse through endothelial lipid membranes [257], polar substances and bulky uncharged molecules require special solute carriers called transporters. Therefore, the BBB exhibit a broad spectrum of selective transport systems to ensure an optimal supply of CNS with essential substances [258, 259]. While some transport proteins are inserted into both luminal and abluminal membranes of BBB endothelium, others are presented only at the one side of the barrier [260, 261]. Differences in transporter protein localization result in preferential transport direction for specific substances [262]. For example, one of the most important transporter superfamily – ATP-binding cassette (ABC) is functioning primarily as an active efflux pump, ensuring the elimination of lipophilic compounds from NVU [263], therefore performing neuroprotective function against endogenous neurotoxins or xenobiotics [264]. Although most of the macromolecules are obviously restricted from entering the brain through the BBB [264], some proteins and enzymes are required by CNS and are transported across BBB through

endocytosis, which is mainly directed from blood to the brain side [265-267]. These processes occur by 2 principal mechanisms: receptor-mediated transcytosis (RMT) and adsorptive-mediated transcytosis (AMT). In RMT molecules need to be recognized by a specific receptor protein and form a ligand cluster with it, which then split off and enter into vesicle [268]. Molecule together with a receptor is then routed through the cytoplasm and exocytosed on the opposite side of endothelium. The AMT mechanism is peculiar for molecules with strong positive charges, which should be recognized by surface binding sites to induce endocytosis [269]. Compared to other endothelial cells in the human body, the BBB exhibit a very limited amount of endocytotic vesicles [270], thus highlighting its outstanding selectivity and importance for CNS homeostasis, because increased transcytosis rates were observed after traumas or inflammation [271, 272].

3.3.2 *In vitro* models of blood-brain barrier

BBB, as good as other neuronal barriers, is a very complicated system and can be hardly studied directly in living organisms. Consequently, to provide a possibility of BBB investigation multiple model systems were designed to reproduce properties of the BBB *in vitro*. These artificial systems significantly alleviate exploration of the processes occurring across BBB and NVU. The development of BBB models goes in three main directions: static models, dynamic models, and spheroid models [273]. The reliable model must reproduce certain processes occurring around the BBB, thus having a predictive power to make possible extrapolation of obtained results to living organisms. Therefore, some systems are more suitable for modeling certain processes than others and have different limitations.

Static models are almost always presented by Transwell® systems (Fig. 7). These models are consisting of primary or immortalized endothelial cells, growing on a matrix-coated membrane insert [274]. A layer of endothelial cells on a membrane divides the volume of one well into two parts. The upper part plays the role of the capillary lumen or blood-facing side, and the lower part represents the parenchymal compartment or brain-facing side. Transwell® models give great freedom both in terms of the cell line choice and the possibility of different co-cultures with astrocytes, pericytes, and neurons, for better simulation of microvascular environment and interactions within NVU [273, 275]. Among other model types, these have an advantage in the simplicity of application, moderate costs, and ease of access to the cell layer, which makes impedance measurements, sampling, and microscopical evaluation of cells rather easier. These static systems demonstrate high effectiveness in the permeability screenings [276, 277]. However, the absence of blood flow and close neurochemical coupling between neuronal cells and endothelial layer circumscribe the application of such models in a number of cases [278].

Dynamic models were developed for implication in studies, where blood flow generated shear stress and neuron-endothelial contact are of great significance and static models cannot be used. In order to closely mimic the natural BBB conformation, endothelial cells and astrocytes are seeded on the inner and outer surface of permeable capillary [279]. Shear stress, close to that in brain capillaries, is achieved by medium circulation through the capillary. Such systems can be

also equipped with gas-permeable tubing or membranes to maintain the physiological level of the O_2/CO_2 ratio. As these models provide a superior advantage to control shear stress affecting BBB conditions, they were successfully used in studies on antiepileptic drugs [280] and ischemia-induced brain injury [281]. However, limitations associated with a geometric profile of dynamic devices make it not possible to visualize endothelial cells and require higher cell density and longer cultivation times to obtain a stable barrier [282, 283]. Further development of dynamic BBB models led to the appearance of microfluidic devices [276, 284]. Shear stress in these devices generated by medium movement in two perpendicularly crossing channels, divided by perpendicularly oriented microfiber capillaries. Compare to conventional dynamic models microfluidic devices allow easier TEER measurements (described in section 5.1.2) and cell visualization [285]. Also, miniaturized devices require a fewer amount of cells, cultivation time, and technical skills to achieve a stable endothelial monolayer. Although, a small chamber size limits their application for shear stress studies and does not allow to reach TEER values higher than 300 $\Omega \cdot cm^2$. Recent advantages in the development, however, demonstrate their potential for a variety of research topics [286-288].

Spheroid or cell aggregate models are a completely different approach in BBB modeling compared to static and dynamic systems. They are based on the ability of endothelial cells, pericytes, and astrocytes to self-organize into 3-dimensional spheroids with astrocytic core and outer endothelial layer, connected by pericytes [289]. Accordingly, the main property of this system is the direct contact between NVU-forming cells [290], giving them a significant advantage in certain applications compared to other model types. On the other side, there is no suitable way to properly assess barrier integrity or permeability in cell aggregates [291]. Specifics of these models make them more suitable for the investigation of processes in NVU and its constitutional cells, rather than barrier functions.

A variety of requirements for BBB models and evolution CNS barrier concepts make the implementation of artificial BBB systems somewhat complicated. However, a better understanding of BBB nature and improvement of existing models allows them to become an important research tool.

3.3.3 Selenium transport across blood-brain barrier

The essential role of selenium and selenoproteins for brain function is now beyond doubt [54, 94, 95]. At the same time, selenium species exhibit significant toxicity to the brain and their uptake by neuronal cells is highly regulated by the BBB [90, 292]. The first study with ^{75}Se radiotracer by Burk et al. [89] revealed important features of selenium transport to the brain. Injection of ^{75}Se labeled selenite to Se-deficient and control mice resulted in accumulation of ^{75}Se only after the appearance of SelenoP with assimilated ^{75}Se tracer in blood plasma. Moreover, selenium-deficient animals demonstrated five times higher ^{75}Se accumulation in the brain already after 2 hours compared to the control group, while the total rate of ^{75}Se-SelenoP distribution from plasma was the same between groups. Thus, the brain differs significantly from other tissues in terms of selenium supply priority [293].

Since the discovery of the SelenoP function as the sole transport protein for Sec delivery, our understanding of selenium transport to the brain has changed drastically [119]. SelenoP biosynthesis, involving high energy consuming incorporation of multiple Sec residues (see section 3.1.4), additionally depicts the importance of SelenoP for selenium metabolism [294]. Human SelenoP contains ten Sec residues, one of them is always located at the C-terminal region and nine others are separated by a histidine-rich sequence and located closer to the N-terminal end [119]. Main quantities of SelenoP are synthesized in the liver [90, 295, 296], however, neurons [297] and astrocytes [298, 299] are also able to produce it, probably for intra-brain selenium redistribution and antioxidative defense. Being responsible for selenium delivery to the brain, SelenoP greatly contributes to redox and neurochemical signaling pathways [93, 300].

As described in section 3.1.3, SelenoP is synthetized in the liver, delivered by the blood flow to other organs, and is assimilated by endocytosis after binding to LRP8 or LRP2 (Fig. 1). The brain is no exception here and relies on the LRP8 receptor (Fig. 6), these are presented on the luminal side of the BBB endothelium [301, 302]. This mechanism was proven by studies conducted in *SelenoP*$^{-/-}$ knockout mice, which exhibit a significant reduction of SelenoP mRNA expression in the brain compared to wild-type animals [90, 301, 303-305]. SelenoP or LRP8 knockout lead to severe neurological impartments [306, 307], while liver selenium content was not affected [303] or even elevated [304] after SelenoP deletion. However, feeding of *SelenoP*$^{-/-}$ with a Se-sufficient diet resulted in partial recovery of the Se status in the brain, indicating the presence of additional mechanisms for selenium delivery to the brain in forms different from SelenoP.

SelenoP that reaches the BBB must be further utilized for the synthesis of other selenoproteins. Intracellular Sec release from SelenoP can occur in lysosomes [294] of astrocytes in NVU under the action of selenocysteine lyase (Scly) [308], as it was shown that adjacent astrocytes have higher SelenoP expression [302]. Nevertheless, the exact mechanism of SelenoP metabolization in NVU is still not fully clear. Alternative mechanisms of selenium transport to the brain may contribute to the selenosugars [292] or low-molecular-mass species [309]. In this case, selenosugars are the most probable candidates, since they do not exhibit toxic properties to the brain and may share glucose transporters of the BBB [310]. SeMet and selenite also may serve as substrates for the selenoproteome, as enhancement of selenite reduction and trans-selenation pathways (section 3.1.4) was reported in case of SelenoP absence [311, 312]. Sec synthesized by these routes can be utilized in the brain for the further internal synthesis of selenoproteins.

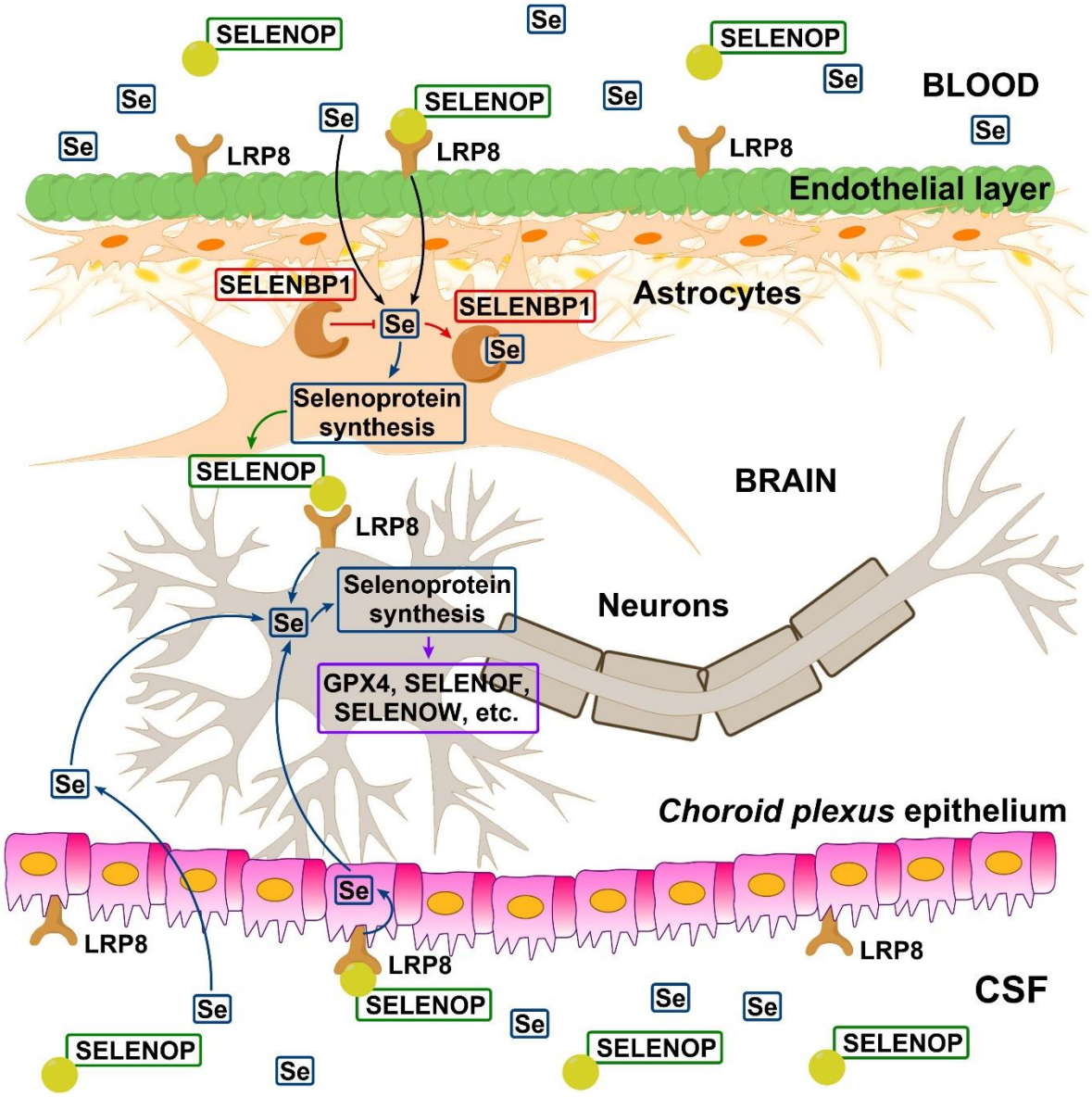

Figure 6. Generalized model of the presumptive ways of selenium transport to the brain [87].

4. Objectives

Selenium (Se) is an essential trace element, known to take part in different physiological processes. Although the Se content in the Earth's crust is relatively low, Se can be found in significant amounts in all living organisms. Considering the presence of endemic areas with both high and low Se contents in soil and water, as well as the presence of Se bioaccumulation chains, Se exposure is varying greatly all over the world. Among other essential elements, Se stands out in that it has a very narrow optimal uptake window between deficiency and overexposure. This, together with the abovementioned highly uneven Se distribution in the environment, makes the assessment of human exposure to Se species an important task and still leaves a lot of questions regarding health-related effects of Se.

In various types of plant and animal-derived food, selenium is presented in the form of organic and inorganic compounds with different nutritional and toxicological properties. Entering the human body almost exclusively via food, selenium is used for the synthesis of selenoproteins – specific peptides, which are having 21 essential amino acid selenocysteine in their active center. These selenoproteins are responsible for the essentialness of Se.

Despite the close attention to Se for many years, one of the widespread Se species – selenoneine (SeN) was discovered in 2010, only. It was identified in the blood and tissues of the bluefin tuna and then found in a number of edible fish species. Thus, being a food-relevant compound and intensively consumed in different regions, SeN was later found to present the main pool of non-protein bound selenium in the blood of such populations. Moreover, SeN is a Se-analogue of a naturally occurring compound with strong antioxidative properties – ergothioneine. In this way, this compound with high antioxidative potential and involvement in human selenium metabolism is of high interest for a comprehensive investigation.

The predisposition to this work was the first successful synthesis of SeN using genetically modified fission yeasts in the University of Graz. Due to the small amount of substance that can be obtained in such a synthetic approach, cell cultures are the most suitable model system for investigation of its toxicological and potential beneficial characteristics. For this purpose, the human hepatocellular carcinoma cell line (HepG2), primary porcine brain endothelial cells (PBCEC), and the human colorectal adenocarcinoma cell line (Caco-2) were used.

Since almost always Se-compounds undergo a metabolic transformation in the liver, hepatic cells were used to assess both potential hepatotoxic effects and possible transformation of SeN in hepatocytes. Besides the transport of Se to the brain in the form of selenoprotein P, an auxiliary transport mechanism was described for several Se-species, when they pass through the blood-brain barrier in their unchanged form. Therefore, the assessment of SeN's ability to pass the blood-brain barrier is of high importance. For this purpose, a model system utilizing PBCECs seeding on the membrane inserts, imitating brain microvascular endothelium was used. This system also allows establishing possible toxic manifestation, occurring during the transfer of SeN and its metabolization within this process. As follow from human data, demonstrating significant

accumulation of SeN in blood, it is bioavailable in the intestine, which was confirmed before in our lab using the Caco-2 intestinal barrier model. In the current work, Caco-2 cells were used for the investigation of SeN's antioxidant potential and its influence on selenoproteins production and activity. Thus, obtained data should give a general concept of SeN distribution in the body and its interaction with the selenoproteome.

5. Experimental

5.1 Cell culture

All cell culture experiments were conducted in a sterile laminar-flow hood with sterilized equipment, materials, and solutions. Cells were cultivated in the incubator at 37 °C, 100% humidity and 5% (v/v) CO_2 content. Solutions and buffers used in cell culture were prepared using deionized (15 MΩ × cm) water and sterile filtered. Plasticware and glassware were autoclaved under standard conditions (pressurized steam, 121 °C, 15 minutes).

Cells were stored at -196 °C in the nitrogen tank. For cryopreservation, cells were resuspended in a freezing medium, containing 90% of fetal calf serum (FCS) and 10% dimethyl sulfoxide (DMSO) (v/v). Cryotubes with cell suspension were placed into a freezing container, ensuring slow cooling at 1 °C/min rate, for the next 24 hours at -80 °C. Afterward tubes were transferred into the nitrogen tank and stored at -196 °C.

5.1.1 Cultivation of HepG2 cells

HepG2 is an immortalized human liver cancer cell line. These cells were derived from the liver tissue of the 15-year-old Caucasian male with hepatocellular carcinoma [313]. HepG2 is an adherent cell line, growing in single layers. They are actively implemented for studies on liver metabolism, xenobiotic toxicity, and genotoxic effects [314]. HepG2 does not exhibit tumorigenic properties, has a high proliferation rate and epithelial morphology with an average chromosome number of 55.

Cells used in this study were purchased from the European Collection of Authenticated Cell Cultures (ECACC 85011430, Salisbury, UK). For cultivation, Eagle's minimal essential medium with 10% (v/v) FCS, 100 U/mL penicillin, 100 µg/mL streptomycin and 1% (v/v) of non-essential amino acids solution was used. Cryopreserved cells (10^6 cells/mL, 1.6 mL total) from the nitrogen tank were thawed in the water bath and gently resuspended in 10 mL of a warm (37 °C) culture medium. The suspension was subsequently centrifuged for 5 minutes (200×g RCF), pellet carefully resuspended in 15 mL of warm culturing medium, and seeded into cell culture flask (25 cm^2 area) with filter screw caps (PTFE hydrophobic membrane, 0.22 µm pore size). After the formation of the confluent monolayer, cells were seeded into cell culture dishes (60 cm^2 area). For repassaging, the medium was aspirated and cells were carefully rinsed with 2 mL of warm trypsin solution (0.25 %) in PBS-EDTA. After rinsing, cells were incubated for 30 s with 2 mL of trypsin solution, which was then aspirated. Within 2-3 minutes in the incubator at 37 °C cells detached from the bottom of the culture dish. Detached cells were thoroughly washed from the bottom of the dish and actively resuspended. In order to measure the amount of cells in obtained suspension Casy-TTC® automatic cell counter was employed. Aliquot of cell suspension (50 µL) was mixed with 5 mL of isotonic electrolyte solution (Casy-Ton®) in Casy-Cup® and measuring

capillary with an electrode was placed the into solution. Because HepG2 cells tend to form aggregates, obtained results on cell concentration were corrected by aggregation factor. At least two measurements were carried out for each sample and results differed by ≤10% were taken for the mean calculation. Finally, a defined volume of cell suspension was mixed with fresh warm medium and placed into dish (60 cm^2 – $1.5 \cdot 10^6$ cells in 10 mL medium; 22 cm^2 – $5 \cdot 10^5$ cells in 3.7 mL medium) or plate (96 well plate, 0.36 cm^2 – 5000 cells in 0.06 mL; 12 well plate, 3.66 cm^2 – 61000 cells in 0.65 mL; 6 well plate, 9.03 cm^2 – 150000 cells in 1.5 mL). Passage of cells was performed every 2-3 days when they reach around 80% confluence by the same procedure. Cells were taken into experiments 48 h after seeding at the logarithmic growth phase. The initial passage number of preserved cells was 106 and cells were used until passage 120.

5.1.2 Cultivation of porcine brain capillary endothelial cells and impedance measurements

Primary porcine brain capillary endothelial cells (PBCEC) were isolated from brain tissues of freshly slaughtered six-month-old pigs and carried out in accordance with previously published protocols [315, 316]. Hemispheres of porcine brains were collected in 70% (v/v) ice-cold ethanol and then placed into ice-cold PBS containing 200 U/mL penicillin and 200 µg/mL streptomycin for transportation. Then, large blood vessels, meninges, and secretory parts were removed. The remaining white and grey matter substance was mechanically homogenized and placed in a preparation medium, containing 0.7 mM L-glutamine, 100 U/mL penicillin, 100 µg/mL streptomycin, and 100 µg/mL gentamycin in Earle's 199 medium. The resulting suspension was added with 1.6% (w/v) of dry unspecific protease/dispase II mixture and stirred for additional 2 hours. Then, 100 mL of digested homogenate were added in 150 mL of 18% (w/v) dextran solution (molecular weight 160 kDa) at 4 °C for separation of the capillary fraction. Isolated capillaries were precipitated by centrifugation (6890×g RCF, 10 min, 4 °C). The obtained capillary pellet was resuspended in 10 mL of proliferation medium, containing 10% FCS, 50 U/mL penicillin, 50 µg/mL streptomycin, 50 µg/mL gentamycin, and 0.7 mM L-glutamine in Earle's 199 medium, and actively mixed by releasing suspension from 10 mL pipette against the bottom of the beaker. The suspension was filtered through 180 µm nylon mesh to remove larger capillaries. In order to achieve disruption of capillaries into smaller fragments mixture of 0.1% (w/v) dispase/collagenase II was added to the suspension and incubated for 60 minutes in the flasks with a magnetic stirrer at 37 °C. Hereupon, cells were precipitated by centrifugation (110×g RCF, 10 min, r.t.) and resuspended in the same volume of proliferation medium. Endothelial cells were separated by discontinuous percoll gradient precipitation: 15 mL of 1.08 g/mL percoll solution was placed first, carefully covered with 20 mL of 1.04 g/mL percoll solution, and 10 mL of endothelial cells suspension were placed on the top. Tubes with gradient solution were placed into a centrifuge with a swing-bucket rotor and centrifuged for 10 minutes (1250×g RCF, r.t.). The red-stained interface layer in the lower half of the gradient was separated by aspiration and diluted in the proliferation medium. Final centrifugation was carried out at 110×g RCF for 10 minutes. Obtained pellets were diluted in proliferation medium and seeded into 75 cm^2 culture flasks precoated with rat tail collagen (RTC). On the next day, cultures were washed twice with

PBS solution, added with Ca/Mg solution and 250 nM of puromycin, to remove cell debris and non-adherent cells. Further, cells were trypsinized and cryopreserved as described for HepG2 cells (section 5.1.1).

Cryopreserved PBCECs were used for toxicity and permeability studies in accordance with published data [317]. Frozen cells were shortly (90 seconds) thawed in the water bath and transferred into a 50 mL falcon tube. A warm proliferation medium was carefully added above the thawed suspension and mixed by the slow rotation of the tube. Afterward, the suspension was centrifuged (150×g, 10 min), supernatant discarded and pellet dissolved in a warm proliferation medium. For cytotoxicity studies, 100 µL of cell suspension was placed into RTC precoated 96 well plate. For transfer studies, RTC coated Transwell® filter inserts with polycarbonate membrane for 12 well plate (1.12 cm2, 0.4 µm pore size) and CellZscope® device were used. Before placing the Transwells® with cells into CellZscope®, wells of the device were filled with 1 mL of warm proliferation medium (basolateral compartment) and the device was placed into the incubator for 3 hours to ensure a constant temperature of 37 °C. Transwell® inserts were then placed into CellZscope® device and 0.5 mL of cell suspension was carefully added into each Transwell® from glass pipette. After 48 hours, the medium was changed to a differentiation medium, containing 50 U/mL penicillin, 50 µg/mL streptomycin, 50 µg/mL gentamycin, 4.1 mM L-glutamine, and 550 nM hydrocortisone in DMEM/Ham's F12 medium. Following the medium exchange, cells were cultured for additional 48 hours to achieve complete differentiation. At the end of differentiation, the PBCEC monolayer represents barrier functions of the brain capillary endothelium. Membrane with cell layer divides the volume of the CellZscope® well into apical (upper) and basolateral (lower) compartments, corresponding to the blood-facing side of the capillary lumen (apical) and brain parenchymal (basolateral) side (Fig. 7).

For incubation, 50 µL medium was removed from each well of a 96 well plate or 250 µL from the apical compartment of each Transwell®. Medium, containing incubation substances, was added in the same amounts. During transfer experiments, 20 µL of medium from apical and 40 µL from basolateral compartments, were taken for ICP-MS measurements of total selenium content. At the end of the experiments, filters were washed twice with warm PBS and cut out from the insert frame using a sterile scalpel. If cell samples were not analyzed on the same day, they were stored in the 1.5 mL sealed microtubes under argon.

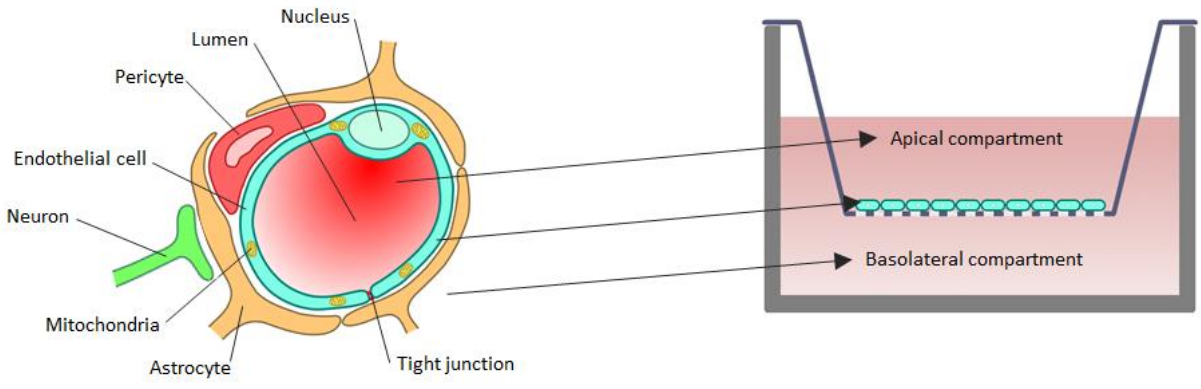

Figure 7. Representation of the used blood-brain barrier model.

To control the integrity of the PBCEC barrier during transfer experiments the CellZscope® device was used. Barrier parameters were monitored by transendothelial electrical resistance (TEER) and capacitance measurements [318]. Measurements were taken every 1.5 hours during transfer experiments. TEER and capacitance values were calculated from the impedance of the cell layer and medium between the upper electrode on the lid of the device and the bottom electrode in every well (Fig. 8). In order to measure the impedance of the cells, a small alternating current voltage (V_{AC}) is applied between the upper and bottom electrodes. During measurements V_{AC} frequency changed from 10 to 10^5 Hz, thus providing frequency-dependent impedance magnitude. Device software is mathematically subtracting constant phase element (CPE) resistance on the surface of electrodes contact and medium resistance in apical and basolateral compartments ($R_{medium\ A}$ and $R_{medium\ B}$), thereby providing TEER and capacitance values expressed from different parts of impedance spectra.

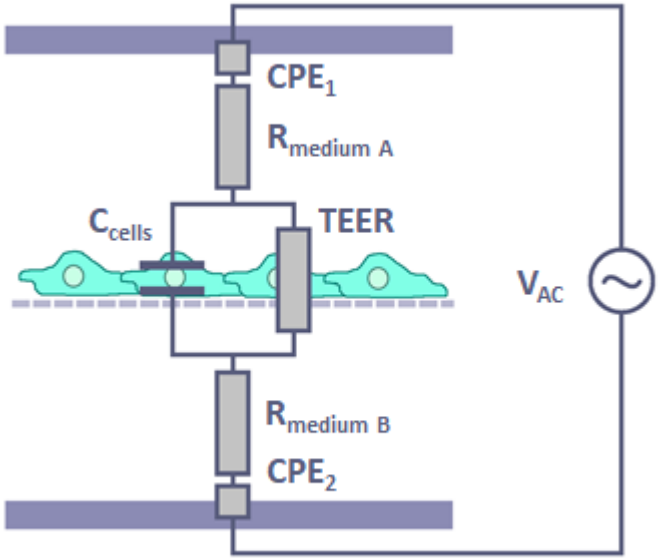

Figure 8. Schematic representation of the equivalent measuring circuit in the CellZscope® device (adapted from manufacturers technical manual).

TEER values are proportional to the constant resistance of the cell layer, hereby correlating with the tightness of the barrier dependent on the tight junction (TJ) density [319]. Capacitance, correspondingly, represents the electrical reactance that is determined by the capacitance of upper and lower membrane layers, thus depicting cell viability.

As cutoff parameters for PBCEC barrier integrity, TEER values higher than 600 Ω·cm² and capacitance in the range between 0.45 – 0.60 µF/cm² were taken, ensuring the integrity of confluent PBCEC monolayer. Only cell layers corresponding to these parameters at the start and during experiments were taken into results.

5.1.3 Cultivation of Caco-2 cells

Caco-2 is an immortalized human epithelial cell line, originally derived from colorectal adenocarcinoma. The most advantageous property of Caco-2 cells is their ability to spontaneously differentiate into a monolayer, representing many properties of intestinal

enterocytes with microvilli similar to those found in the small intestine. In the process of layer formation, Caco-2 cells start to polarize and acquire apical brush structure with microvilli. Caco-2 is one of the most well-described and frequently used cell lines in laboratory studies [320]. This model is often used for drug permeability screenings as well as metabolic studies [321], and shows a good correlation with drug absorption in human jejunum [322], especially for passive diffusion [323].

Caco-2 cells were obtained from the European Collection of Cell Cultures (ECACC 86010202, Salisbury, UK). Cultivation medium for Caco-2 was identical to those for HepG2 cells (section 5.1.1): MEM with 10% (v/v) FCS, 100 U/mL penicillin, 100 µg/mL streptomycin and 1% (v/v) of non-essential amino acids solution. Cryopreserved cells were thawed and seeded into the filter screw cap flasks in the same way as HepG2 cells. For all experiments, cells were seeded at $5 \cdot 10^4$ cells per cm^2 density. After defreezing at the initial passage number 53, cells were cultivated in the flasks for four days and then subcultured three times every two days to achieve a stable phenotype and a sufficient amount of cells. Prior to experiments, cells were cultivated for 11 days until complete differentiation was reached and taken into experiments on DIV 11 with passage number 56. The culture medium was changed every 2-3 days during proliferation and differentiation stages.

5.2 Cytotoxicity testing

Prior to conducting any cell culture experiments, the toxicity of applied compounds was assessed by at least two different endpoints.

5.2.1 Lysosomal integrity

Lysosomes are dynamic organelles in eukaryotic cells and act as a main catabolic center, where macromolecules are degraded by phagocytosis or autophagy [324]. Therefore, lysosomes perform energy supply functions and act as a cellular recycling center. They are also involved in processes of maintenance of cellular homeostasis. Functions and stability of lysosomes rely on specific ATPase, which pumps protons inside lysosomes at the expense of ATP energy. Loss of lysosomal membrane integrity often occurs during cell death and expulsion of lysosomal content into the cytoplasm is known to cause “lysosomal cell death” [325].

In the current work, lysosomal integrity was assessed by Neutral red staining. Neutral red is a phenazine stain, which is used as a vital stain. It is able to penetrate cellular membranes and accumulates in the lysosomes of viable cells. The ability of lysosomes to accumulate neutral red is dependent on their pH gradient. At the physiological pH, neutral red is presented as a neutral molecule and can be taken up by the cells. As soon as neutral red enters lysosomes it receives a positive charge due to the lower pH in the lysosomes and stays retained inside [326]. Therefore, only viable cells are able to maintain neutral red uptake, and the amount of dye, accumulated in the cell layer, reflects their viability. Since selenium compounds are known to induce oxidative

stress, lysosomal integrity was chosen as a viability marker, because lysosomes are highly sensitive to RONS exposure [327, 328].

For this assay, cells were seeded in 96 well plates. Neutral red stock solution (1 g/L) was prepared in deionized water and filtered in sterile conditions through a 0.45 µm filter in order to remove residual dye crystals and ensure solution sterility. After incubation with studied compounds, the medium was discarded and cells were washed once with a warm medium to remove leftovers of incubated compounds. For the dye loading, the stock solution was diluted at 1:12.5 for HepG2 and Caco-2 cells, and 1:5 for PBCECs with a warm culture medium. Cells were incubated with dye solution for 3 hours in the incubator. After stain uptake, cells were promptly washed with 100 µL of 0.5% formaldehyde solution in PBS-UVC. The dye retained in the cell lysosomes was extracted using 100 µL of acidified (1% v/v acetic acid) ethanol-PBS mixture (50/50 v/v), which was loaded for 10 minutes and kept at 37 °C. After incubation, plates were gently shaken to equally distribute the stain in solution, and absorbance was measured with a microplate reader at 540 nm wavelength. Obtained absorbance values were related to control cells and expressed as a percent of viable cells.

5.2.2 Dehydrogenase activity

Nicotine adenine nucleotide (NADH) and nicotinamide adenine dinucleotide phosphate (NADPH) are central units in metabolism, involved in redox reactions and electron transfer. They serve as electron donors for intracellular dehydrogenases, which oxidize organic substrates.

Resazurin is a phenoxazine dye, which can be converted by mitochondrial diaphorase in the presence of NADPH during aerobic cellular respiration [329]. Reduction of resazurin results in the formation of pink-colored resorufin (Fig. 9), which exhibits strong fluorescence and indicates the metabolic activity of cells. Due to the differences in absorbance spectra of resazurin and resorufin, the only reduced form can be detected by its fluorescence.

At the end of incubation, HepG2 cells seeded in 96 well plates were washed with warm medium and 100 µL of 1:100 diluted stock solution of resazurin (2.5 g/L) was applied. After three hours in incubator fluorescence of resorufin was measured at 590 nm wavelength (excitation at 540 nm). Obtained fluorescence values were related to control values and expressed as a percent of viability.

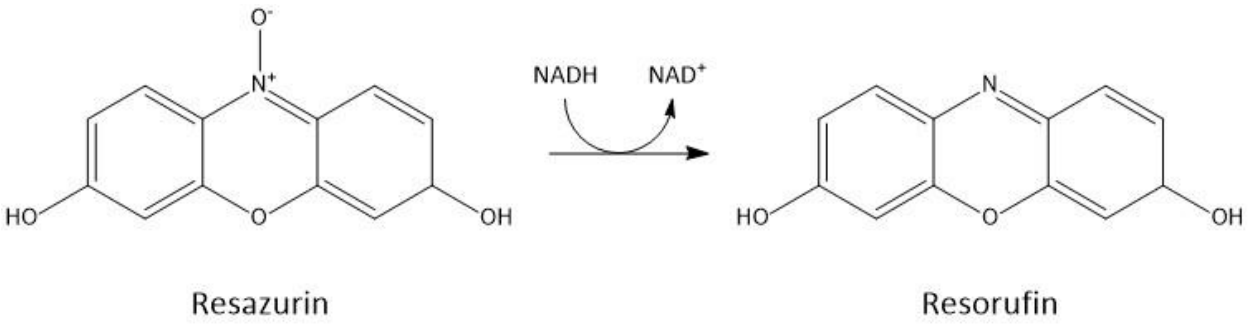

Figure 9. Reduction of resazurin to its analytical form resorufin (adapted from wikipedia.org).

To assess dehydrogenase activity in PBCECs, cell counting kit 8 (CCK-8) was used due to its higher sensitivity in comparison with resazurin. CCK-8 kit contains WST-8 dye (2-(2-methoxy-4-nitrophenyl)-3-(4-nitrophenyl)-5-(2,4-disulfophenyl)-2H-tetrazolium monosodium salt), which is a water-soluble dye from the MTT spectrum of formazan stains. Formazan dyes are reduced in viable cells by NADH/NADPH-dependent dehydrogenases and converted to their violet form (Fig. 10). Therefore, the amount of reduced colored dye dependent on the activity of cytosolic and mitochondrial dehydrogenases and directly proportional to the number of living cells.

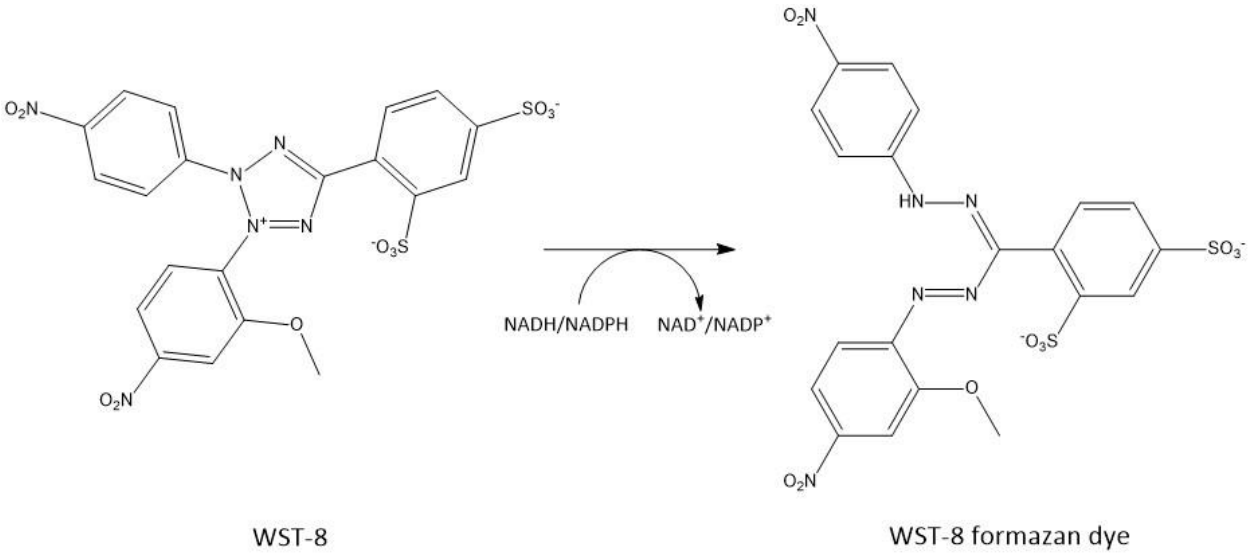

Figure 10. Reduction of WST-8 to its analytical formazan form (adapted from manufacturer's protocol).

The CCK-8 assay was carried out in accordance with the manufacturer's protocol. After incubation of PBCECs in 96 well plates with studied compounds, 10 µL of staining solution were added to each well and incubated for 1 hour. Detection of violet formazan dye was performed using a plate reader at 450 nm wavelength. For evaluation, individual measurements were related to the average absorbance of control wells.

5.2.3 Hoechst staining

Hoechst stains are bis-benzimides compounds with fluorescent properties. Hoechst 33258 stain is able to penetrate cell membranes and bind to the double-stranded DNA, thus correlating with the amount of intact cells.

After incubation of Caco-2 cells with studied compounds and *tert*-butyl hydroperoxide (TBHP) in 96 well plates, the culture medium was removed and cells were fixated with 100 µL of 3.7% (v/v) formaldehyde solution in PBS-UVC at 37 °C. After 10 minutes, a fixating solution was replaced by 100 µL of permeabilization buffer, containing 2.2% (v/v) of Triton X-100 in PBS-UVC, for 10 minutes. In the next step, permeabilization buffer was discarded and 100 µL of 6 µM Hoechst 33258 stain solution in PBS-UVC was added to each well for 30 minutes. At the end of incubation with staining solution, cells were washed using 100 µL of PBS-UVC to remove dye leftovers.

Fluorescence was measured using a microplate reader (excitation – 355 nm, emission – 460 nm). For calculations, fluorescence intensities of incubated wells were related to the untreated controls.

5.3 Protein content determination

Protein content in the cell lysates was determined by the Bradford protein assay. It is based on the spectral absorbance shift of the Coomassie Brilliant Blue R-250 dye when it binds to proteins. For quantification, bovine serum albumin (BSA) standards with concentration range 0-200 µg/mL were prepared freshly and analyzed together with samples at each plate. Samples were diluted twenty times with respective buffer and 20 µL of the diluted sample were placed into the plate in triplicates. Bradford reagent was diluted in water (two parts staining solution, seven parts water) and 180 µL of diluted stain was added to the standards and samples. Plates were incubated for 5 minutes in the darkness at room temperature. Detection of protein-bound stain was performed at 595 nm.

5.4 Assessment of cellular RONS level

5(6)-Carboxy-2',7'-dichlorodihydrofluorescein diacetate (carboxy-H2DCFDA) is a fluorescent probe, used to measure intracellular peroxides formation. After entering the cell, carboxy-H2DCFDA is hydrolyzed by intracellular esterases to carboxy-dihydrodichlorofluorescein (carboxy-H2DCF), which further undergoes oxidative cyclization with the formation of fluorescent carboxy-dichlorofluorescein (carboxy-DCF) (Fig. 11). Therefore, the intensity of DCF fluorescence is proportional to the amount of RONS presented in the cells [330, 331].

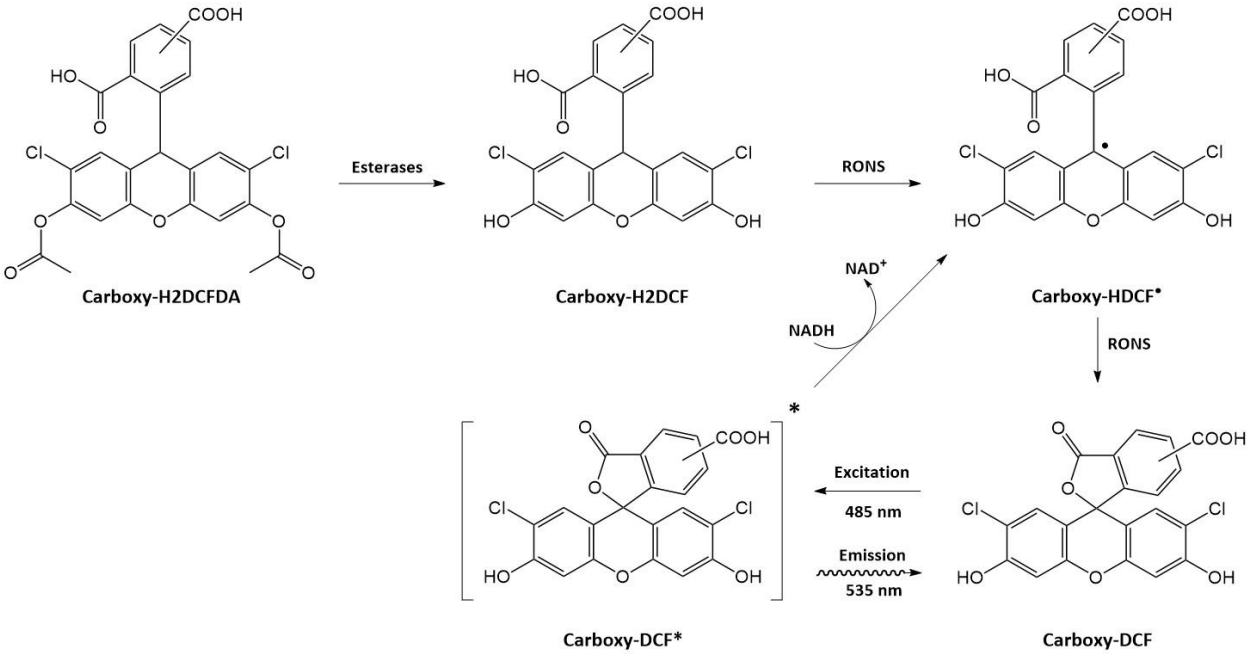

Figure 11. Transformation of carboxy-H2DCFDA and formation of DCF; adapted from [332].

To establish a protocol for carboxy-H2DCFDA assay in Caco-2 cells, different parameters like stain concentration, incubation time, TBHP concentration, and readout time were optimized. Assays were performed three times with different cell passages. The stock solution of carboxy-H2DCFDA was prepared in DMSO with 50 mM concentration. As carboxy-H2DCFDA exhibits cytotoxicity, its concentration and staining time were optimized in the first order. For this purpose, Caco-2 cells seeded in 96 well plates were washed twice with a warm culture medium and 60 µL of fresh medium containing 15, 25, or 40 µM of carboxy-H2DCFDA were applied for 10, 20, or 30 minutes. For RONS induction, pure TBHP was dissolved in deionized water to obtain a 10 mM concentration and this stock solution was then added to the culture medium. After loading with the dye, cells were washed twice and a medium containing 100 µM TBHP was applied for 3 hours for RONS generation. Fluorescence was detected by a microplate reader (excitation – 485 nm, emission – 535 nm). Obtained data demonstrate no significant increase of fluorescence after incubation with 25 and 40 µM of dye compare to 15 µM concentration (Fig. 12). Due to the toxicity of carboxy-H2DCFDA lowest concentration was chosen for assay. An increase in incubation time resulted in the very low elevation of analytical signal and the lowest incubation time (10 minutes) was selected to avoid toxic affection of the cells.

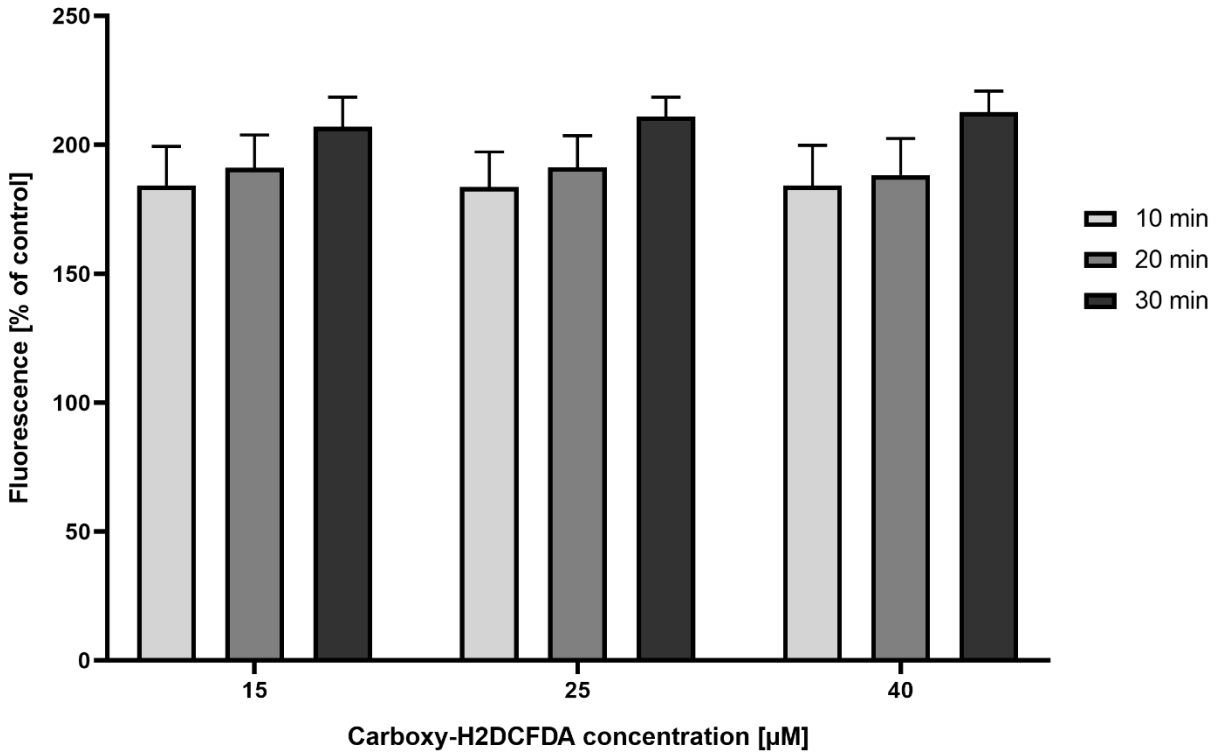

Figure 12. Optimization of DCF concentration and incubation time. Shown are mean values + SD, expressed as % of control, calculated from three independent experiments with six replicates each.

At the next step, TBHP exposure as RONS inducing stimulus was optimized. After incubation of Caco-2 cells with 15 µM dye for 10 minutes, TBHP concentrations of 25, 50, 100, and 200 µM were applied and fluorescence intensity was measured at the zero-time point and further at 0.5-5 hours. The highest TBHP concentration induced the strongest fluorescence response (Fig. 13). However, microscopic evaluation of cells after incubation with 200 µM TBHP showed the

appearance of shrunken cells already after 1 hour. Therefore, 100 µM concentration was selected as optimal, which provides sufficient signal increase compared to control (200%), while not affecting them. Incubation longer than 1 hour does not provide any additional signal enhancement. Thereby, 100 µM concentration of TBHP was incubated for 1 hour in all further experiments.

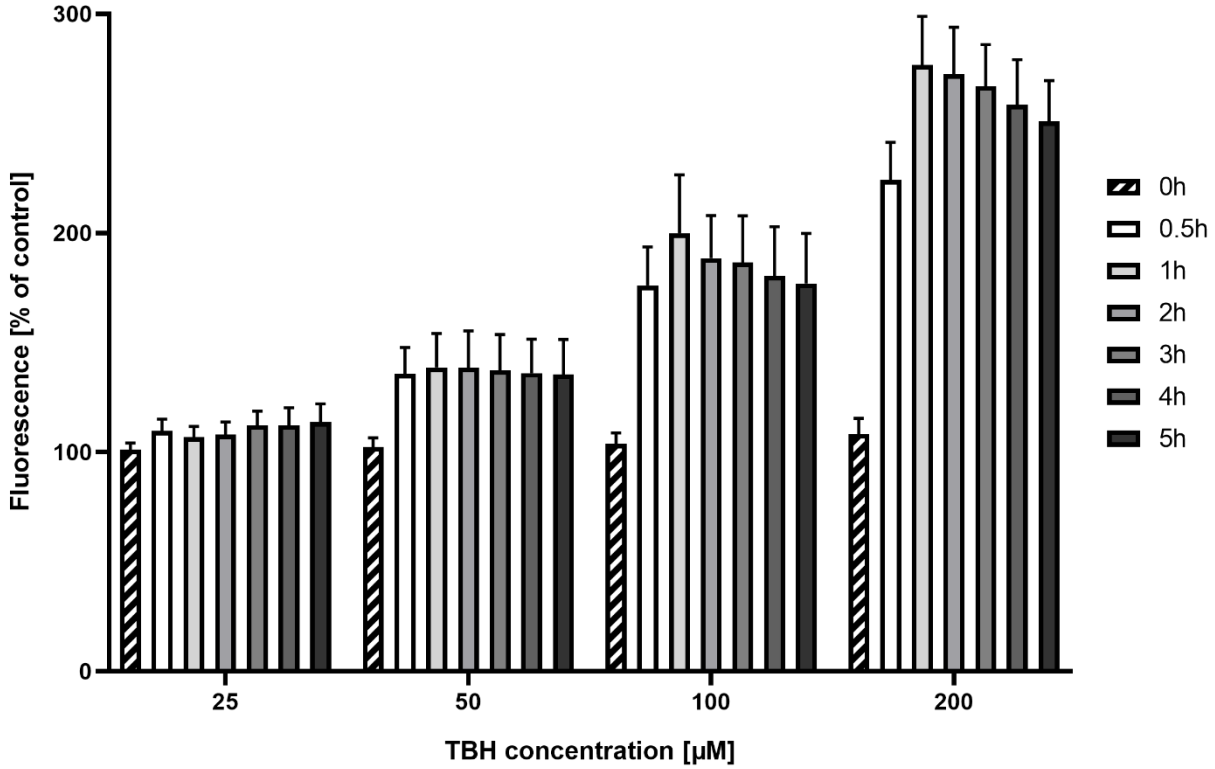

Figure 13. Optimization of TBHP load and readout time. Shown are mean values + SD, expressed as % of control, calculated from three independent experiments with six replicates each.

Summing up the optimized parameters, further assays were conducted with 15 µM carboxy-H2DCFDA incubated for 10 minutes, followed by RONS induction with 100 µM TBHP applied for 1 hour. As different cell passages exhibit slight differences in fluorescence intensities, data from conducted tests were normalized to positive control cells (incubated with TBHP only) and expressed as a percent of positive control.

5.5 Assessment of GPx activity

Intracellular GPx activity in Caco-2 cells was measured according to the protocol of Weydert and Cullen [333]. This assay is based on the indirect measurements of GPx activity, which is detected by the speed of the NADPH consumption. GPx acts in conjugation with GSH, glutathione reductase (GR), and hydrogen peroxide as a source of radicals (Fig. 14). When hydrogen peroxide is added to the reaction mixture it induces action of GPx and oxidation of GSH to GSSG.

Subsequently, GSSG is reduced back to GSH by GR in the presence of NADPH. Therefore, the speed of NADPH consumption is dependent on the speed of GSH oxidation, which correlates with GPx activity in the mixture.

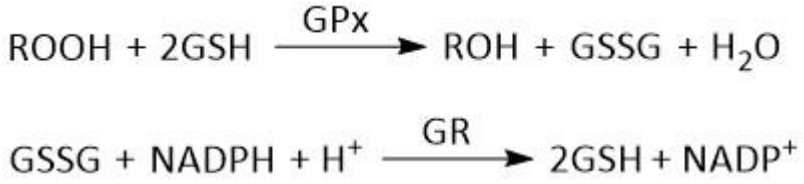

Figure 14. GPx assay principle; adapted from [333].

Caco-2 cells were seeded in 6 well plates (9.026 cm^2) for GPx measurements. After cell differentiation and incubation with studied compounds, cells were washed twice with warm PBS and covered with 0.5 mL of warm trypsin solution (0.25 %) in PBS-EDTA for 30 seconds. Trypsinization was continued for 3 minutes in the incubator and cells were collected in 2 ml of fresh medium. Obtained cell suspensions were centrifuged (250×g RCF, 3 min, 4 °C) and the supernatant aspirated. Cell pellets were resuspended in 1 ml of ice-cold PBS and transferred to 1.5 mL screw-cap tubes for bead mill homogenizer. Cells were precipitated again and 250 µL of freshly prepared homogenization buffer (100 mM Tris, 300 mM KCl, 0.1% (v/v) Triton X-100, 0.1% (v/v) protease inhibitor cocktail set III) were added to the pellet together with 15 ceramic beads (ZrO_2, 0.5 mm diameter). To avoid overheating during homogenization, samples were shaken twice for 20 seconds at 7 m/s speed. Between cycles, samples were cooled in ice for 2 minutes. Homogenized samples were centrifuged (15000×g RCF, 10 min, 4 °C) and kept on ice. Supernatant samples (20 µL) were taken for protein content analysis (section 5.3).

The assay was conducted in the 96 well plates. Plates and solutions were kept on ice during preparation to avoid the reduction of GPx activity. Each sample was placed in at least six wells to obtain a reliable mean value. For control samples, 17.5 µL of cell homogenate and 5 µL for treated samples were placed in the wells. Homogenization buffer was added to the 5 µL of sample to obtain 17.5 µL of total volume. Blank wells were filled with 17.5 µL of homogenization buffer only. Directly prior to analysis, reaction mixture was prepared, containing 96 mM Tris, 4.8 mM EDTA, 0.96 mM NaN_3, 0.1% (v/v) Triton X-100, 0.22 mM NADPH, 13 mM $NaHCO_3$, 3.4 mM GSH, 1.1 nM HCl, 0.66 U/mL GR and 18 mM $(NH_4)_2SO_4$. The reaction mixture (222.5 µL) was added to the cell homogenates and the plate was placed into the plate reader. Prior to the start of the analysis, the plate was pre-warmed in the thermoregulated compartment of the reader for 10 minutes at 37 °C. After the plate reaches a temperature of 37 °C, 10 µL of 0.00375% (v/v) H_2O_2 was added to each well by an automatic reagent injector system connected with the plate reader. The addition of H_2O_2 initiates GPx activity and reaction cycle showed in Figure 14. From this moment, NADPH concentration was reducing and NADPH absorbance was measured at 340 nm wavelength. Measurements were taken every 30 seconds to obtain enough points for reliable linear regression.

Obtained data was firstly evaluated for each well. Outliers were excluded and linear regression was made for the remaining points. If more than three outliers were found for the well or R^2 less

than 0.9 was obtained this well was excluded from evaluation. The absolute value of the regression slope is presenting the NADPH consumption rate and was used as an analytical signal. Slope values were averaged for blank wells and subtracted from control and treated samples. In the cases when slope values of control samples were lower than blank values, they were also excluded. Consistent slope values were then averaged and absolute activity of GPx in cell homogenate calculated. Absolute GPx activity was normalized to the protein content in the homogenate. Obtained values were further related to control samples and expressed as a percent of GPx activity in untreated cells.

Formula 1 – Calculation of GPx activity in cell lysates.

$$GPx\ activity = \frac{\frac{A_{sample\ end} - A_{sample\ start}}{t} - \frac{A_{blank\ end} - A_{blank\ start}}{t}}{\varepsilon_{NADPH} \times d \times c_{protein}} \times F_1 \times F_2$$

$A_{sample\ end}$: absorbance of the sample at the end of the measurement
$A_{sample\ start}$: absorbance of the sample at the start of the measurement
$A_{blank\ end}$: absorbance of the blank at the end of the measurement
$A_{blank\ start}$: absorbance of the blank at the start of the measurement
t: time corresponding to the linear regression range
F_1 : dilution factor of the lysate
F_2 : dilution factor of the diluted (F_1) lysate in the total reaction volume
ε_{NADPH} : molar extinction coefficient of NADPH (6.22 mL/µmol×cm)
d: the thickness of solution layer in the well
$c_{protein}$: protein concentration in the cell lysate

5.6 Sample preparation for ICP-MS and HPLC-ICP-MS measurements

HepG2 and Caco-2 cells were seeded in 6 well plates. Medium samples were placed into 1.5 mL microtubes and stored in the freezer (-20 °C). After incubation for 72 hours with studied compounds, cells were washed two times with 2 mL of warm PBS (37 °C) and 0.5 mL of 0.25% trypsin solution in PBS-EDTA were added for 30 seconds. Trypsin was then aspirated and plates incubated for 3 minutes at 37 °C. Cells were detached with 2 mL of ice-cold PBS-UVC with 5% (v/v) FCS. Cell suspensions were kept on ice during all following steps. In the case of HepG2, cells 50 µL of cell suspension were taken for determination of cell number and cell volume by Casy-TTC® automatic cell counter (section 5.1.1). In the case of Caco-2 cells, 20 µL of cell suspension were taken for protein content analysis, as described in section 5.3. The cell suspension was centrifuged (280×g RCF, 5 min, 4 °C) and the supernatant was discarded. To remove non-covalently bound selenium compounds from the cell surface, cell pellets were resuspended in 1 mL of ice-cold PBS, transferred into 1.5 mL microtubes, centrifuged (2200×g RCF, 5 min, 4 °C) and the supernatant discarded. Obtained cell pellets were stored in the freezer (-20 °C). The procedure of PBCEC sample collection is described in section 5.1.2.

For total selenium quantification, HepG2 and Caco-2 cell pellets were digested using a closed vessel microwave digestion system. Cell pellets were resuspended in 500 µL of deionized water and transferred quantitatively into 20 mL polyethylene digestion vessels. Storage tubes were then washed with 425 µL of deionized water in order to collect all remaining cells and this water was also transferred to the digestion vessel. At the next step, 500 µL of concentrated nitric acid, as well as 75 µL of 100 µg/L solution of ^{77}Se isotope enriched selenite were added to the vessel. Isotope spike was used both for isotope dilution measurements and as an internal standard to control possible losses during sample preparation and ionization interferences. Loaded vessels were closed using a dynamometric wrench and placed into MARS 6 microwave digestion system. Samples were heated to 220 °C for 15 minutes at 650 W power and the temperature was hold for 20 minutes. After cooling to a temperature lower than 50 °C vessels were taken out and the inner cap and walls of the vessel were washed with two 463 µL portions of deionized water to transfer all droplets to the solution. Digestates were transferred to the 15 mL falcon tubes and stored at 4 °C until the day of analysis. Directly before measurements, 75 µL of isopropanol were added to the digestates for carbon enhancement of ionization in plasma. The resulting volume of the sample was 2.5 mL, thus giving a 3 µg/L concentration of ^{77}Se isotope spike, 20% (v/v) content of nitric acid, and 3% (v/v) of isopropanol.

PBCEC cell layers on the filters were lysed in RIPA buffer, containing 10 mM Tris, 150 mM NaCl, 1 mM EDTA, 1% (v/v) Triton X-100, 1% (v/v) sodium deoxycholate and 0.1% (v/v) SDS. RIPA buffer was prepared freshly each time and cooled down to 4 °C prior to use. Filters in 1.5 mL microtubes were covered with 200 µL of RIPA buffer and thoroughly vortexed. Then tubes were centrifuged shortly to shift all filters to the tube bottom and keep them fully covered with buffer. Samples were incubated for 15 minutes at 4 °C and then centrifuged (10000×g RCF, 20 min, 4 °C). Supernatant aliquots (10 µL) were taken for protein content analysis (section 5.3). The rest of the supernatant was transferred to the new tube and stored at -20 °C. Prior to analysis, 180 µL of cell lysate was diluted 1:5 by mixing with 648 µL of deionized water, 18 µL concentrated nitric acid, 27 µL of 100 µg/L solutions of ^{77}Se isotope spike, and 27 µL isopropanol. The resulting volume of the sample was 900 µL and contained 3 µg/L of ^{77}Se, 2% (v/v) nitric acid, and 3% (v/v) isopropanol.

Medium samples from transfer experiments were diluted 35 times and contained 3 µg/L of ^{77}Se, 2% (v/v) nitric acid and 3% (v/v) isopropanol. Samples were diluted 35 times since apical medium samples had only 20 µL volume and 700 µL is a minimal required volume for a single selenium measurement.

PBCEC medium and cell lysate samples from transfer experiments were also sent to the University of Graz on dry ice and stored at -80 °C before analysis. Samples were centrifuged (21000×g RCF, 10 min, 4 °C) and diluted with deionized water or used undiluted.

Calibration standards with 0.1, 0.5, 1, 5, 10 and 20 µg/L were prepared from 10 mg/L Se stock solution through serial dilutions. As in samples, 3 µg/L of ^{77}Se, 2% (v/v) nitric acid and 3% (v/v) isopropanol were added to calibration standards. For reverse standardization of isotope dilution set of standards including 5 µg/L of natural selenium (^{nat}Se), 5 µg/L of ^{77}Se and 5 µg/L of 1:1 ^{nat}Se and ^{77}Se mixture were prepared in 2% (v/v) nitric acid with addition of 3% (v/v) isopropanol. Two

calibration approaches were used for measurement quality control. However, due to the higher sensitivity of the isotope dilution approach, it was used for all total Se calculations.

Medium samples from Caco-2 cells for SelenoP speciation were frozen (-20 °C) and used undiluted. Calibration of SelenoP measurements was performed by the set of SeMet standards with concentrations 0.1, 1, 5, 10, and 50 µg Se/L.

5.7 Total selenium quantification by ICP-MS

For over twenty years, inductively coupled plasma mass spectrometry (ICP-MS) has been the primary method for the determination of metals and metalloids, such as selenium, arsenic, or antimony, in all types of biological matrices [334-336]. High sensitivity and selectivity of ICP-MS based on the fundamental property of all atoms as a charge-to-mass ratio. This provides the widest dynamic range (up to nine orders of magnitude), possibility of simultaneous multi-element detection, and determination of different isotopes of the same element [337]. In ICP-MS, samples are introduced to the plasma torch, working on three coaxial argon flows, where the central channel is used for sample introduction and two others for maintenance of plasma argon supply. Plasma is generated by a high-frequency magnetic field, provided by an inductor coil placed around the torch, which accelerates electrons from ignition spark and ionizes argon atoms. Samples must be introduced as gas or finely dispersed solid or liquid particles to ensure full ionization in plasma. In the case of liquid samples, different nebulizers and spray chambers are used for the generation of sample aerosol. When particles enter the plasma they evaporate, molecules transferred by them break apart and constituent atoms ionized. Ions further transferred to the inner vacuumed space of the instrument through sampling and skimmer cones by extraction lens. Transferred ions are then focused into an ion-beam by electromagnetic optics. When ions forming this ion beam passing through electrostatic or magnetic sectors they are deflected at different angles, depending on their charge-to-mass ratios. Detection of ions is performed by Faraday cups or secondary electron multipliers. As different elements can have overlapping isotope masses and argon plasma mostly consist of Ar^+ ions, a variety of spectral interferences occur from isobaric isotopes or dimer ions, mostly formed by conjugation with Ar^+ ions and having close masses. However, these interferences can be overcome by an increase of mass-analyzer resolution (as in sector field instruments) or employment of reaction cells, where undesirable dimeric ions can be destroyed and target analytes modified with atoms like oxygen or nitrogen and detected as a dimer at the new mass free of interferences. This is of special concern for selenium because the most abundant selenium isotopes ^{80}Se and ^{78}Se are heavily affected by $^{40}Ar^{40}Ar^+$ and $^{40}Ar^{38}Ar^+$ ions, which are formed in argon plasma to a greater extend.

Agilent 8800 triple quadrupole ICP-MS was utilized for selenium content determination. The instrument was operated in reaction mode with 0.4 mL/min O_2 and 1 mL/min H_2 flows. Hydrogen was used to reduce the formation of different argon-element dimers. Oxygen was applied to perform a mass shift of selenium from ^{78}Se and ^{80}Se masses, affected by argon interference, to $^{78}Se^{16}O^+$ and $^{80}Se^{16}O^+$ masses. Parameters for selenium detection are presented in Table 1.

Table 1 – ICP-MS operating parameters for selenium quantification.

Nebulizer	MicroMist™, Meinhard type glass concentric nebulizer
Spray chamber	Scott type, quartz
Temperature of the spray chamber	2 °C, controlled by Peltier-element housing
Sampling and skimmer cones	Nickel
RF generator power	1550 W
Reflected power	< 5 W
Extraction lens voltage	5.0 V
Plasma gas flow	15.0 L/min
Auxiliary gas flow	0.90 L/min
Nebulizer gas flow	1.05 L/min
O_2 flow in reaction cell	0.40 L/min
H_2 flow in reaction cell	1.00 L/min
Detected masses	*m/z* $^{80}Se^+ \rightarrow {}^{96}SeO^+$
	m/z $^{78}Se^+ \rightarrow {}^{94}SeO^+$
	m/z $^{77}Se^+ \rightarrow {}^{93}SeO^+$
	m/z $^{80}Se^+ \rightarrow {}^{80}Se^+$
	m/z $^{78}Se^+ \rightarrow {}^{78}Se^+$
	m/z $^{77}Se^+ \rightarrow {}^{77}Se^+$
Integration time	0.100 s
Pump speed	0.33 mL/min (6 rpm)

Data was exported from instrument software in form of intensities and calculations were performed manually by isotope dilution approach. Concentration calculations by isotope dilution were adapted from the work of Rodríguez-González et al. [338]. The basic concept of the isotope dilution method is based on the measurement of isotope ratios in the sample where the isotopic composition was altered by the addition of isotope enriched spiking solution (Fig. 15). Thus, measurements of isotopic distribution in the spiked sample and a known amount of added isotopic spike allow calculating initial amount of target isotope in the sample before spiking. Since this method requires only isotope ratios and known natural isotopic distributions, it does not

require external calibration. Due to this fact isotope dilution method is less affected by sample matrix composition and exhibits higher sensitivity, compared to conventional calibration [339].

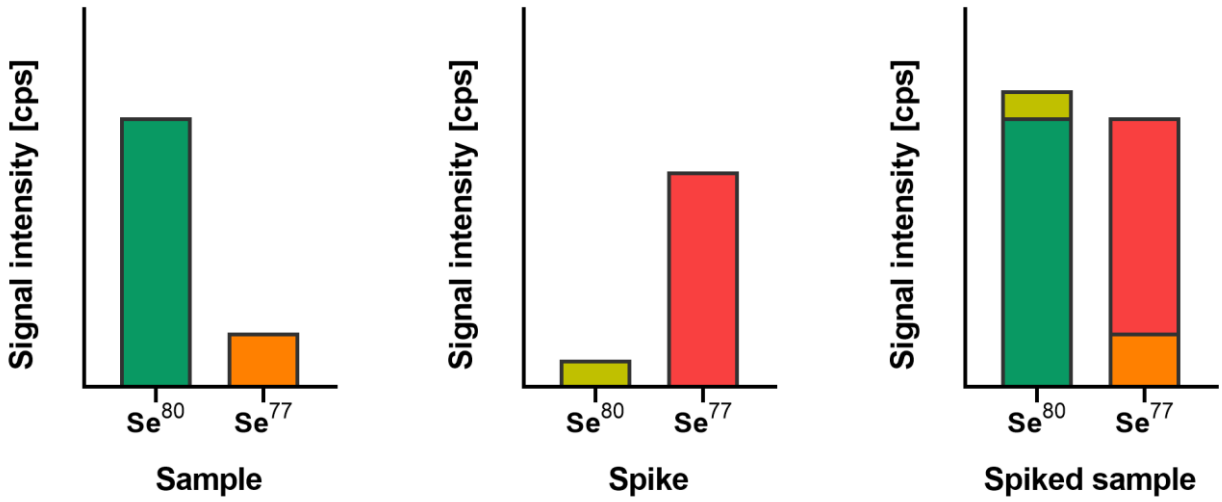

Figure 15. Principle of isotope dilution-based ISP-MS measurements.

In the simplest case, when pure isotope can be added to the sample, calculations are very simple and do not require prerequisite steps. However, usually isotope enriched mixtures do not consist of a single isotope. Therefore, a double dilution procedure is utilized, where initial standardization of spiking solution is required. The first step includes reverse isotope dilution measurements, where the isotope composition of enriched mixture is determined from the set of standards. They should include pure spiking solution, standard with natural isotopic composition, and their mixture with known ratio. Calculations are performed by Formula 2 in accordance with the work of Rodríguez-González et al [338].

Formula 2 – Reverse calculation of ^{77}Se concentration in isotope spiking solution. Adapted from [338].

$$c\,{}^{77}Se_{spike} = c\,{}^{77}Se_{natural} \times \frac{A\,{}^{77}Se_{natural}}{A\,{}^{77}Se_{spike}} \times \times \frac{I\,{}^{80}Se_{natural} / I\,{}^{77}Se_{natural} - I\,{}^{80}Se_{50/50\,mix} / I\,{}^{77}Se_{50/50\,mix}}{I\,{}^{80}Se_{50/50\,mix} / I\,{}^{77}Se_{50/50\,mix} - I\,{}^{80}Se_{spike} / I\,{}^{77}Se_{spike}}$$

c $^{77}Se_{spike}$: determined ^{77}Se concentration in isotope spiking solution
c $^{77}Se_{natural}$: concentration of ^{77}Se in the sample with natural isotope distribution
A $^{77}Se_{natural}$: the abundance of ^{77}Se in the sample with natural isotope distribution
A $^{77}Se_{spike}$: abundance of ^{77}Se in isotope spiking solution
I $^{80}Se_{natural}$: intensity of ^{80}Se signal in solution with natural isotope distribution
I $^{77}Se_{natural}$: intensity of ^{77}Se signal in solution with natural isotope distribution
I $^{80}Se_{spike}$: intensity of ^{80}Se signal in isotope spiking solution
I $^{77}Se_{spike}$: intensity of ^{77}Se signal in isotope spiking solution
I $^{80}Se_{50/50\ mix}$: intensity of ^{80}Se signal in an equimolar mixture of natural selenium and isotope spike

$I\ ^{77}Se_{50/50\ mix}$: intensity of ^{77}Se signal in an equimolar mixture of natural selenium and isotope spike

When amounts of spiking isotope (^{77}Se) and residual isotopes (^{80}Se, ^{78}Se) are determined, they are used for direct calculations of ^{80}Se in samples (Formula 3).

Formula 3 – Calculation of total selenium content in the sample by isotope dilution. The formula presented for calculation is based on ^{80}Se intensities; the same applies for ^{78}Se. Adapted from [338].

$$c\ Se_{total} = c\ Se_{spike} \times \frac{V_{sample}}{V_{spike}} \times \frac{M\ Se_{natural}}{M\ Se_{spike}} \times \frac{A\ ^{77}Se_{sample}}{A\ ^{80}Se_{sample}} \times \times \frac{I\ ^{80}Se_{sample} / I\ ^{77}Se_{sample} - I\ ^{80}Se_{spike} / I\ ^{77}Se_{spike}}{1 - I\ ^{80}Se_{sample} / I\ ^{77}Se_{sample} \times I\ ^{80}Se_{natural} / I\ ^{77}Se_{natural}}$$

$c\ Se_{total}$: determined total selenium concentration in the sample
$c\ Se_{spike}$: total selenium concentration in isotope spiking solution
V_{sample} : volume of sample solution
V_{spike} : volume of isotope spiking solution
$M\ Se_{natural}$: molar mass of natural selenium
$M\ Se_{spike}$: molar mass of selenium in isotope spiking solution
$A\ ^{77}Se_{sample}$: abundance of ^{77}Se in the sample with isotope spike
$A\ ^{80}Se_{sample}$: abundance of ^{80}Se in the sample with isotope spike
$I\ ^{80}Se_{sample}$: intensity of ^{80}Se signal in the sample with isotope spike
$I\ ^{77}Se_{sample}$: intensity of ^{77}Se signal in the sample with isotope spike
$I\ ^{80}Se_{spike}$: intensity of ^{80}Se signal in isotope spiking solution
$I\ ^{77}Se_{spike}$: intensity of ^{77}Se signal in isotope spiking solution
$I\ ^{80}Se_{natural}$: intensity of ^{80}Se signal in solution with natural isotope distribution
$I\ ^{77}Se_{natural}$: intensity of ^{77}Se signal in solution with natural isotope distribution

In the case of HepG2 cells, selenium concentration was normalized to the cell volume. For Caco-2 cells and PBCECs, data was related to the protein concentration.

5.8 Speciation studies

5.8.1 SelenoP speciation in Caco-2 medium samples

High-performance liquid chromatography (HPLC) with ICP-MS detection was used for SelenoP measurements in medium samples of Caco-2 cells. Element-specific detection was performed with the same instrument settings as described in section 5.7. Speciation of SelenoP was

performed with 1 mL HiTrap Heparin HP column. Parameters of chromatographic separation are provided in Table 2.

Table 2 – Chromatographic conditions for SelenoP speciation.

Column	1 mL HiTrap Heparin HP
Injection volume	100 µL
Flow rate	1.0 mL/min
Mobile phases	A: 0.17 M ammonium acetate, 10 µg/L Ge, 2% (v/v) ethanol, pH 7
	B: 1.30 M ammonium acetate, 10 µg/L Ge, 2% (v/v) ethanol, pH 7
Elution program	0.0 – 1.0 min: 100% A 1.0 – 4.5 min: 100% B
	4.5 – 5.5 min: 100% A

Quantification of HPLC-ICP-MS measurements was performed by external calibration with SeMet standards. Due to the low matrix content in the post-column eluent, measurements were not performed by isotope dilution. Germanium was used in buffers as the internal standard for the correction of ionization interferences.

5.8.2 Speciation of selenium compounds in PBCEC samples

Mass spectrometry with electrospray ionization (ESI) and Orbitrap mass-analyzer was used together with HPLC separation at the University of Graz for detection of unknown selenium species in PBCEC medium and cell lysate after incubation with SeN. Chromatographic conditions are provided in Table 3. Obtained mass spectra were used to determine possible structures of detected species.

Table 3 – Chromatographic conditions for detection of selenium species by HPLC-ESI-Orbitrap-MS.

Column	Dionex IonPac™ AS14 (5 µM; 3 × 150 mm)
Column temperature	30 °C
Injection volume	10 µL
Flow rate	0.5 mL/min
Mobile phase	5 mM ammonium malonate, pH 9.5
Elution mode	Isocratic

Quantitative measurements of selenium species were performed at the University of Graz by HPLC-ICP-MS with parameters provided in Table 4.

Table 4 – Chromatographic conditions for HPLC-ICP-MS measurements of PBCEC samples.

Column	Atlantis® dC18 (5 µM; 4.6 x 150 mm)
Column temperature	30 °C
Injection volume	10 µL
Flow rate	1.0 mL/min
Mobile phase	20 mM ammonium formate, 3% (v/v) methanol, pH 3.0
Elution mode	Isocratic

6. Results and discussion

6.1 Toxicity and uptake studies in HepG2 cells

Investigation of the properties of SeN started with the assessment of its toxicity in the HepG2 cell line. This immortalized cell line, derived from hepatocellular adenocarcinoma, is a valuable tool for the assessment of toxic and metabolic properties of Se compounds [167, 340-342]. Studies in hepatocytes are an important part of Se compounds' investigation since the liver plays one of the central roles in Se metabolism (see section 3.1.4) [343]. Neutral red staining was chosen as a viability marker since it allows the assessment the lysosomal condition (detailed description in section 5.2.1). Lysosomes are known to be affected during Se-induced toxicity [344, 345] and serve as a sensitive endpoint for toxicological evaluation [346]. Resazurin staining was used as a second viability test for confirmation of the neutral red results. This assay is based on the conversion of resazurin into fluorescent resorufin by intracellular dehydrogenases (detailed description in section 5.2.2). The resazurin assay was demonstrated to be an effective and reliable method for cytotoxicity screening of Se species [347].

For comparison of SeN effects, the two reference Se compounds selenite and MeSeCys were incubated in the same manner for 48 hours. Selenium compounds were incubated at the following concentration ranges: selenite, 0.7 – 33 µM; MeSeCys, 50 – 400 µM; and SeN in dimer form, 1 – 100 µM. Even though physiological total Se concentrations in plasma are only a few micromoles, toxic concentrations are in the higher range and therefore, applied concentrations should induce observable toxic effects. Results of neutral red and resazurin cytotoxicity tests are presented in Figures 16 and 17, respectively. Effective concentrations of applied Se species are listed in Table 5. The concentration at which the viability of the cells was reduced by 30% compared to control is marked as EC30. The half-maximal inhibitory concentration (IC50) was determined as the concentration point where the viability of treated cells represents 50% of those of control.

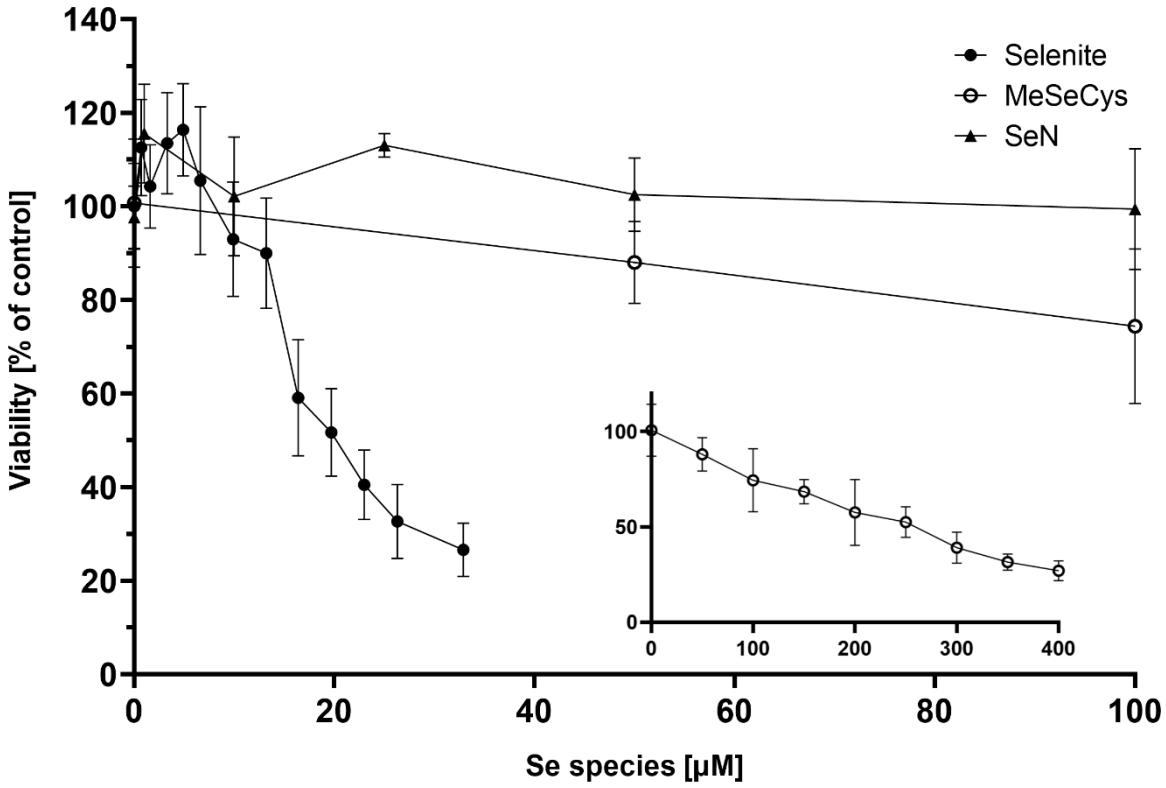

Figure 16. HepG2 cell viability after 48-hour incubation with Se species determined by neutral red uptake assay. The inner graph corresponds to the full concentration range of MeSeCys incubation. Shown are mean values ± SD of 3 independent experiments with six replicates each for selenite and MeSeCys, and three replicates for SeN.

Obtained data for selenite show good accordance with earlier published data [348, 349], where IC50 in HepG2 was found to be around 15 µM. While IC50 obtained in the neutral red assay was 20.2 µM, the resazurin assay showed a lower value of 15.9 (Table 5). However, since these assays are based on different metabolic activities, such a difference was expected and a comparison of neutral red and resazurin assay data shows that dehydrogenase activity in HepG2 cells is often affected at lower concentrations [350, 351]. Similar curve shapes for selenite in Figures 16 and 17 also indicate that both assays show a similar dose-dependence. The lowest values of toxic concentrations for selenite are in good accordance with the well-known fact that selenite is one of the most toxic Se species [352]. It is noteworthy that selenite at doses of few micromolar on the contrary slightly increased the number of cells, which could be seen in both assays (Fig. 16 and 17). This is a typical picture of a dose-response curve for essential micronutrients. In contrast to selenite, incubation with MeSeCys decreased the viability of HepG2 cells at much higher concentrations. The lower toxicity of MeSeCys and other organic Se compounds compared to the inorganic forms is well documented [353, 354]. This is usually attributed to the higher stability of oxidized intermediates, which are stabilized by the amino acid structure. Also, such organic Se species are less potent in interactions with peptide thiol groups due to the lower redox potential [355]. As the mechanism of MeSeCys toxicity, in particular, is not clear, another assumption is based on the different speeds of metabolic transformations. MeSeCys shows a slower rate of

conversion to methylselenol than selenite. Therefore, excessive amounts of metabolic intermediate, which can interact with thiol groups, are produced slower during incubation with organic Se species [356]. Also, as amino acid species, MeSeCys may be unspecifically incorporated into proteins, thus potentially affecting their structure, but being removed from the metabolically active pool. MeSeCys toxicity usually does not appear at concentrations present in food, however via supplementation may cause toxic effects. The LD50 of MeSeCys in mice is around 11 mg/kg bw [185]. Opposite to selenite, MeSeCys demonstrates a faster dose-response in the neutral red assay, and obtained EC30 and IC50 values differ significantly from resazurin data. This may be attributed to a much "milder" manifestation of the MeSeCys effect, which is expressed in a linear shape of dose-response. Also, compared to selenite, which should promote elevated RONS formation in mitochondria, MeSeCys does not act as pro-oxidant [357] and thus exhibit lower toxicity to mitochondrial dehydrogenases. In such a mode of toxicity, the effective concentrations tend to differ significantly, since they depict slow inhibition of certain cell functions without a sharply pronounced cell death event as in the case of selenite.

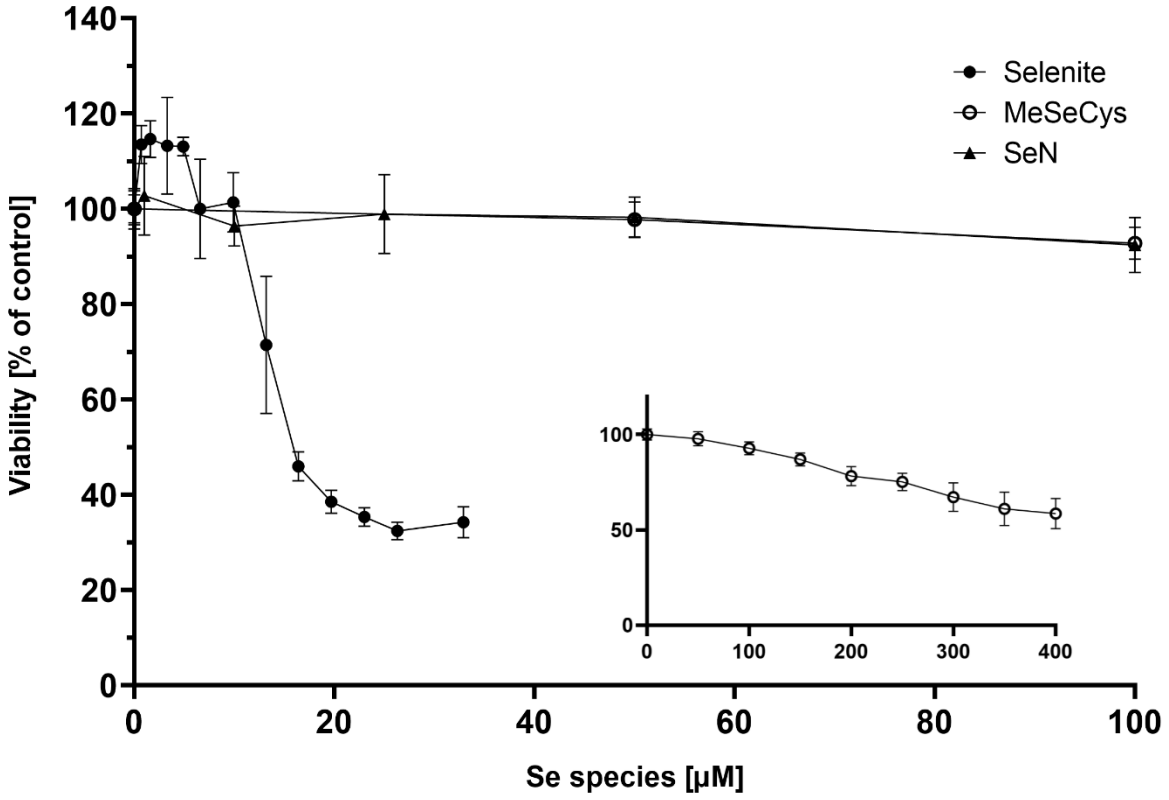

Figure 17. HepG2 cell viability after 48-hour incubation with Se species determined by resazurin assay. The inner graph corresponds to the full concentration range of MeSeCys incubation. Shown are mean values ± SD of 3 independent experiments with six replicates each for selenite and MeSeCys, and three replicates for SeN.

Data for SeN show that it is not affecting cell viability in concentrations up to 100 µM. Higher concentrations of SeN were not applied due to the tightly limited amount of SeN available for experiments. The absence of toxicity in the physiological range can be assumed from

biomonitoring studies, indicating high SeN content in the blood of fish-eating populations without the development of toxic manifestations [188, 190, 194]. Thus, the absence of observable toxic effects of SeN goes in hand with human data.

Table 5 – Effective concentrations of Se species in HepG2 cells assessed by neutral red and resazurin staining after 48-hour incubation.

	Neutral red		Resazurin	
	EC30 (µM)	IC50 (µM)	EC30 (µM)	IC50 (µM)
Selenite	15.2	20.2	13.3	15.9
MeSeCys	137	258	282	> 400
Selenoneine	> 100	> 100	> 100	> 100

Uptake studies for SeN were performed in the same concentration range (up to 100 µM) where it was found to be non-toxic for HepG2 cells. After 48-hour incubation, cells were collected and digested as described in section 5.6. Total Se content in cells was normalized to the cell volume and expressed in µM for easier comparison.

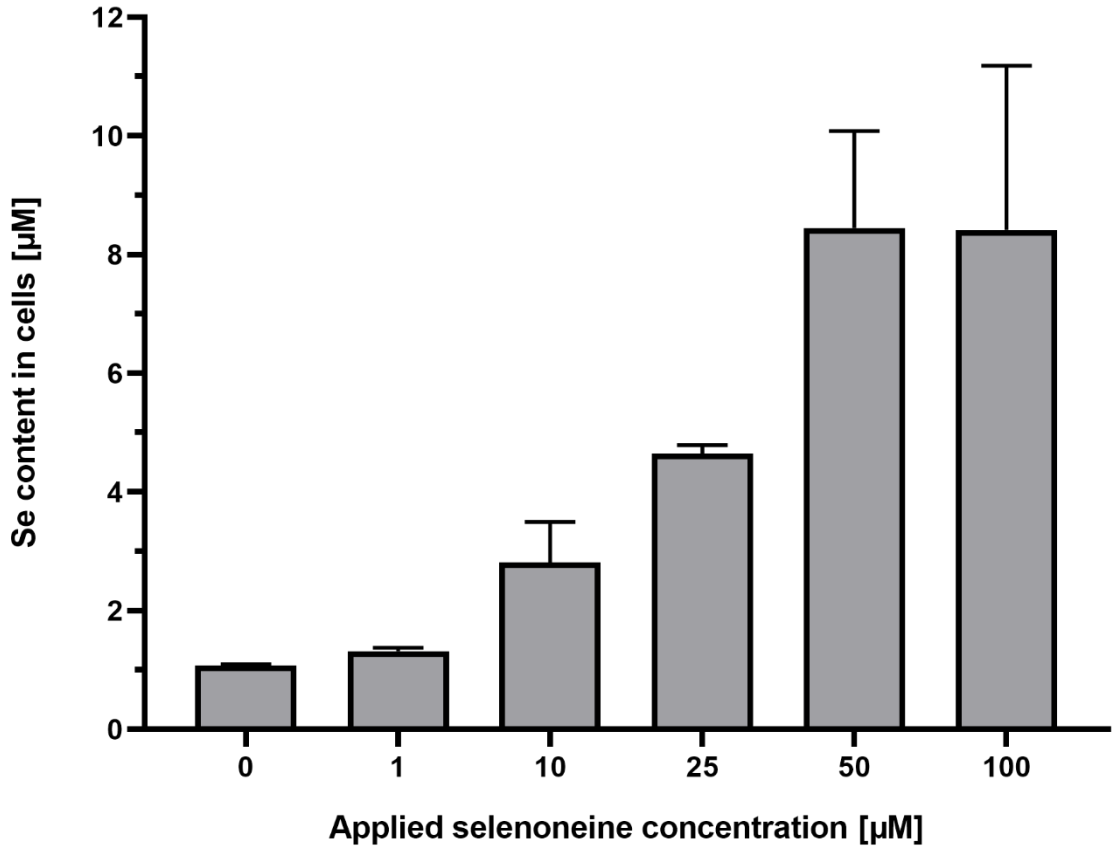

Figure 18. Cellular Se content in HepG2 cells after 48-hour incubation with SeN. Shown are the mean values of 3 independent experiments with two replicates each + SD.

Data in Figure 18 represent total Se concentrations found in cells after incubation with SeN. There is a significant linear increase with growing SeN concentration until 50 µM. Also, incubation with 100 µM resulted in an only 3-fold increase of Se content compared to 10 µM. To express the dynamics of this process, accumulation factors were calculated and are presented in Table 6.

Table 6 – Accumulation factors of HepG2 cells after 48-hour incubation given as the ratio of intracellular Se concentration (µM) to incubated SeN concentration (µM). Shown are the mean values of 3 independent experiments with two replicates each.

Incubated SeN concentration (µM)	Se concentration in the medium at the end of incubation (µM)	Accumulation factor
1	0.92	0.24
10	9.84	0.17
25	22.8	0.14
50	42.9	0.14
100	94.3	0.07

Accumulation factors were calculated as the ratio of cellular Se content to incubated concentrations. As it can be seen, the increase of SeN content in the medium is inversely correlated with accumulation factors. This indicates that SeN is not actively transported into the cells. Also, typical accumulation factors for metabolically active Se compounds are usually higher than 1 and do not decrease significantly in the lower µM range [358]. Se concentration in the medium was also measured at the end of the incubation to ensure the stability of SeN. No significant decrease of Se concentration indicates that extremely low Se uptake was not associated with the unavailability of SeN. Thus, despite the observed increase of Se content in the cell, it was most probably not associated with SeN uptake, but only with surface absorption.

6.2 *In vitro* blood-brain barrier model studies

The CNS is a subtle regulated system and requires precise maintenance of its homeostasis (for details see section 3.3.1). The BBB performs both protective and transport functions, defending the CNS from toxic agents and supplying it with essential nutrients. Therefore, the ability of chemical compounds to be transferred across the BBB or affect the barrier condition is of high importance. Regarding Se delivery to the brain, its transport through the BBB is commonly accepted to occur *via* SelenoP. However, studies with SelenoP knockout mice demonstrated that such Se species as selenosugars [292], selenite [311], and SeMet [312] may attribute to Se delivery into the brain. Correspondingly, the ability of SeN to be transferred into the brain is of high significance for the decryption of SeN properties.

6.2.1 Assessment of Se species toxicity in PBCECs

First of all, the toxicity of SeN and reference Se species (selenite, MeSeCys) was assessed in PBCECs. Cells were seeded in 96 well plates and incubated for 72 hours. Afterward, neutral red staining and CCK8 assay were performed as described in sections 5.2.1 and 5.2.2, respectively. Selenite was incubated in concentration range 0.1 – 100 µM, MeSeCys 1 – 400 µM, and SeN 10 – 100 µM. As it was described for HepG2 cells, neutral red staining provides information about the lysosomal condition, which can be affected by Se compounds. As a second endpoint, mitochondrial activity was assessed using the CCK8 kit, which is based on a standard formazan assay with WST-8 dye. Mitochondrial activity is known to be dependent on Se supply and affected under Se overexposure [359, 360]. Therefore, mitochondrial activity represents a valuable toxicological endpoint for the assessment of Se toxicity.

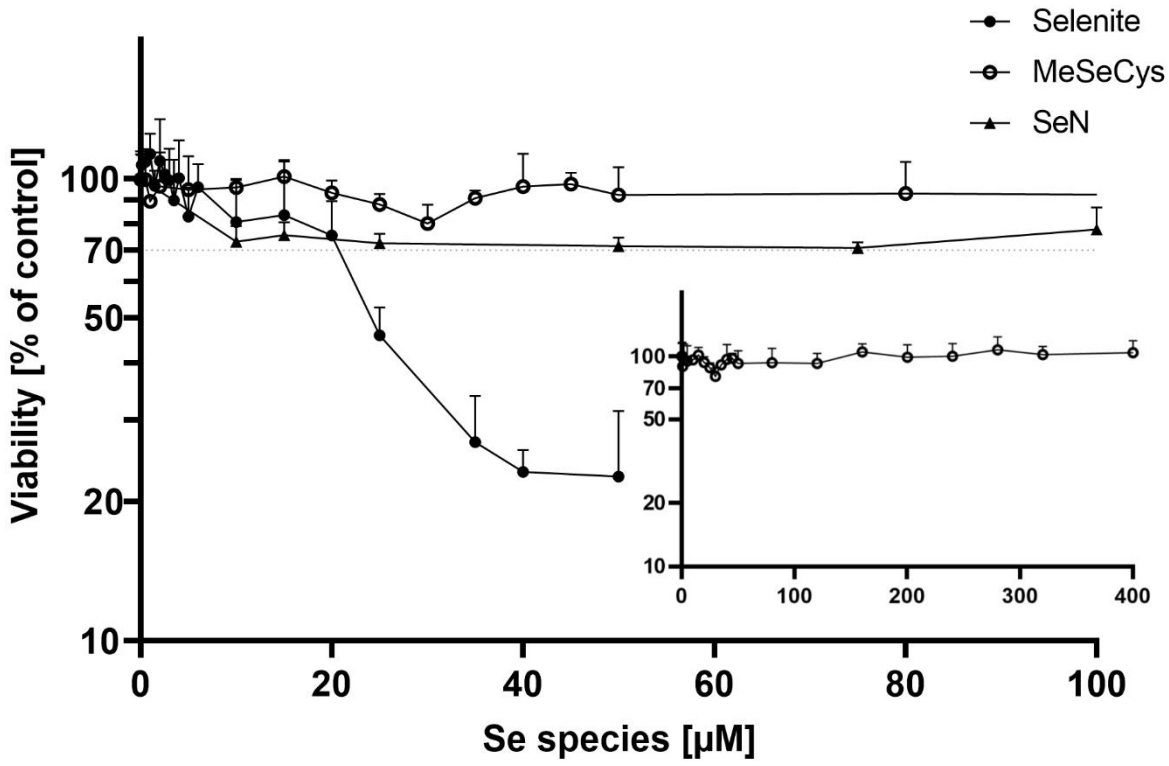

Figure 19. PBCEC cell viability after 72-hour incubation with Se species determined by neutral red uptake assay [361]. The inner graph corresponds to the full concentration range of MeSeCys incubation. Shown are mean values + SD of 3 independent experiments with six replicates each for selenite and MeSeCys, and three replicates for SeN.

Results of neutral red and CCK8 assays in PBCECs are presented in Figures and , correspondingly. As well as for HepG2 cells, selenite was found to exert the most pronounced toxic effect. Moderately higher EC30 and IC50 (Table 7) values, most probably associated with lower metabolic activity in PBCECs, are comparable to liver cells with regard to the generation of highly reactive Se intermediates [87]. Therefore, selenite toxicity in endothelial cells is most probably attributed to its higher pro-oxidant activity, while hepatocytes may additionally suffer from the

excessive generation of species like methylselenol or hydrogenselenide. When comparing effective concentrations obtained in lysosomal integrity and dehydrogenase activity assays, PBCECs exhibit significant differences compared to liver cells. For endotheliocytes, 2-fold higher toxic concentrations for selenite were observed, while values for hepatocytes were close to each other. This can be explained by lower mitochondrial content in the brain capillaries, compared to hepatic tissue. While liver cells have around 25% of mitochondria in their cytoplasm [362], endothelial cells of the BBB contains 8-11% [363]. Therefore, the stronger metabolic activity of hepatocytes ensured by prominent mitochondrial function, leads to the enhanced formation of RONS under selenite pro-oxidant action. Also, obtained ratios of effective concentrations in neutral red and CCK8 assays for PBCECs and HepG2 correlate with their mitochondrial content.

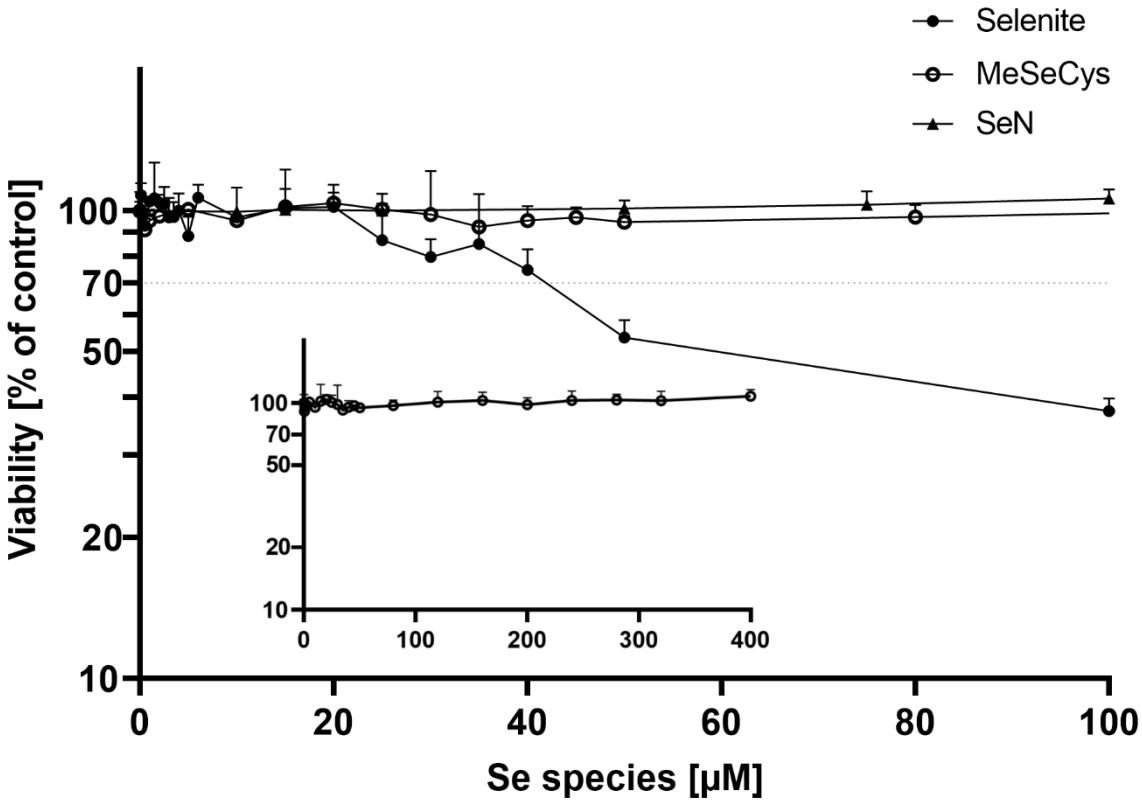

Figure 20. PBCEC cell viability after 72-hour incubation with Se species determined by CCK8 assay [361]. The inner graph corresponds to the full concentration range of MeSeCys incubation. Shown are mean values + SD of 3 independent experiments with six replicates each for selenite and MeSeCys, and three replicates for SeN.

MeSeCys caused no decrease in PBCECs' viability even at the extreme concentration of 400 µM. Compared to HepG2 cells, the absence of MeSeCys toxicity in PBCECs is most probably associated with the lack of active selenoprotein synthesis in the capillary endothelium and, therefore, the absence of highly reactive intermediates.

The applied range of SeN concentrations partially overlaps with SeN content in human blood. In accordance with other Se compounds, SeN content in human blood shows significant regional

variability. While people in Europe have less than 0.1 µM of SeN in blood [364], people consuming fish as a main source of protein have up to 40 µM of SeN in blood [188]. Therefore, the observed absence of SeN toxicity in both assays connects with the lack of endemic neurological impairments in such populations.

Table 7 – Effective concentrations of Se species in PBCECs assessed by neutral red and CCK8 assay after 72-hour incubation.

	Neutral red		Resazurin	
	EC30 (µM)	IC50 (µM)	EC30 (µM)	IC50 (µM)
Selenite	20.7	24.0	42.0	59.9
MeSeCys	> 400	> 400	> 400	> 400
Selenoneine	> 100	> 100	> 100	> 100

6.2.2 Transfer studies

To explore the bioavailability of SeN to the CNS, time-dependent transfer experiments were carried out using the *in vitro* BBB model. This model consists of a confluent monolayer of PBCECs seeded on permeable Transwell® inserts (details in section 5.1.2). Compounds were applied from the apical side, thus imitating the entry of Se species from blood to the brain. Transwell® inserts with cells were placed into cellZscope® device for TEER and capacitance measurements during transfer experiments. Control of impedance characteristics of PBCEC monolayers allows to ensure barrier stability during transfer experiments and indicates if the barrier incurs damage during transfer. All Se species were applied at concentrations of 1 and 10 µM. SeN was additionally incubated at a concentration of 0.1 µM. As MeSeCys and SeN do not exhibit toxicity in PBCECs at much higher concentrations and selenite was applied in concentrations below EC30, no barrier disruption could be observed by TEER and capacitance values (Fig. A, B; Fig. A, B; Fig. A, B).Transfer data, presented in Figure C, showed that upon incubation with 1 µM selenite 33 ± 13.7% of applied Se were transferred to the basolateral compartment. However, this was not statistically significant due to the high standard deviation. The permeability coefficient calculated for 1 µM selenite was (6.3 ± 3.3) × 10^7 cm/s (Table 8). When a 10 µM selenite was applied, much higher amounts of Se were found in the basolateral compartment – 63 ± 4%. Correspondingly, the permeability coefficient increased up to (10.7 ± 1.5) × 10^7 cm/s. Interestingly, the mode of selenite transfer occurred most active between 24 and 48 hours for both applied concentrations. Possibly, selenite causes slight barrier permeabilization, since a concentration of 10 µM was quite high with regard to obtained EC30 values for PBCECs (section 6.2.1, Table 7).

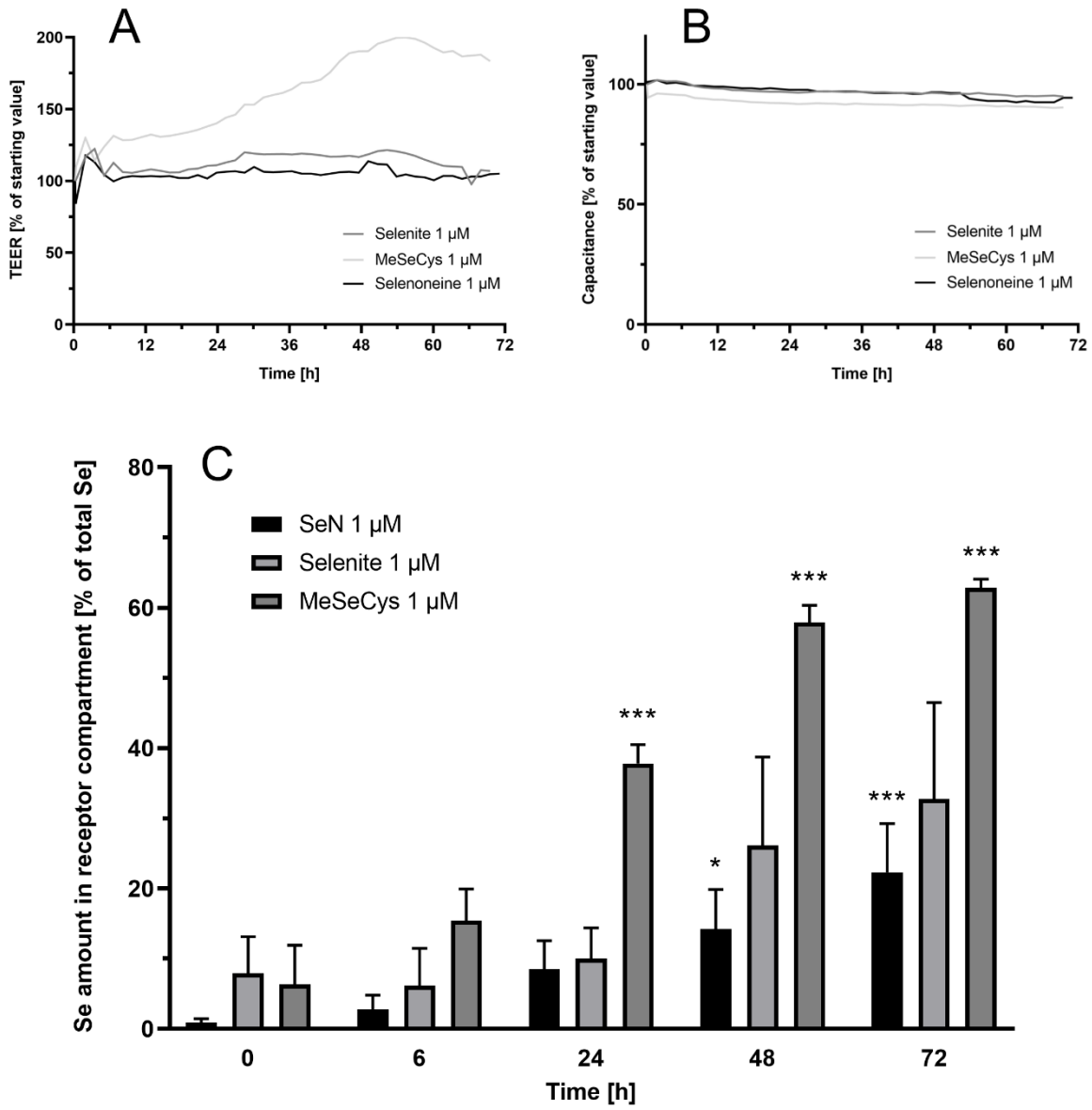

Figure 21. Results of the transfer studies with 1 µM of Se species applied from the apical side for 72 hours. A: TEER values of PBCEC barrier during transfer experiments, presented as percentage of starting value for each sample. B: Capacitance values of PBCEC barrier during transfer experiments, presented as percentage of starting value for each sample. C: Percentage of Se transferred into the basolateral compartment from total Se amount in well. Shown are mean values, calculated from three independent experiments for selenite and MeSeCys, and four experiments for SeN with two replicates each. Statistically significant difference was calculated in relation to the starting value using one-way ANOVA followed by Dunnett's test, * $P < 0.05$, *** $P < 0.001$.

At a concentration of 1 µM, MeSeCys already showed most pronounced transfer, where 63 ± 2% of Se were carried to the basolateral compartment (Fig. C), corresponding to a permeability coefficient of (10.8 ± 1.3) × 10^7 cm/s (Table 8). Increase of the MeSeCys concentration did not affect the mode of MeSeCys transfer, demonstrating the same transfer efficiency (64 ± 2%, P = (10.4 ± 0.2) × 10^7 cm/s) and time dependence (Fig. C). Obtained permeability coefficients for MeSeCys are very close for those reported for sucrose in the same PBCEC model [365], which are

corresponding to the *in vivo* data for sucrose as an important glucose supplier for the brain. The concentration-independent character of MeSeCys transfer indicates its active mode of action. Most probably this is attributed to the alanine, serine, cysteine, and threonine transporter 1 (ASCT1) and 2 (ASCT2) since they are responsible for cysteine delivery to the brain [366].

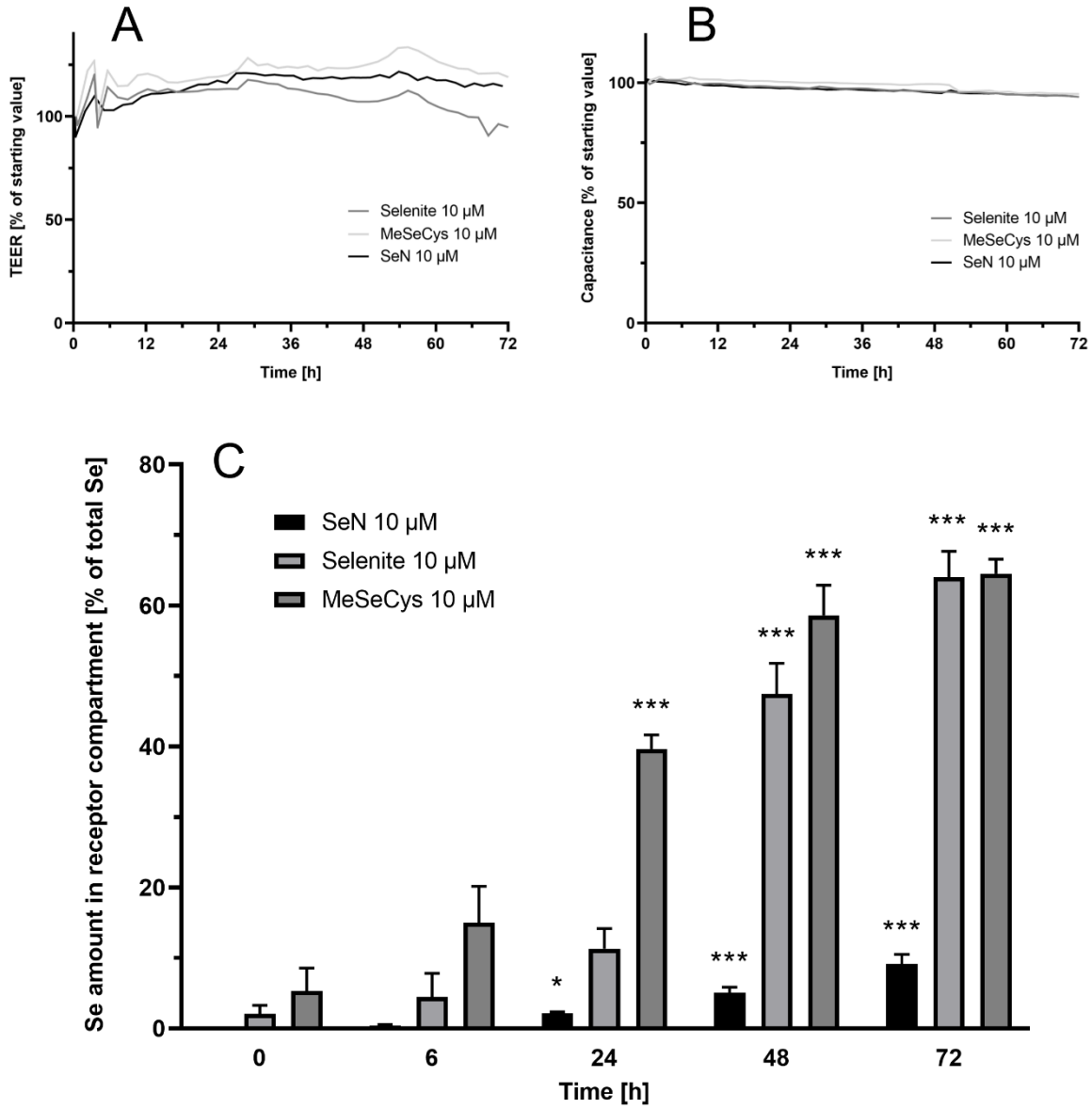

Figure 22. Results of the transfer studies with 10 µM of Se species applied from the apical side for 72 hours. A: TEER values of PBCEC barrier during transfer experiments, presented as percentage of starting value for each sample. B: Capacitance values of PBCEC barrier during transfer experiments, presented as percentage of starting value for each sample. C: Percentage of Se transferred into the basolateral compartment from total Se amount in well. Shown are mean values, calculated from three independent experiments with two replicates each. Statistically significant difference was calculated in relation to the starting value using one-way ANOVA followed by Dunnett's test, * $P < 0.05$, *** $P < 0.001$.

SeN in these experiments was characterized by the lowest obtained permeability coefficients (Table 8). Significant Se transfer was observed for SeN already within 24 hours for a concentration of 10 µM. However, for 0.1 µM significant Se accumulation in the basolateral compartment was

observed only at the end of incubation time (Fig. C). Amounts of transferred Se were very similar for concentrations of 0.1 and 1 µM: 24 ± 6% and 22 ± 7%, respectively, in accordance with permeability coefficients (Table 8). However, incubation with 10 µM SeN resulted in much lower Se transfer – only 9.0 ± 1.5%. Also, double-sided incubation was performed once to control the possible side-directed transfer of SeN [361] and no shift of equilibrium was observed under equal SeN concentrations on both sides of the barrier. Altogether this indicates a passive diffusion mechanism for SeN. If OCTN1, the main transporter for SeN, would be present in PBCECs, it should provide fast and efficient SeN transport, like in HEK293 [212] or Caco-2 [163] cells. Nevertheless, studies on the distribution of sulfur analog of SeN – ET in rats demonstrate significant accumulation of ET in the rat brain [367], even though the rat BBB does not have OCTN1 transporter [368]. Therefore, obtained data for SeN transfer in the PBCEC barrier model does not contradict *in vivo* studies and indicate the presence of other possible mechanisms of SeN transfer, besides the OCTN1 transporter.

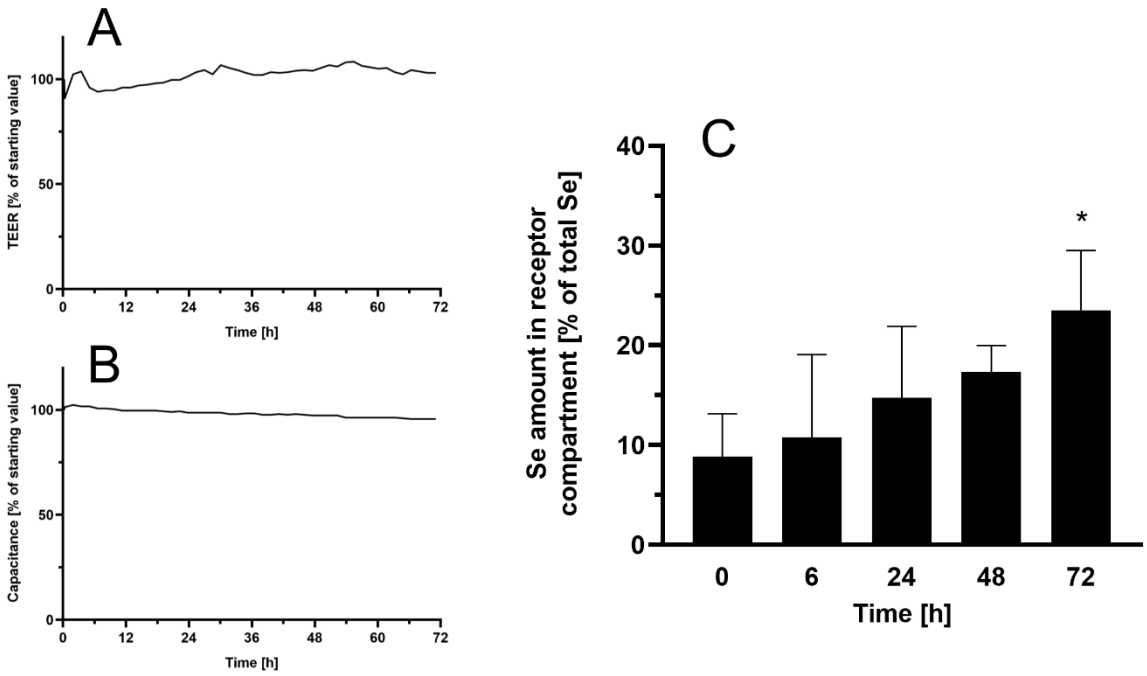

Figure 23. Results of the transfer studies with 0.1 µM of SeN applied from the apical side for 72 hours. A: TEER values of PBCEC barrier during transfer experiments, presented as percentage of starting value for each sample. B: Capacitance values of PBCEC barrier during transfer experiments, presented as percentage of starting value for each sample. C: Percentage of Se transferred into the basolateral compartment from total Se amount in well. Shown are mean values, calculated from three independent experiments with two replicates each. Statistically significant difference was calculated in relation to the starting value using one-way ANOVA followed by Dunnett's test, * $P < 0.05$.

Table 8 – Permeability coefficients calculated from transfer experiments for selenite, MeSeCys, and SeN after 72-hour incubation.

Compound	Concentration (µM)	P (cm/s) × 10^7
SeN	0.1	4.0 ± 1.0
	1	3.7 ± 1.3
	10	1.57 ± 0.3
Selenite	1	6.3 ± 3.3
	10	10.7 ± 1.5
MeSeCys	1	10.8 ± 1.3
	10	11.3 ± 0.9

The selenium content, measured in PBCEC cell lysates after transfer experiments, showed no differences from control for all applied Se species. HPLC-ICP-MS together with HPLC-ESI-Orbitrap-MS measurements were performed at the University of Graz. Metabolomic data demonstrated that both in the medium samples and in the cell lysates, there are metabolites of applied Se species. Concluding, SeN demonstrated slow but substantial transfer in the used BBB model and was not metabolized by endotheliocytes.

6.3 Studies in Caco-2 intestinal cells

Previous studies in our group demonstrated that SeN is not toxic for Caco-2 cells [163]. Also, these cells are able to effectively take up significant amounts of SeN [163]. This is an important property of SeN from two points of view of its properties. First of all, SeN may act as a selenium source for intestinal cells, which are requiring it for maintenance of their functions (section 3.1.5). Secondly, the gastrointestinal tract is often influenced by elevated RONS levels, thus SeN may enhance the intestinal antioxidative capacity. These two questions are addressed in the current chapter.

6.3.1 Antioxidant activity in Caco-2 cells

For the detection of RONS in Caco-2 cells, a carboxy-H_2DCFDA molecular probe was used (detailed description in section 5.4). Cells were pre-incubated with different concentrations of selenite, SeMet, SeN, and ET for different terms, loaded with carboxy-H_2DCFDA, and then oxidative stress was induced using 150 µM TBHP.

Firstly, all studied compounds were incubated for 72 hours in concentrations from 10 to 500 nM. Data on cells' response to RONS induction is presented in Figure . All selenium species caused a statistically significant reduction of RONS level starting from a concentration of 100 nM. SeN effect was already significant at 50 nM and very close to selenite. At the highest dose, reduction

of RONS level by SeN (66%) was very close to those for selenite and SeMet (60%). ET effect was incomparably weak with regard to SeN. Only at a concentration of 500 nM, a significant decline in RONS level was observed.

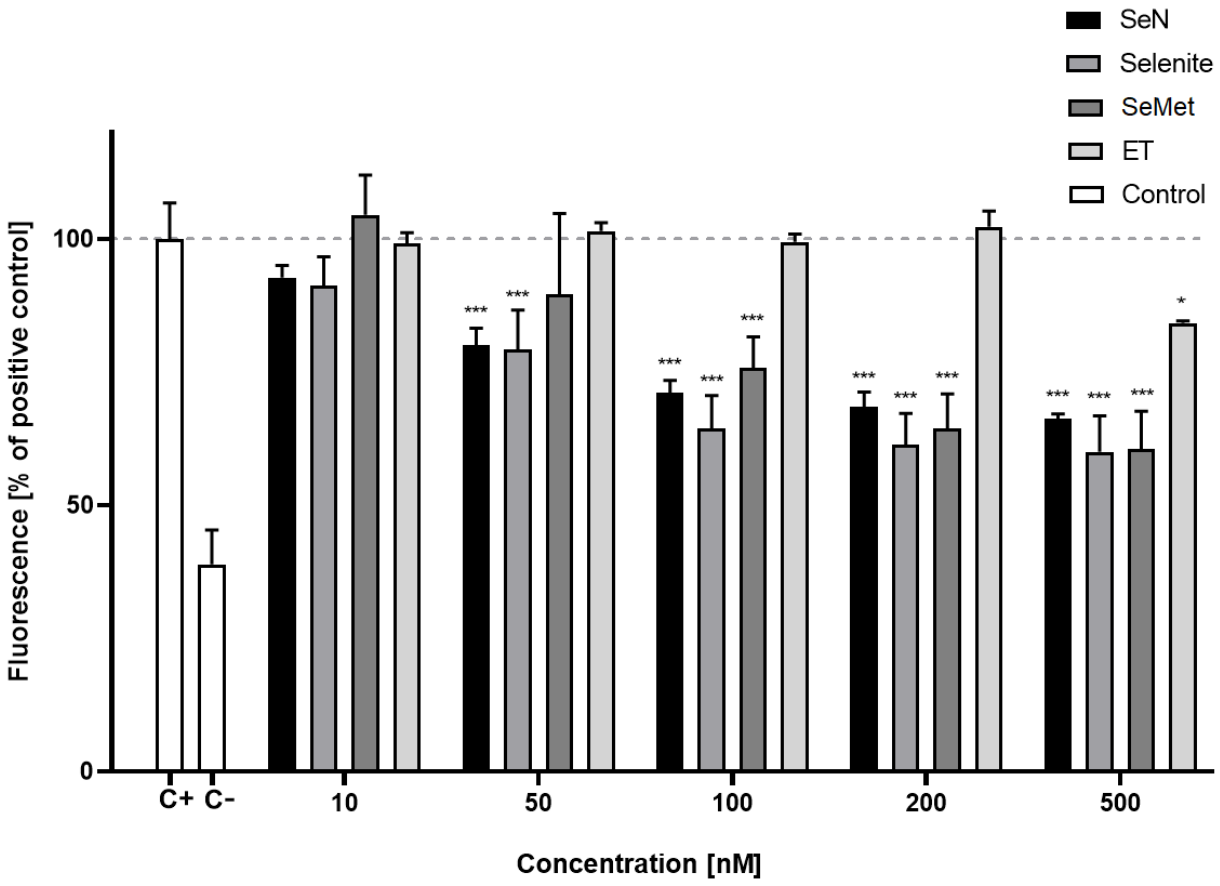

Figure 24. Induction of RONS in Caco-2 cells by 150 µM TBHP after 72-hour pre-incubation with 10-500 nM of Se species or ET. Untreated control is marked as "C-". Positive control cells treated with TBHP only are marked as "C+". Results are presented as % of fluorescence of positive control cells. Shown are mean values + SD of at least two independent experiments with six replicates each. Statistically significant difference was calculated in relation to the positive control using one-way ANOVA followed by Dunnett's test, * $P < 0.05$, *** $P < 0.001$.

Since already at a concentration of 200 nM Se species cause a decrease in RONS activity close to a plateau level, the 200 nM was chosen for a time-dependent incubation. The results on RONS quenching at different time points are presented in Figure . Here, as for the concentration-dependent incubation, SeN showed an effect similar to those for selenite and SeMet. Selenite caused the fastest reduction of RONS – already after 3 hours. With a longer incubation time, all Se compounds exhibited a consistent effect on the RONS level. Thus, being a Se analog of ET, SeN is acting almost like selenite or SeMet, rather than ET. Much higher activity of RONS quenching induced by 2,2-diphenyl-1-picrylhydrazyl has already been reported for SeN compared to ET in experiments with SeN-enriched fish extracts [187]. Thus, the higher antioxidant activity of SeN is now confirmed by the current experiments with the pure compound.

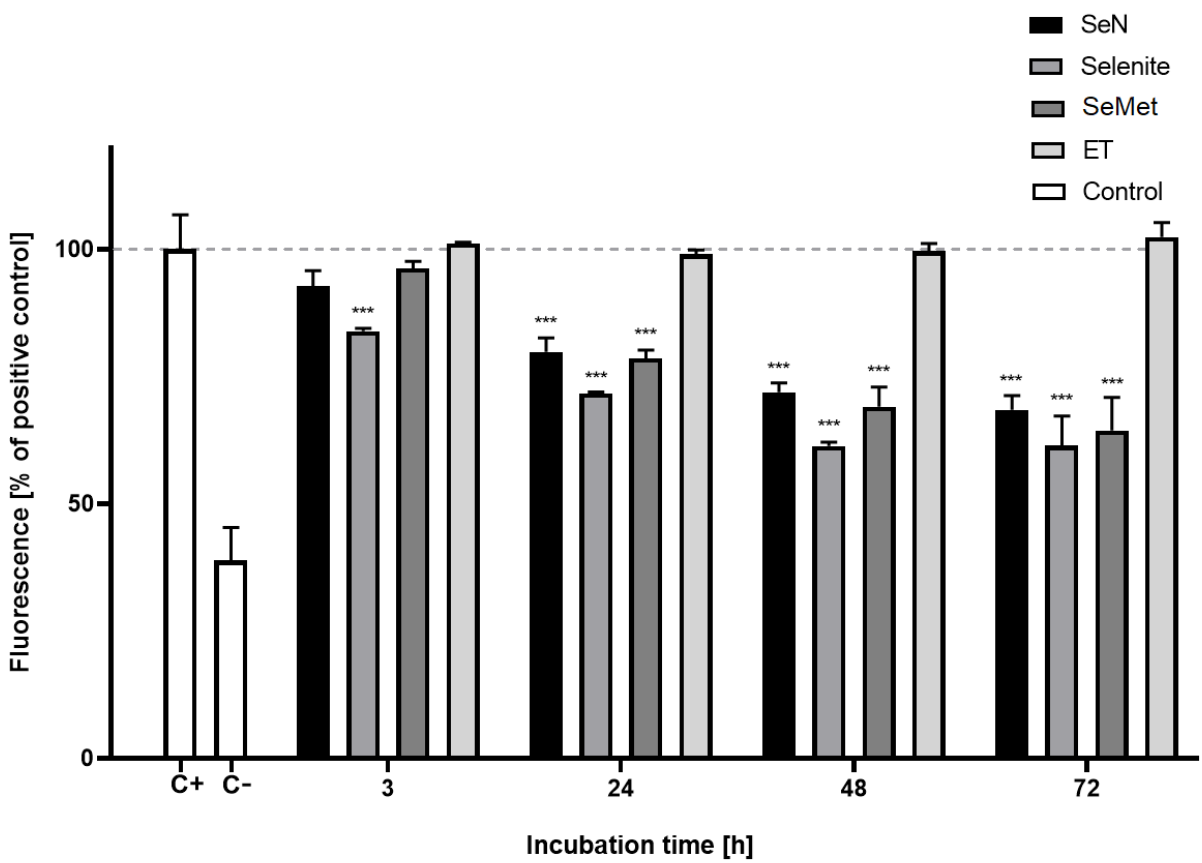

Figure 25. Induction of RONS in Caco-2 cells by 150 µM TBHP after pre-incubation with 200 nM of Se species or ET for 3-72 hours. Untreated control is marked as "C-". Positive control cells treated with TBHP only are marked as "C+". Results are presented as % of fluorescence of positive control cells. Shown are mean values + SD of at least two independent experiments with six replicates each. Statistically significant difference was calculated in relation to the positive control using one-way ANOVA followed by Dunnett's test, * $P < 0.05$, *** $P < 0.001$.

In order to assess the integral effect of SeN and other compounds on cell viability under oxidative conditions, neutral red and Hoechst staining were performed. Caco-2 cells were pre-incubated with 100 nM of Se species or ET for 72 hours and then subjected to different concentrations of TBHP for 24 hours. Results for neutral red uptake are presented in Figure . The positive control curve (C+) corresponds to the cells, which were not treated with Se species or ET before TBHP incubation.

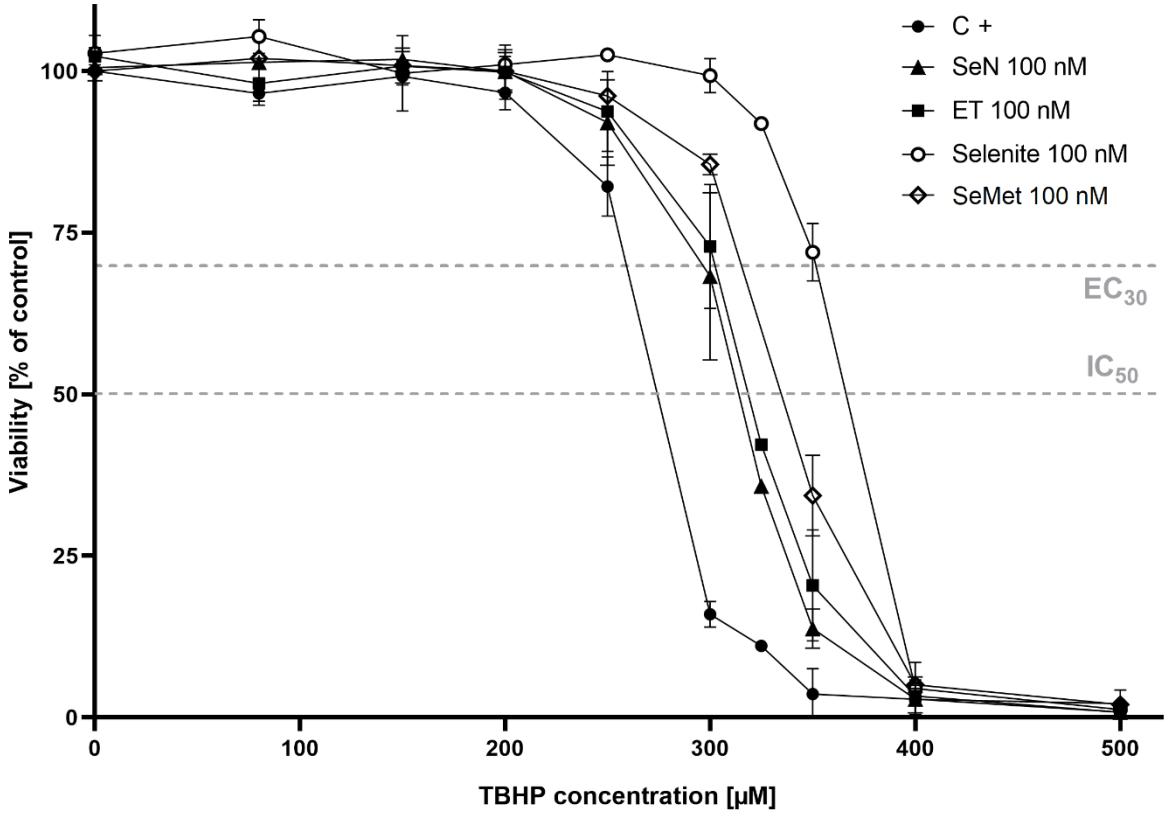

Figure 26. Viability of the Caco-2 cells determined by neutral red uptake after 72-hour preincubation with 100 nM of Se species or ET and subsequent 24-hour treatment with indicated TBHP concentrations. Positive control cells treated with TBHP only are marked as "C+". Shown are mean values ± SD, expressed as % of the untreated control value, calculated from three independent experiments with six replicates each.

All applied compounds significantly increased the viability of Caco-2 cells, reflecting increased resistance to induced oxidative damage (Table 9). Selenite caused the most significant shift in the EC30 value, from 260 µM for positive control to 355 µM. SeMet was less effective, with an EC30 value of 315 µM. Both ET and SeN caused a similar effect, which was significant compared to the positive control, but also less pronounced than for selenite and SeMet. Also, incubation with 200 nM of SeN and ET was performed in the same manner and obtained results were equal to those for 100 nM concentration. Hoechst staining was less sensitive (Fig.), however, it showed the same pattern as in the neutral red assay and confirmed the observed statistically significant increase in viability for all applied compounds.

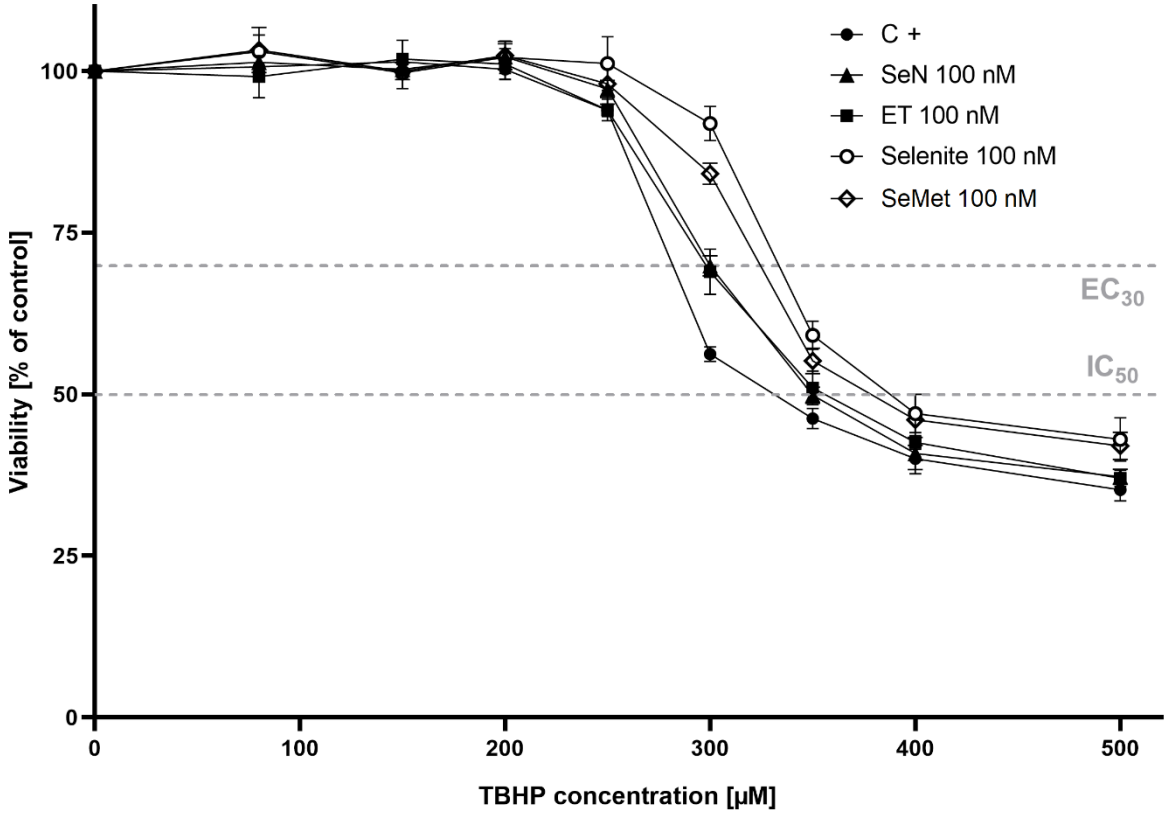

Figure 27. Viability of Caco-2 cells determined by Hoechst staining after 72-hour preincubation with 100 nM of Se species or ET and subsequent 24-hour treatment with indicated TBHP concentrations. Positive control cells treated with TBHP only are marked as "C+". Shown are mean values ± SD, expressed as % of the untreated control value, calculated from three independent experiments with six replicates each.

The higher antioxidant activity of SeN compared to ET can be explained by their redox stability. Treatment of ET and SeN with hydrogen peroxide showed different rates of oxidized intermediates' formation [216]. Selenium is a better nucleophile than sulfur and this is reflected in the higher stability of SeN intermediates after reaction with hydrogen peroxide. When ET being oxidized to the first intermediate – sulfinic acid (Fig. A), it is rapidly converted to sulfonic acid (Fig. C) or undergoes desulfuration with the formation of trimethylhistidine (Fig. B). Studies in biological samples demonstrated the presence of these intermediates after ET administration [217], thus showing low stability of the sulfinic acid form. In contrast to ET, oxidation of SeN slows down at the stage of the seleninic acid intermediate, and further oxidation to selenonic acid or deselenation to trimethylhistidine shows a much slower reaction rate. Moreover, in the presence of GSH, the stable seleninic acid intermediate is reduced back to SeN at a high rate. Thus, SeN is not only more resistant to oxidative degradation than ET but also can be restored by GSH. Compared to other Se compounds, which in high concentrations promote the formation of RONS including intensification of iron oxidation in the Fenton reaction, SeN conversely can reduce iron oxidation in erythrocytes [191]. This effect of SeN may be attributed to its complexing ability, thus lowering available amounts of iron for the reaction with peroxides.

Table 9 – Effects of selenite, SeMet, SeN, and ET on the effective TBHP concentrations and area under the curve (AUC).

	Neutral Red			Hoechst		
	EC30	IC50	AUC	EC30	IC50	AUC
Positive control	260	275	7607 ± 226	280	332	13330 ± 104
SeN 100 nM	297	312	11145 ± 448 *	300	350	14425 ± 117 *
ET 100 nM	303	320	11821 ± 434 *	300	358	14289 ± 178 *
Selenite 100 nM	355	368	16485 ± 180 *, a	332	390	16339 ± 215 *, a
SeMet 100 nM	315	338	13429 ± 247 *, a, b	325	380	15578 ± 184 *, a, b

Statistically significant difference was calculated in relation to the control value (*), SeN (a), and selenite (b) using one-way ANOVA followed by Dunnett's test, $P < 0.001$.

6.3.2 Involvement of SeN in selenium metabolism

Since SeN has an amino acid structure and is effectively assimilated by Caco-2 cells, it can be a source of Se for selenoprotein synthesis. Since antioxidant enzymes play a crucial role in intestinal functions (see section 3.1.5), the potential role of SeN in the modulation of these functions is of considerable interest. Accordingly, the effect of SeN on two of the most important selenoproteins, GPx and SelenoP, has been studied.

GPx activity was measured in Caco-2 cell lysates (procedure described in section 5.5) after 72-hour incubation with Se species or ET (Fig.). Selenite, as a reference compound, demonstrated fast and efficient induction of GPx activity, which was significant already at a concentration of 10 nM. At 200 nM, the selenite effect reached its plateau, causing a 3-fold increase in GPx activity. The impact of SeMet on GPx activity was comparable with selenite at the higher dosages. In the lower concentration range, the effect of SeMet developed slower, because it is known, that SeMet is also unspecifically incorporated into proteins instead of plain Met [369], and thus lowering its availability for selenoprotein synthesis. A less pronounced but still significant effect on GPx activity was observed for ET, which is in accordance with earlier studies [370]. Unlike both Se species and ET, SeN had no effect on the GPx activity.

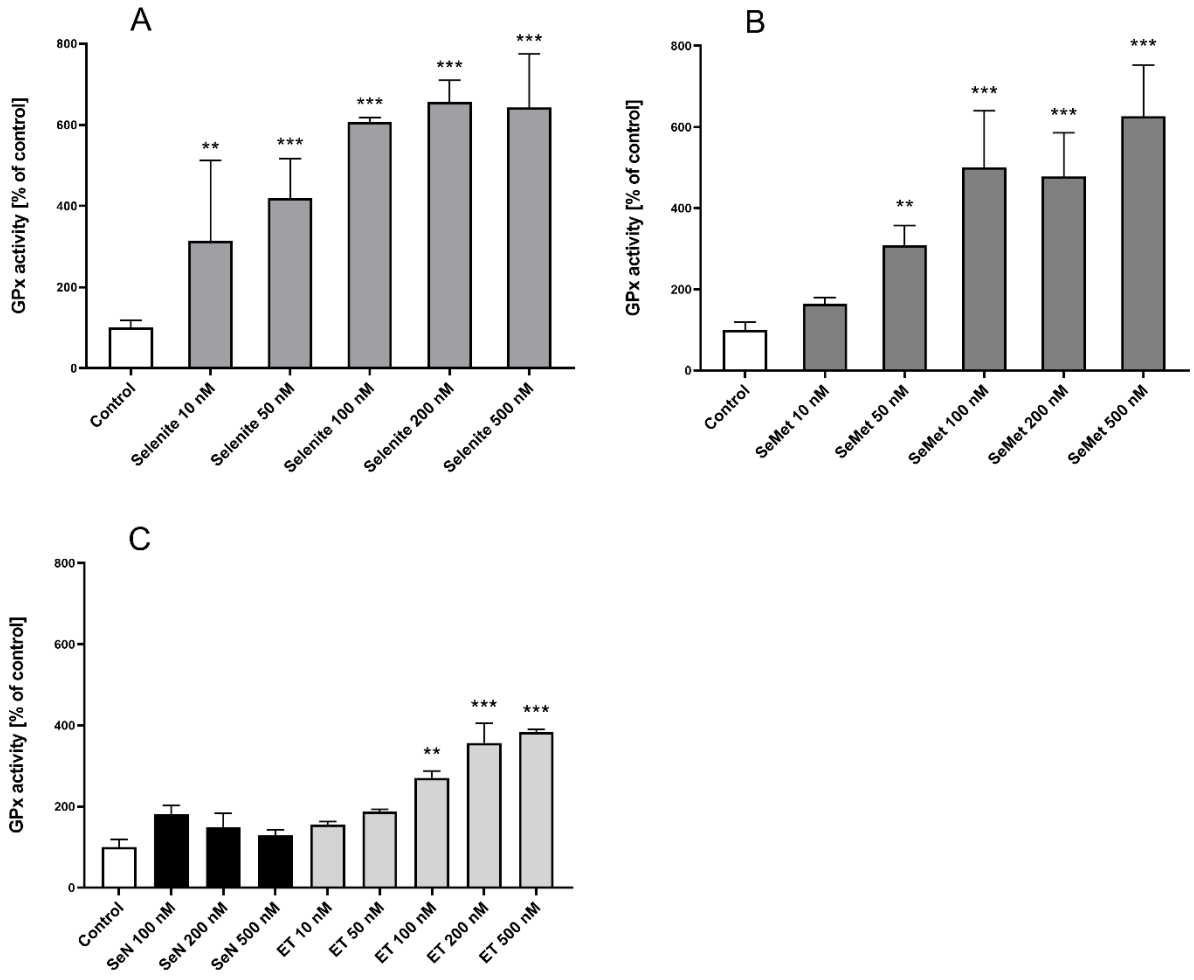

Figure 28. Effect of selenite (A), SeMet (B), SeN (C), and ET (C) on the GPx activity in Caco-2 cells after 72-hour incubation. Shown are mean values + SD, expressed as % of the control value, calculated from three independent experiments with two replicates each. Statistically significant difference was calculated in relation to the control value using one-way ANOVA followed by Dunnett's test, ** $P < 0.01$, *** $P < 0.001$.

The SelenoP concentration was measured in the culture medium since it is excreted by intestinal cells [371]. The amount of SelenoP secreted in the medium correlated with the bioavailability of Se species since SelenoP serves as the main protein for Se transport (see section 3.1.4). Selenium concentration in Caco-2 cells was also measured to ensure the bioavailability of the applied species for Caco-2 cells. Compared to selenite and SeMet, SeN showed the most apparent uptake (Fig.), possibly due to the presence of OCTN1 in Caco-2 cells. Also, ratios of intracellular Se content to applied concentrations were not decreasing for SeN (Table 10), as they do for selenite and SeMet. This means that SeN can be taken up at the same ratio, even at higher concentrations. However, SeN exhibited no effect on SelenoP production by Caco-2 cells (Fig.), while selenite and SeMet, known to be a Se source, increased SelenoP secretion significantly. While the effectiveness of SelenoP synthesis by selenite is slowly decreasing (Table 10), the SeMet effect is remaining on the same level, probably due to the abovementioned unspecific incorporation of SeMet into proteins.

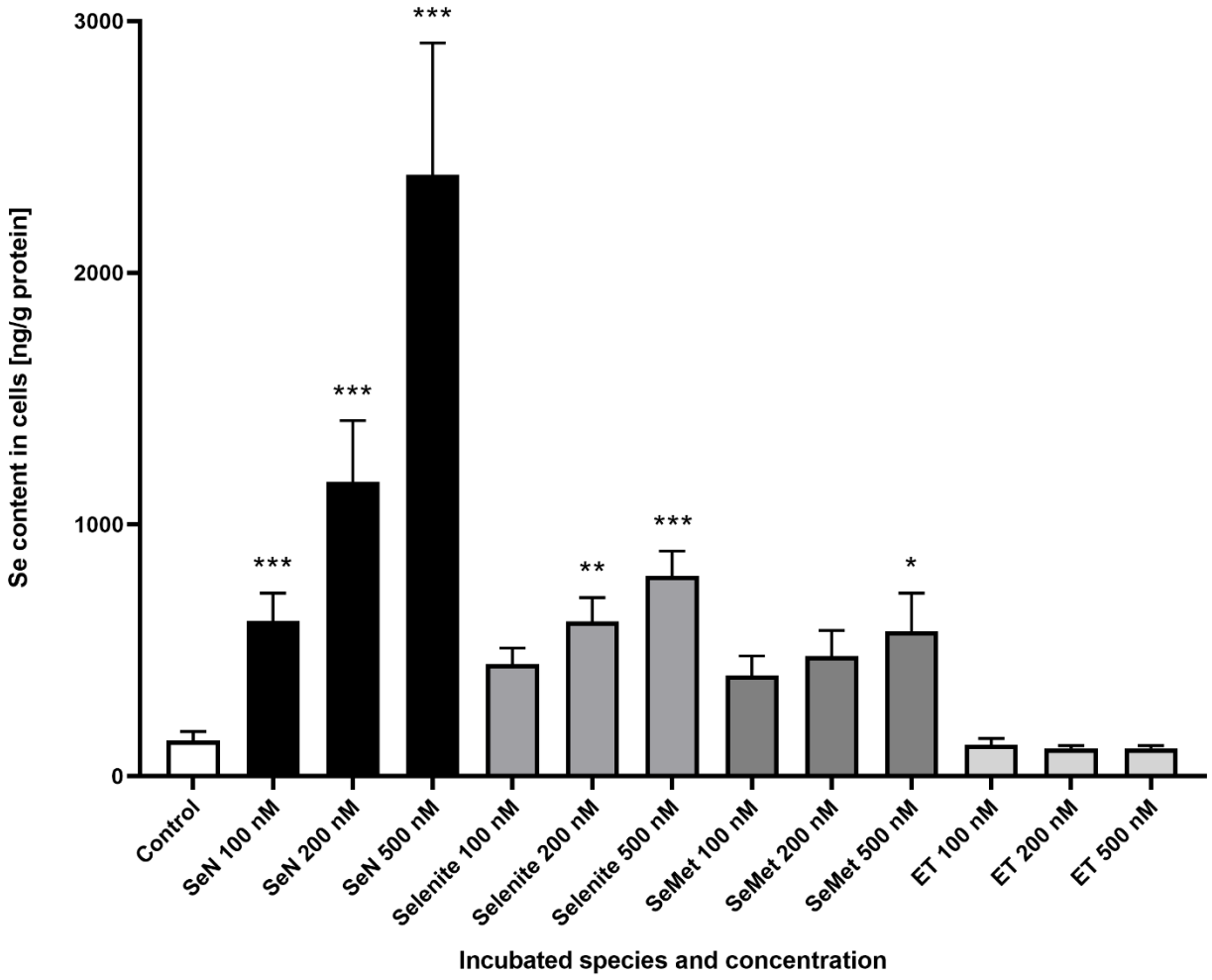

Figure 29. Selenium concentration in Caco-2 cells after 72-hour incubation with selenite, SeMet, SeN and ET. Shown are mean values + SD, calculated from four independent experiments. Statistically significant difference was calculated in relation to the control value using one-way ANOVA followed by Dunnett's test, *P < 0.05, ** P < 0.01, *** P < 0.001.

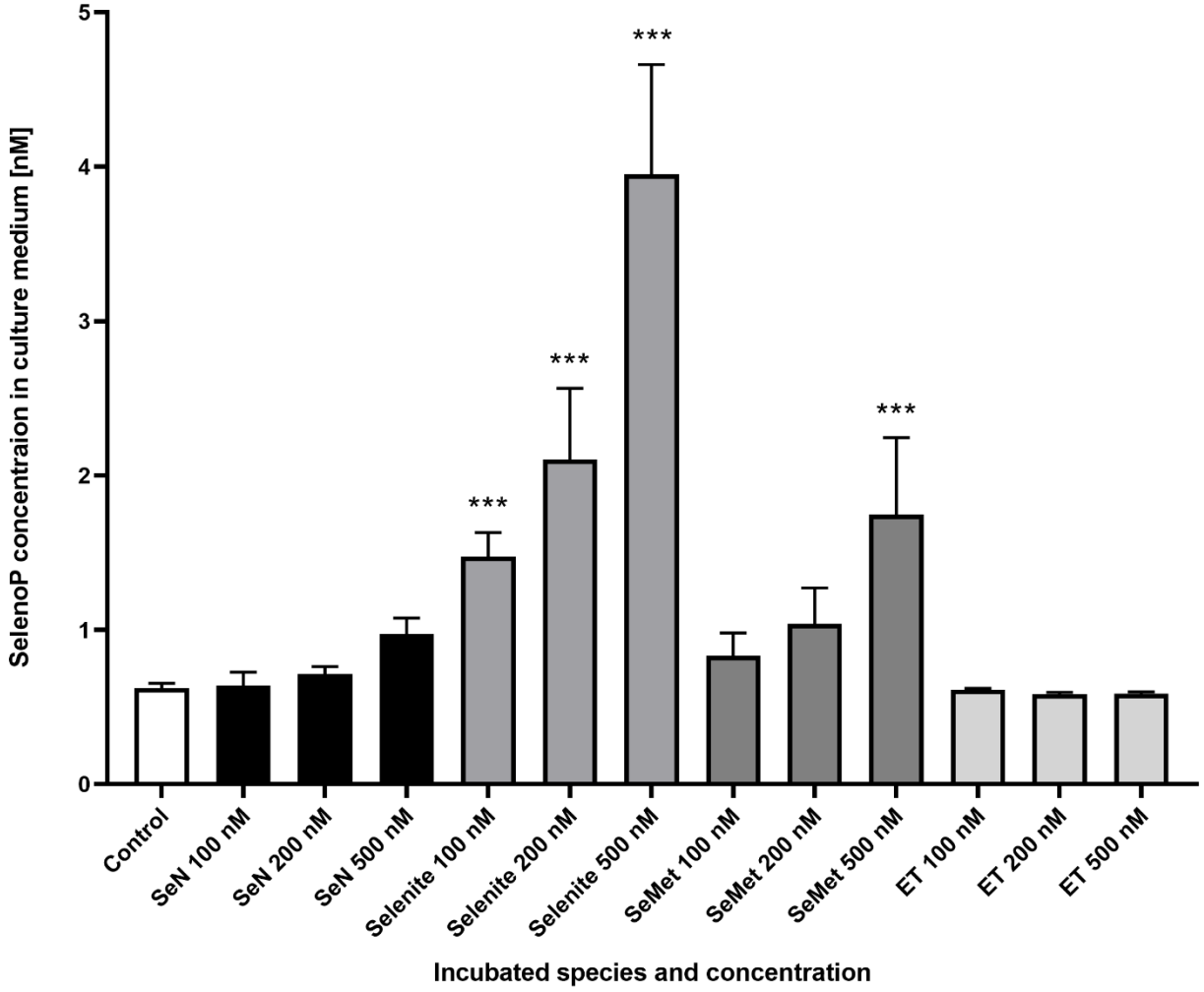

Figure 30. SelenoP concentration in the culture medium of Caco-2 cells after 72-hour incubation with selenite, SeMet, SeN, and ET. Shown are mean values + SD, calculated from four independent experiments. Statistically significant difference was calculated in relation to the control value using one-way ANOVA followed by Dunnett's test, ** $P < 0.01$, *** $P < 0.001$.

The absence of a SeN effect on GPx activity and SelenoP production, while it is effectively taken up by the Caco-2 cells, clearly indicates its unavailability for the selenoproteome. The absence of further SeN metabolites, other than MeSeN, in human samples, was already indicating this indirectly [193, 196]. The unavailability of SeN for Se metabolism can be most likely explained from the point of its chemical structure. While commonly in food present Se compounds like selenite or selenoamino acids undergo reduction to hydrogen selenide (see section 3.1.4), conversion of SeN seems not to be possible in the same way as easily. While organic Se species have an amino acid structure with free or methylated selenol groups, SeN has a strong cyclic conjugation between free electron pairs of the selenol group, double bonds, and nitrogen atoms in the imidazole ring. This conjugation allows SeN to exhibit a significant degree of tautomerization (Fig. 5), enhance its antioxidative properties compared to ET, and also provide it with strong metal-complexing ability. However, from the point of Se metabolism, such conjugated selenol groups cannot be easily removed via the trans-selenation pathway and used as a substrate for Sec synthesis (Fig. 2). Accordingly, data from SeN studies in the nematode

Caenorhabditis elegans are proving the inability of SeN to modulate functions of selenoproteins [372]. When SeN was incubated for 18 hours, it was efficiently taken up by the nematodes. However, an increase in RONS scavenging ability was observed only 48 hours post-treatment and when no SeN was left inside the nematode. This indicates that antioxidative action was not caused by SeN by itself, but by other molecular mechanisms.

Table 10 – Ratios of total Se content in Caco-2 cells and SelenoP concentration in culture medium to applied concentrations of Se species ± SD after 72-hour incubation.

	Concentration [nM]	Se content in cell [ng g^{-1} protein] / Applied concentration [nM]	SelenoP concentration [nM] / Applied concentration [nM]
SeN	100	4.77 ± 0.85	0.15 ± 0.02
	200	5.14 ± 1.07	0.45 ± 0.03
	500	4.50 ± 1.05	0.70 ± 0.07
Selenite	100	3.05 ± 0.43	8.52 ± 0.90
	200	3.08 ± 0.47	7.40 ± 1.63
	500	1.59 ± 0.20	6.66 ± 1.20
SM	100	2.60 ± 0.50	2.08 ± 0.37
	200	2.40 ± 0.50	2.08 ± 0.47
	500	1.15 ± 0.30	2.25 ± 0.64

7. Conclusion

Being discovered only 10 years ago, SeN attracted significant attention due to its wide distribution in edible fish species and outstanding antioxidant activity [373]. Until recently, SeN properties were not properly studied due to the absence of synthetic approaches to obtain a pure compound. However, its detection in human blood in different regions worldwide has raised a reasonable interest in it as a participant of human selenium metabolism and safe nutritional antioxidant.

In the current study, the properties of SeN were described from the points of its toxicity, antioxidant properties, and involvement in selenium metabolism. SeN was shown to be non-toxic in HepG2 liver cells, primary capillary endotheliocytes from the porcine brain, and intestinal Caco-2 cells. Hepatocytes were found to be not able to take up SeN and, consequently, use it for selenoproteins production. Transfer studies using an *in vitro* BBB model demonstrated that SeN is able to passively cross the BBB endothelium and is not anyhow metabolized during this process. Earlier supposed higher antioxidant activity of SeN compared to its sulfur isolog ET was now confirmed in Caco-2 cells and found to be close to those for nutritional selenium compounds. However, SeN hardly can be involved in selenium metabolism and being utilized for the selenoprotein synthesis. Summing up, we can say that SeN is of great interest for investigation of its antioxidative properties and endemic exposure, but not as a metabolically active selenium compound. It can act as a dietary antioxidant and be used to prevent the effects of intestinal diseases and other pathologies associated with increased RONS formation, which requires further comprehensive investigation.

8. Appendix

8.1 Equipment

Analytical balances Atilon	Satorius (Göttingen)
Autoclave DX-65	Systec (Wettenberg)
Biological Safety Cabinet InCu saFe®	Panasonic (Wiesbaden)
Biological Safety Cabinet Safe 2020, Class II	Thermo Scientific (Langenselbold)
CASY® cell counter and analyzer	Roche (Mannheim)
CellZscope™	Nanoanalytics (Münster)
Centrifuge Mikro 200 R	Hettich (Tuttlingen)
Centrifuge Labofuge 400R	ThermoFisher Scientific (Hanau)
Fluid aspiration system BVC 21	Vacuubrand (Wertheim)
Freezer	Bosch (Stuttgart)
Fridges	Privileg (Stuttgart), Siemens (Berlin)
HPLC column Atlantis® dC18* 5 µm, 4.6 x 150 mm	Waters Corporation (Milford, USA)
HPLC column Dionex IonPac™ AS14* 5 µm, 3.0 x 150 mm	ThermoFisher Scientific (Waltham, USA)
HPLC column Gemini C6-Phenyl* 3 µm, 4,6 x 150 mm	Phenomnex (Torrance, USA)
HPLC system Infinity 1260	Agilent (Waldbronn)
HPLC System Dionex 3000*	ThermoFisher Scientific (Waltham, USA)
Incubator B-15	ThermoFisher Scientific (Dreieich)
Incubator INCU-Line	VWR (Darmstadt)

Laboratory Gas Burner Fuego SCS basic	WLD-TEC GmbH (Göttingen)
Magnetic stirrer	Ika Labortechnik (Staufen)
Microplate reader Infinite® 200 Pro	Tecan Deutschland (Crailsheim)
Microscope	Helmut Hund GmbH (Wetzlar)
Microwave digestion system MARS 6 with 30 mL TFA digestion liners	CEM (Kamp-Lintfort)
Multichannel pipette Xplorer 300	Eppendorf (Hamburg)
Nitrogen tank MVE Cryosystem 4000	Cryo Solutions (Hertogenbosch, Netherlands)
pH-Meter Lab 850	Schott (Mainz)
Pipettes Reference and Reference 2	Eppendorf (Hamburg)
Pipettus	TPP (Trasadingen, Switzerland) Satorius (Göttingen)
Preparative affinity chromatography column HiTrap Heparin HP, 1 mL	GE Healthcare (Freiburg)
Software MassHunter ICP-QQQ-MS, Version 4.2	Agilent (Waldbronn)
Triple quadrupole ICP-MS, 8800 Series	Agilent (Waldbronn)
UHMR ESI-Quadrupole-Orbitrap™-MS Q Exactive™ *	ThermoFisher Scientific (Waltham, USA)
Ultrasonic homogenizer Labsonic® M	Satorius (Göttingen)
Vortex Genius 3	Ika Labortechnik (Staufen)
Water bath	Haake (Karlsruhe)
Water purification system Milli-Q Elix 15	Millipore GmbH (Schwalbach)

8.2 Chemicals

Acetic acid	Sigma-Aldrich (Steinheim)
Ammonia solution	Merck (Darmstadt)
Ammonium acetate	Merck (Darmstadt)
Ammonium formate	Sigma-Aldrich (Steinheim)
Ammonium malonate	Sigma-Aldrich (Steinheim)
Ammonium sulfate	Roth (Karlsruhe)
Bicinchoninic acid	Bio-Rad (Feldkirchen)
Bovine serum albumin	Sigma-Aldrich (Steinheim)
tert-Butyl hydroperoxide	Sigma-Aldrich (Steinheim)
5(6)-Carboxy-2',7'-dichlorodihydrofluorescein diacetate	ThermoFisher Scientific (Hennigsdorf)
tris(2-Carboxyethyl)phosphine	Sigma-Aldrich (Steinheim)
Coomassie brilliant blue R-250 staining solution	Bio-Rad (Feldkirchen)
Copper sulfate, anhydrous	Sigma-Aldrich (Steinheim)
Deoxycholic acid sodium salt	Roth (Karlsruhe)
Dimethyl sulfoxide, ≥ 99.9%	Merck (Darmstadt)
DMEM/Ham's F12 medium	Biochrom (Berlin)
Earle's 199 medium	Biochrom (Berlin)
Ergothioneine	Tetrahedron (Vincennes, France)
Ethanol 96%, denatured	VWR (Fontenay-sous-Bois, France)
Ethanol, HPLC grade	Roth (Karlsruhe)

Ethylenediaminetetraacetic acid disodium salt	Sigma-Aldrich (Steinheim)
Fetal calf serum (FCS)	PAA Laboratories (Pasching, Austria)
Gentamycin	Biochrom (Berlin)
Germanium standard solution (1 g/L Ge, 2% HNO_3)	Merck (Darmstadt)
L-Glutamine, 0.7 mM	Biochrom (Berlin)
L-Glutathione reduced	Sigma-Aldrich (Steinheim)
Glutathione Reductase, from baker's yeast (S. cerevisiae)	Roche (Mannheim)
Hoechst solution (20 mM)	Bio-Rad (Feldkirchen)
Hydrochloric acid	Roth (Karlsruhe)
Hydrocortisone solution (50 µM)	Sigma-Aldrich (Steinheim)
Hydrogen peroxide, 30%	Merck (Darmstadt)
Isopropanol ≥ 99,999%	Sigma-Aldrich (Steinheim)
Isotopically enriched (^{77}Se) metallic Se	Eurisotop SAS (Saarbrücken)
MEM-Earle's w L-Glutamin, w/o NaHCO3	Biochrom (Berlin)
Methanol, LC-MS grade	VWR (Darmstadt)
Methylselenocysteine, > 98%	Sigma-Aldrich (Steinheim)
NADPH tetrasodium salt	Sigma-Aldrich (Steinheim)
Neutral Red	Roth (Karlsruhe)
Nitric acid, 65% Suprapur	Merck (Darmstadt)
Non-essential amino acids (NEA)	Biochrom (Berlin)
Penicillin-Streptomycin (10,000 U/mL)	Gibco (Dublin, Ireland)

Potassium chloride (KCl), > 99,5%	Roth (Karlsruhe)
Potassium hydroxide (KOH), > 90%	Roth (Karlsruhe)
Potassium dihydrogen phosphate (KH_2PO_4), ≥ 99%	Roth (Karlsruhe)
di-Potassium hydrogen phosphate (K_2HPO_4), > 99%	Roth (Karlsruhe)
Protease Inhibitor Cocktail Set III	Millipore (Darmstadt)
Resazurin	Sigma-Aldrich (Steinheim)
Selenium standard solution (1 g/L Se, 2% HNO_3)	Merck (Darmstadt)
Selenomethionine, ≥ 99%	Fluka (St. Gallen, Switzerland)
Sodium azide	Sigma-Aldrich (Steinheim)
Sodium carbonate (Na_2CO3), > 99,5%	Roth (Karlsruhe)
Sodium chloride (NaCl), > 99,9%	Roth (Karlsruhe)
Sodium dihydrogen phosphate (NaH_2PO_4), > 99%	Roth (Karlsruhe)
Sodium dodecyl sulfate	VWR (Darmstadt)
Sodium hydrogen carbonate (NaHCO3), > 99%	Roth (Karlsruhe)
di-Sodium hydrogen phosphate (Na_2HPO_4), > 99,5%	Roth (Karlsruhe)
Sodium hydroxide (NaOH), > 90%	Roth (Karlsruhe)
Sodium selenite pentahydrate, ≥ 99,0%	Sigma-Aldrich (Steinheim)
Tris	Sigma-Aldrich (Steinheim)
Triton X-100	Sigma-Aldrich (Steinheim)
Trypsin, 5 g/L	Sigma-Aldrich (Steinheim)

Tuning solution (10 mg/L Ce, Co, Li, Tl, Y; 2% HNO_3)	Agilent (Waldbronn)

8.3 Consumables

6 Well plate	TPP (Trasadingen, Switzerland)
12 Well plate	TPP (Trasadingen, Switzerland)
24 Well plate	TPP (Trasadingen, Switzerland)
96 Well plate	TPP (Trasadingen, Switzerland)
Butane CV360	CampinGAZ (Hattersheim)
Casy®Cups	Roche (Mannheim)
Casy®Ton Solution	Roche (Mannheim)
Casy®Clean Solution	Roche (Mannheim)
Cell culture dishes, 6, 10, 15 cm	TPP (Trasadingen, Switzerland)
Cellulose acetate syringe filter, 0.2 and 0.45 µm	VWR (Darmstadt), Corning (Wiesbaden)
Cryotubes, 1.6 mL	Sarstedt (Nümbrecht)
Disposable syringes, 2, 5, 10 mL	Braun (Melsungen)
Glass bottles, 50, 100, 250, 500, 1000 mL	Schott (Mainz)
Glass pipettes	VWR (Darmstadt)
Glass vials, 1.5 mL, 32 x 11.6 mm	VWR (Darmstadt)
Micro tubes, 1.5 and 5.0 mL	Eppendorf (Hamburg)
Micro tubes, 2.0 mL	VWR (Darmstadt)
Parafilm®	Serva Feinbiochemica (Heidelberg)

Pipette tips, 10, 200, 1000 µL	Brand (Westheim)
Pipette tips, 5 mL	Eppendorf (Hamburg)
Plastic tubes, 15 and 50 mL	Corning (Wiesbaden)
Screw neck cell culture flasks, 25 and 75 cm^2	Corning (Wiesbaden)
Transwell® filter inserts for 12-well plates	Corning (Wiesbaden)
Vial screw caps, 9 mm, with 1 mm septum	VWR (Darmstadt)

8.4 Buffers, eluents and solutions

Affinity chromatography mobile phase A, pH 7.0	0.17 M Ammonium acetate 10 µg/L Ge 2% (v/v) Ethanol
Affinity chromatography mobile phase B pH 7.0	1.3 M Ammonium acetate 10 µg/L Ge 2% (v/v) Ethanol
Anion-exchange chromatography mobile phase, pH 9.5	5 mM Ammonium malonate
GPx homogenization buffer	100 mM Tris 300 mM KCl 0.1% Triton X-100 0.1% Protease Inhibitor Cocktail Set III
GPx reaction solution	96 mM Tris 4.8 mM EDTA 0.96 mM NaN_3 0.1% (v/v) Triton X-100 0.22 mM NADPH 13 mM $NaHCO_3$ 3.4 mM GSH 1.1 nM HCl 0.66 U/mL GR 18 mM $(NH_4)_2SO_4$

GPx substrate	0.00375% H_2O_2 in deionized water
GR buffer, pH 6.0	3.2 M $(NH_4)_2SO_4$ in deionized water
HepG2/Caco-2 medium, pH 6.8	MEM 10% FCS 100 U/mL Penicillin 100 µg/mL Streptomycin 1% (v/v) NEA
PBCEC proliferation medium	Earle's 199 Medium 10% FCS 50 U/mL Penicillin 50 µg/mL Streptomycin 50 µg/mL Gentamycin 0.7 mM L-Glutamine
PBCEC differentiation medium	DMEM/Ham's F12 Medium 50 U/mL Penicillin 50 µg/mL Streptomycin 50 µg/mL Gentamycin 4.1 mM L-Glutamine 550 nM Hydrocortisone
PBS, pH 7.4	100 mM NaCl 7 mM Na_2HPO_4 4.5 mM KCl 3 mM KH_2PO_4
PBS-EDTA, pH 7.4	100 mM NaCl 7 mM Na_2HPO_4 4.5 mM KCl 3 mM KH_2PO_4 0.5 mM EDTA
PBS-UVC, pH 7.4	136.8 mM NaCl 8.45 mM Na_2HPO_4 2.15 mM KCl 1.18 mM KH_2PO_4
Reversed-phase chromatography mobile phase, pH 3.0	20 mM Ammonium formate 3% Methanol

RIPA buffer, pH 7.6	150 mM NaCl 10 mM Tris 1 mM EDTA 1% (v/v) Triton X-100 24 mM DOC 3.5 mM SDS
Trypsin solution	PBS-EDTA 0.25% (v/v) Trypsin

Curriculum Vitae

This page contains personal data and was removed from the document.

This page contains personal data and was removed from the document.

Fundings

1. G-RISC mobility funds for young scientists.
   Project B-2018a-1 “Molybdenum speciation in human cerebrospinal fluid”
   Supervisor: Prof. Dr. Bernhard Michalke, Research Unit Analytical BioGeoChemistry
   Helmholtz Zentrum München, Neuherberg, Germany

2. G-RISC mobility funds for young scientists.
   Project B-2017a-3 “Protein binding and speciation of molybdenum in biological fluids”
   Supervisor: Prof. Dr. Bernhard Michalke, Research Unit Analytical BioGeoChemistry
   Helmholtz Zentrum München, Neuherberg, Germany

Conference abstracts

1. “Direct Detection of Arsenic in Human Urine by High-Resolution ICP-MS”
   Ivanenko N., Ivanenko A., Solovyev N., Navolotskii D., **Drobyshev E.**
   Annual conference of the Institute of Chemistry “Mendeleev-2013”
   Saint Petersburg, Russia, April 2013

2. “Pharmacokinetics and toxicity of a novel radiomitigator BP-C2, a complex of molybdenum with benzyl polycarboxylic acids, originating from lignin.”
   Drobyshev E., Kraev S., Maydin M., Gubareva E., Semenov A., Ivanenko N., Solovyev N.
   32th Annual Conference of the German Society for Minerals and Trace Minerals (GMS) in cooperation with the German Federal Institute for Risk Assessment (BfR)
   Berlin, Germany, October 2016

3. “New experimental model of beryllium toxicity.”
   Drobyshev E., Solovyev N., Gaikova O., Ivanenko N., Ivanov M., Kashuro V., Kybarskaya L., Dagaev S.
   16th International Symposium on Trace Elements in Man and Animals (TEMA-16)
   Saint Petersburg, Russia, June 2017

4. “Molybdenum protein binding in human serum and cerebrospinal fluid.”
   Drobyshev E., Solovyev N., Michalke B.
   33th Joint Annual Meeting of the German Society for Minerals and Trace Elements (GMS) with Zinc-UK and Zinc-Net COST Training School
   Aachen, Germany, September 2017

5. “Characterizing selenoneine by the use of in vitro models.”
   Drobyshev E., Ebert F., Müller S.M., Bornhorst J., Kuehnelt D., Schwerdtle T.
   7th International Symposium of the Federation of European Societies on Trace Elements and Minerals (FESTEM) together with the 35th Annual GMS Meeting
   Potsdam, Germany, April 2019

Publications

Thesis related publications:

1. "Selenoneine Antioxidant Action in Caco-2 Cells? in Comparison with Ergothioneine and other Small Selenium Species."
   Drobyshev E., Kühnelt D., Kopp J., Kipp A., Ebert F., Schwerdtle T.
   Under submission

2. "Capabilities of Selenoneine to Cross the *In Vitro* Blood-Brain Barrier Model."
   Drobyshev E., Raschke S., Glabonjat R.A., Bornhorst J., Ebert F., Kühnelt D., Schwerdtle T.
   Metallomics, **2021**, 13, doi.org/10.1093/mtomcs/mfaa007

Other publications:

1. "Selenium at the neural barriers: a review"
   Solovyev N., **Drobyshev E.**, Blume B., Michalke B.
   Frontiers in Neuroscience, **2021**, 15, p. 88

2. "New insight in beryllium toxicity excluding exposure to beryllium-containing dust: Accumulation patterns, target organs, and elimination."
   Drobyshev E., Kybarskaya L., Dagaev S., Solovyev N.
   Archives of Toxicology, **2019**, 93, p. 859-869

3. "Selenium-rich mushrooms cultivation on a wheat straw substrate from seleniferous area in Punjab, India."
   Solovyev N., Prakash N.T., Bhatia P., Prakash R., **Drobyshev E.**, Michalke M.
   Journal of Trace Elements in Medicine and Biology, **2018**, 50, p. 362-366

4. "Selenium, selenoprotein P, and Alzheimer's disease: is there a link?"
   Solovyev N., **Drobyshev E.**, Bjørklund G., Lysiuk R., Dubrovskii Y., Rayman, M.P.
   Free Radical Biology and Medicine, **2018**, 127, p. 124-133

5. "Accumulation Patterns of Subchronic Aluminum Toxicity Model After Gastrointestinal Administration in Rats."
   Drobyshev E., Solovyev N., Gorokhovskiy B., Kashuro, V.A.
   Biological Trace Element Research, **2018**, 185, p. 384-394

6. "The importance of speciation analysis in neurodegeneration research."
   Michalke B., Willkommen D., **Drobyshev E.**, Solovyev N.
   Trends in Analytical Chemistry, **2018**, 104, p. 160-170

7. "Anticancer activity and tissue distribution of platinum (II) complex with lignin-derived polymer of benzene-poly-carboxylic acids."

Solovyev N., Fedoros E., **Drobyshev E.**, Ivanenko N., Pigarev S., Tyndyk M., Anisimov V., Vilpan Y., Panchenko A.
Journal of Trace Elements in Medicine and Biology, **2017**, 43, p. 72-79

8. "Direct isotope analysis of Chernobyl microparticles using time-of-flight mass spectrometry with pulsed glow discharge."
Ganeev A., Gubal A., Korotetski B., Bogdanova O., Burakov B., Titova A., Solovyev N., Ivanenko N., **Drobyshev E.**, Iakovleva E., Sillanpää, M.
Microchemical Journal, **2017**, 132, p. 286-292

9. "Trace element biomonitoring in hair of school children from a polluted area by sector field inductively coupled plasma mass spectrometry."
Drobyshev E., Solovyev N., Ivanenko N., Kombarova M., Ganeev A.
Journal of Trace Elements in Medicine and Biology, **2017**, 39, p. 14-20

10. "Results and prospects of development of new polyphenolic drugs for cancer patients."
Anisimov V., Larsen S., Lofberg S., Baldueva I., Malek A., Nielsen T.K., Fedoros E., Perminova I., **Drobyshev E.**, Bykov V., Panchenko A., Scherbakov A., Belyaev, A.
Oncotarget, **2017**, 8, p. 100951-100956

11. Patent RU 2641380: "Method for Beryllium Intoxication Simulation"
Drobyshev E., Solovyev N., Gaikova O., Ivanenko N., Ivanov M., Kashuro V., Kybarskaya L., Dagaev S.
October **2016**

12. "Biomonitoring of 20 trace elements in blood and urine of occupationally exposed workers by sector field inductively coupled plasma mass spectrometry."
Ivanenko N., Ivanenko A., Solovyev N., Zeimal' A., Navolotskii D., **Drobyshev E.**
Talanta, **2013**, 116, p. 764-769

9. References

1. Greenwood, N.N., *Chemistry of the elements*. Second edition. ed, ed. A. Earnshaw. 1998, Oxford ;: Butterworth-Heinemann.
2. Malisa, E.P., *The Behaviour of Selenium in Geological Processes.* Environmental Geochemistry and Health, 2001. **23**(2): p. 137-158.
3. Gupta, M. and S. Gupta, *An Overview of Selenium Uptake, Metabolism, and Toxicity in Plants.* Frontiers in Plant Science, 2017. **7**(2074).
4. Rayman, M.P., H.G. Infante, and M. Sargent, *Food-chain selenium and human health: spotlight on speciation.* British Journal of Nutrition, 2008. **100**(2): p. 238-253.
5. Rayman, M.P., *Selenium and human health.* The Lancet, 2012. **379**(9822): p. 1256-1268.
6. Vinceti, M., et al., *Chapter One - The Epidemiology of Selenium and Human Cancer*, in *Advances in Cancer Research*, K.D. Tew and F. Galli, Editors. 2017, Academic Press. p. 1-48.
7. *Environmental Health Criteria: Selenium*. 1987, World Health Organization: Geneva.
8. Yang, G.Q., et al., *Endemic selenium intoxication of humans in China.* The American Journal of Clinical Nutrition, 1983. **37**(5): p. 872-881.
9. Fairweather-Tait, S.J., et al., *Selenium in Human Health and Disease.* Antioxidants & Redox Signaling, 2010. **14**(7): p. 1337-1383.
10. Combs, G.F., Jr., *Biomarkers of selenium status.* Nutrients, 2015. **7**(4): p. 2209-2236.
11. Davis, T.Z. and J.O. Hall, *Chapter 34 - Selenium*, in *Reproductive and Developmental Toxicology (Second Edition)*, R.C. Gupta, Editor. 2017, Academic Press. p. 595-605.
12. Jablonska, E. and M. Vinceti, *Selenium and Human Health: Witnessing a Copernican Revolution?* Journal of Environmental Science and Health, Part C, 2015. **33**(3): p. 328-368.
13. Efsa Panel on Dietetic Products, N. and Allergies, *Scientific Opinion on Dietary Reference Values for selenium.* EFSA Journal, 2014. **12**(10): p. 3846.
14. *Institute of Medicine. Dietary Reference Intakes for Vitamin C, Vitamin E, Selenium, and Carotenoids*. 2000, Washington, DC: The National Academies Press. 528.
15. Carlson, B.A., et al., *Mammalian selenocysteine tRNA*, in *Selenium: Its Molecular Biology and Role in Human Health*, D.L. Hatfield, Editor. 2001, Springer US: Boston, MA. p. 23-32.
16. Gladyshev, V.N. and G.V. Kryukov, *Evolution of selenocysteine-containing proteins: Significance of identification and functional characterization of selenoproteins.* BioFactors, 2001. **14**(1-4): p. 87-92.
17. Imai, H., et al., *Early embryonic lethality caused by targeted disruption of the mouse PHGPx gene.* Biochemical and Biophysical Research Communications, 2003. **305**(2): p. 278-286.
18. Rayman, M.P., *The importance of selenium to human health.* The Lancet, 2000. **356**(9225): p. 233-241.
19. Gladyshev, V.N. and D.L. Hatfield, *Analysis of Selenocysteine-Containing Proteins.* Current Protocols in Protein Science, 2000. **20**(1): p. 3.8.1-3.8.18.
20. Schomburg, L., *Selenium, selenoproteins and the thyroid gland: interactions in health and disease.* Nat Rev Endocrinol, 2012. **8**(3): p. 160-71.
21. Schomburg, L., *Dietary Selenium and Human Health.* Nutrients, 2017. **9**(1).

22. Solovyev, N., F. Vanhaecke, and B. Michalke, *Selenium and iodine in diabetes mellitus with a focus on the interplay and speciation of the elements.* Journal of Trace Elements in Medicine and Biology, 2019. **56**: p. 69-80.
23. Kieliszek, M. and S. Błażejak, *Current Knowledge on the Importance of Selenium in Food for Living Organisms: A Review.* Molecules, 2016. **21**(5).
24. Savaskan, N.E., et al., *Selenium deficiency increases susceptibility to glutamate-induced excitotoxicity.* The FASEB Journal, 2003. **17**(1): p. 112-114.
25. Aaseth, J., et al., *Treatment strategies in Alzheimer's disease: a review with focus on selenium supplementation.* BioMetals, 2016. **29**(5): p. 827-839.
26. Labunskyy, V.M., D.L. Hatfield, and V.N. Gladyshev, *Selenoproteins: molecular pathways and physiological roles.* Physiological reviews, 2014. **94**(3): p. 739-777.
27. Benstoem, C., et al., *Selenium and its supplementation in cardiovascular disease--what do we know?* Nutrients, 2015. **7**(5): p. 3094-3118.
28. Moslemi, M.K. and S. Tavanbakhsh, *Selenium-vitamin E supplementation in infertile men: effects on semen parameters and pregnancy rate.* International journal of general medicine, 2011. **4**: p. 99-104.
29. Pieczyńska, J. and H. Grajeta, *The role of selenium in human conception and pregnancy.* Journal of Trace Elements in Medicine and Biology, 2015. **29**: p. 31-38.
30. Dominiak, A., et al., *Selenium in the Therapy of Neurological Diseases. Where is it Going?* Current neuropharmacology, 2016. **14**(3): p. 282-299.
31. Rita Cardoso, B., et al., *Selenium status in elderly: Relation to cognitive decline.* Journal of Trace Elements in Medicine and Biology, 2014. **28**(4): p. 422-426.
32. Benton, D. and R. Cook, *The impact of selenium supplementation on mood.* Biological Psychiatry, 1991. **29**(11): p. 1092-1098.
33. Vinceti, M., et al., *Selenium for preventing cancer.* The Cochrane database of systematic reviews, 2014. **2014**(3): p. CD005195-CD005195.
34. Kamwesiga, J., et al., *Effect of selenium supplementation on CD4+ T-cell recovery, viral suppression and morbidity of HIV-infected patients in Rwanda: a randomized controlled trial.* AIDS, 2015. **29**(9).
35. Gladyshev, V.N. and D.L. Hatfield, *Selenocysteine-containing proteins in mammals.* Journal of Biomedical Science, 1999. **6**(3): p. 151-160.
36. Stadtman, T.C., *Selenocysteine.* Annual Review of Biochemistry, 1996. **65**: p. 83-100.
37. Arnér, E.S.J., *Selenoproteins—What unique properties can arise with selenocysteine in place of cysteine?* Experimental Cell Research, 2010. **316**(8): p. 1296-1303.
38. Weekley, C.M. and H.H. Harris, *Which form is that? The importance of selenium speciation and metabolism in the prevention and treatment of disease.* Chem Soc Rev, 2013. **42**(23): p. 8870-94.
39. Zhong, L.W. and A. Holmgren, *Essential role of selenium in the catalytic activities of mammalian thioredoxin reductase revealed by characterization of recombinant enzymes with selenocysteine mutations.* Journal of Biological Chemistry, 2000. **275**(24): p. 18121-18128.
40. Collet, J.-F. and J. Messens, *Structure, Function, and Mechanism of Thioredoxin Proteins.* Antioxidants & Redox Signaling, 2010. **13**(8): p. 1205-1216.
41. Fátima, N., et al., *Role of selenium and glutathione peroxidase on development, growth, and oxidative balance in rat offspring.* REPRODUCTION, 2013. **146**(6): p. 659-667.
42. Ardanaz, N., et al., *Lack of Glutathione Peroxidase 1 Accelerates Cardiac-Specific Hypertrophy and Dysfunction in Angiotensin II Hypertension.* Hypertension, 2010. **55**(1): p. 116-123.

43. Canli, Ö., et al., *Glutathione peroxidase 4 prevents necroptosis in mouse erythroid precursors.* Blood, 2016. **127**(1): p. 139-148.
44. Bianco, A.C. and B.W. Kim, *Deiodinases: implications of the local control of thyroid hormone action.* The Journal of Clinical Investigation, 2006. **116**(10): p. 2571-2579.
45. Yang, G., et al., *The Role of Selenium in Keshan Disease*, in *Advances in Nutritional Research*, H.H. Draper, Editor. 1984, Springer US: Boston, MA. p. 203-231.
46. Yao, Y., F. Pei, and P. Kang, *Selenium, iodine, and the relation with Kashin-Beck disease.* Nutrition, 2011. **27**(11): p. 1095-1100.
47. Wang, L., et al., *Serious Selenium Deficiency in the Serum of Patients with Kashin–Beck Disease and the Effect of Nano-Selenium on Their Chondrocytes.* Biological Trace Element Research, 2020. **194**(1): p. 96-104.
48. Chen, J., *The Role of Selenium in Special Endemic Diseases and Cancer in China*, in *Trace Elements in Man and Animals 6*, L.S. Hurley, et al., Editors. 1988, Springer US: Boston, MA. p. 149-153.
49. Spallholz, J.E., L.M. Boylan, and H.S. Larsen, *Advances in Understanding Selenium's Role in the Immune System.* Annals of the New York Academy of Sciences, 1990. **587**(1): p. 123-139.
50. Kiremidjian-Schumacher, L., et al., *Supplementation with selenium and human immune cell functions.* Biological Trace Element Research, 1994. **41**(1): p. 115.
51. Guimarães, M.J., et al., *Identification of a novel selD homolog from Eukaryotes, Bacteria, and Archaea: Is there an autoregulatory mechanism in selenocysteine metabolism?* Proceedings of the National Academy of Sciences, 1996. **93**(26): p. 15086.
52. Oldereid, N., Y. Thomassen, and K. Purvis, *Selenium in human male reproductive organs.* Human reproduction, 1998. **13 8**: p. 2172-6.
53. Ursini, F., et al., *Dual Function of the Selenoprotein PHGPx During Sperm Maturation.* Science, 1999. **285**(5432): p. 1393.
54. Weber, G.F., et al., *Glutathione peroxidase deficiency and childhood seizures.* The Lancet, 1991. **337**(8755): p. 1443-1444.
55. Ramaekers, V.T., et al., *Selenium Deficiency Triggering Intractable Seizures.* Neuropediatrics, 1994. **25**(04): p. 217-223.
56. Flores-Mateo, G., et al., *Selenium and coronary heart disease: a meta-analysis.* The American journal of clinical nutrition, 2006. **84**(4): p. 762-773.
57. Hawkes, W.C. and L. Hornbostel, *Effects of dietary selenium on mood in healthy men living in a metabolic research unit.* Biological Psychiatry, 1996. **39**(2): p. 121-128.
58. Benton, D. and R. Cook, *Selenium supplementation improves mood in a double-blind crossover trial.* Psychopharmacology, 1990. **102**(4): p. 549-550.
59. Rotruck, J.T., et al., *Selenium: Biochemical Role as a Component of Glutathione Peroxidase.* Science, 1973. **179**(4073): p. 588.
60. Marín-García, J., *Chapter 14 - Oxidative Stress and Cell Death in Cardiovascular Disease: A Post-Genomic Appraisal*, in *Post-Genomic Cardiology (Second Edition)*, J. Marín-García, Editor. 2014, Academic Press: Boston. p. 471-498.
61. Espinoza, S.E., et al., *Glutathione Peroxidase Enzyme Activity in Aging.* The Journals of Gerontology: Series A, 2008. **63**(5): p. 505-509.
62. Cohen, G. and P. Hochstein, *Glutathione Peroxidase: The Primary Agent for the Elimination of Hydrogen Peroxide in Erythrocytes*.* Biochemistry, 1963. **2**(6): p. 1420-1428.
63. Arthur, J.R., *The glutathione peroxidases.* Cellular and Molecular Life Sciences CMLS, 2001. **57**(13): p. 1825-1835.

64. Meyer, M., H.L. Pahl, and P.A. Baeuerle, *Regulation of the transcription factors NF-κB and AP-1 by redox changes.* Chemico-Biological Interactions, 1994. **91**(2): p. 91-100.
65. Yu, B.P. and H.Y. Chung, *Adaptive mechanisms to oxidative stress during aging.* Mechanisms of Ageing and Development, 2006. **127**(5): p. 436-443.
66. Brigelius-Flohé, R., *Tissue-specific functions of individual glutathione peroxidases.* Free Radical Biology and Medicine, 1999. **27**(9): p. 951-965.
67. Imai, H. and Y. Nakagawa, *Biological significance of phospholipid hydroperoxide glutathione peroxidase (PHGPx, GPx4) in mammalian cells.* Free Radical Biology and Medicine, 2003. **34**(2): p. 145-169.
68. Ryoji, F. and K. Takashi, *Tissue Distribution, Molecular Cloning, and Gene Expression of Cytosolic Glutathione Peroxidase in Japanese Monkey.* Zoological Science, 2003. **20**(7): p. 861-868.
69. Brigelius-Flohé, R. and M. Maiorino, *Glutathione peroxidases.* Biochimica et Biophysica Acta (BBA) - General Subjects, 2013. **1830**(5): p. 3289-3303.
70. de Haan, J.B., et al., *Mice with a Homozygous Null Mutation for the Most Abundant Glutathione Peroxidase, Gpx1, Show Increased Susceptibility to the Oxidative Stress-inducing Agents Paraquat and Hydrogen Peroxide.* Journal of Biological Chemistry, 1998. **273**(35): p. 22528-22536.
71. Ho, Y.-S., et al., *Mice Deficient in Cellular Glutathione Peroxidase Develop Normally and Show No Increased Sensitivity to Hyperoxia*.* Journal of Biological Chemistry, 1997. **272**(26): p. 16644-16651.
72. Cheng, W.-H., et al., *Cellular Glutathione Peroxidase Is the Mediator of Body Selenium To Protect against Paraquat Lethality in Transgenic Mice.* The Journal of Nutrition, 1998. **128**(7): p. 1070-1076.
73. Chu, F.F., J.H. Doroshow, and R.S. Esworthy, *Expression, characterization, and tissue distribution of a new cellular selenium-dependent glutathione peroxidase, GSHPx-GI.* Journal of Biological Chemistry, 1993. **268**(4): p. 2571-2576.
74. Esworthy, R.S., et al., *Low glutathione peroxidase activity in Gpx1knockout mice protects jejunum crypts from γ-irradiation damage.* American Journal of Physiology-Gastrointestinal and Liver Physiology, 2000. **279**(2): p. G426-G436.
75. Dittrich, A.M., et al., *Glutathione peroxidase-2 protects from allergen-induced airway inflammation in mice.* European Respiratory Journal, 2010. **35**(5): p. 1148.
76. Florian, S., et al., *Loss of GPx2 increases apoptosis, mitosis, and GPx1 expression in the intestine of mice.* Free Radical Biology and Medicine, 2010. **49**(11): p. 1694-1702.
77. Takahashi, K. and H.J. Cohen, *Selenium-dependent glutathione peroxidase protein and activity: immunological investigations on cellular and plasma enzymes.* Blood, 1986. **68**(3): p. 640-645.
78. Avissar, N., et al., *Human kidney proximal tubules are the main source of plasma glutathione peroxidase.* American Journal of Physiology-Cell Physiology, 1994. **266**(2): p. C367-C375.
79. Maser, R.L., B.S. Magenheimer, and J.P. Calvet, *Mouse plasma glutathione peroxidase. cDNA sequence analysis and renal proximal tubular expression and secretion.* Journal of Biological Chemistry, 1994. **269**(43): p. 27066-27073.
80. Howie, A.F., et al., *Thyroidal extracellular glutathione peroxidase: a potential regulator of thyroid-hormone synthesis.* The Biochemical journal, 1995. **308 (Pt 3)**(Pt 3): p. 713-717.

81. Tham, D.M., et al., *Expression of extracellular glutathione peroxidase in human and mouse gastrointestinal tract.* American Journal of Physiology-Gastrointestinal and Liver Physiology, 1998. **275**(6): p. G1463-G1471.
82. Björnstedt, M., et al., *The thioredoxin and glutaredoxin systems are efficient electron donors to human plasma glutathione peroxidase.* The Journal of biological chemistry, 1994. **269**(47): p. 29382-29384.
83. Schuckelt, R., et al., *Phospholipid Hydroperoxide Glutathione Peroxidase is a Seleno-Enzyme Distinct from the Classical Glutathione Peroxidase as Evident from Cdna and Amino Acid Sequencing.* Free Radical Research Communications, 1991. **14**(5-6): p. 343-361.
84. Maiorino, M., et al., *Reactivity of Phospholipid Hydroperoxide Glutathione Peroxidase with Membrane and Lipoprotein Lipid Hydroperoxides.* Free Radical Research Communications, 1991. **12**(1): p. 131-135.
85. Maiorino, M., et al., *Probing the presumed catalytic triad of a selenium-containing peroxidase by mutational analysis.* Zeitschrift fur Ernahrungswissenschaft, 1998. **37 Suppl 1**: p. 118-121.
86. Hoekstra, W.G., *Biochemical function of selenium and its relation to vitamin E.* Federation proceedings, 1975. **34**(11): p. 2083-2089.
87. Solovyev, N., et al., *Selenium at the Neural Barriers: A Review.* Frontiers in Neuroscience, 2021. **15**: p. 88.
88. Kühbacher, M., et al., *The brain selenoproteome: priorities in the hierarchy and different levels of selenium homeostasis in the brain of selenium-deficient rats.* Journal of Neurochemistry, 2009. **110**(1): p. 133-142.
89. Burk, R.F., et al., *Response of rat selenoprotein P to selenium administration and fate of its selenium.* American Journal of Physiology-Endocrinology and Metabolism, 1991. **261**(1): p. E26-E30.
90. Burk, R.F. and K.E. Hill, *Selenoprotein P-Expression, functions, and roles in mammals.* Biochimica Et Biophysica Acta-General Subjects, 2009. **1790**(11): p. 1441-1447.
91. Reeves, M.A. and P.R. Hoffmann, *The human selenoproteome: recent insights into functions and regulation.* Cellular and Molecular Life Sciences, 2009. **66**(15): p. 2457-2478.
92. Zhang, Y., et al., *Comparative analysis of selenocysteine machinery and selenoproteome gene expression in mouse brain identifies neurons as key functional sites of selenium in mammals.* J Biol Chem, 2008. **283**(4): p. 2427-38.
93. Cardoso, B.R., et al., *Selenium, selenoproteins and neurodegenerative diseases.* Metallomics, 2015. **7**(8): p. 1213-1228.
94. Solovyev, N.D., *Importance of selenium and selenoprotein for brain function: From antioxidant protection to neuronal signalling.* Journal of Inorganic Biochemistry, 2015. **153**: p. 1-12.
95. Michalke, B., et al., *The importance of speciation analysis in neurodegeneration research.* TrAC Trends in Analytical Chemistry, 2018. **104**: p. 160-170.
96. Zeevalk, G.D., R. Razmpour, and L.P. Bernard, *Glutathione and Parkinson's disease: Is this the elephant in the room?* Biomedicine & Pharmacotherapy, 2008. **62**(4): p. 236-249.
97. Rao, A.V. and B. Balachandran, *Role of Oxidative Stress and Antioxidants in Neurodegenerative Diseases.* Nutritional Neuroscience, 2002. **5**(5): p. 291-309.
98. Behl, C. and B. Moosmann, *Antioxidant neuroprotection in Alzheimer's disease as preventive and therapeutic approach2 2This article is part of a series of reviews on*

"Causes and Consequences of Oxidative Stress in Alzheimer's Disease." The full list of papers may be found on the homepage of the journal. Free Radical Biology and Medicine, 2002. **33**(2): p. 182-191.

99. Lin, M.T. and M.F. Beal, *Mitochondrial dysfunction and oxidative stress in neurodegenerative diseases.* Nature, 2006. **443**(7113): p. 787-795.
100. Baillet, A., et al., *The Role of Oxidative Stress in Amyotrophic Lateral Sclerosis and Parkinson's Disease.* Neurochemical Research, 2010. **35**(10): p. 1530-1537.
101. Haratake, M., et al., *Elevated amyloid-β plaque deposition in dietary selenium-deficient Tg2576 transgenic mice.* Metallomics, 2013. **5**(5): p. 479-483.
102. Ishrat, T., et al., *Selenium prevents cognitive decline and oxidative damage in rat model of streptozotocin-induced experimental dementia of Alzheimer's type.* Brain Research, 2009. **1281**: p. 117-127.
103. Rueli, R.H.L.H., et al., *Increased selenoprotein P in choroid plexus and cerebrospinal fluid in Alzheimer's disease brain.* Journal of Alzheimer's disease : JAD, 2015. **44**(2): p. 379-383.
104. Bellinger, F.P., et al., *Association of Selenoprotein P with Alzheimer's Pathology in Human Cortex.* Journal of Alzheimer's Disease, 2008. **15**: p. 465-472.
105. Imam, S.Z. and S.F. Ali, *Selenium, an antioxidant, attenuates methamphetamine-induced dopaminergic toxicity and peroxynitrite generation.* Brain Research, 2000. **855**(1): p. 186-191.
106. Bellinger, F.P., et al., *Changes in selenoprotein P in substantia nigra and putamen in Parkinson's disease.* Journal of Parkinson's disease, 2012. **2**(2): p. 115-126.
107. Vinceti, M., et al., *Are environmental exposures to selenium, heavy metals, and pesticides risk factors for amyotrophic lateral sclerosis?* Reviews on Environmental Health, 2012. **27**(1): p. 19-41.
108. Vinceti, M., et al., *Cerebrospinal fluid of newly diagnosed amyotrophic lateral sclerosis patients exhibits abnormal levels of selenium species including elevated selenite.* NeuroToxicology, 2013. **38**: p. 25-32.
109. Uğuz, A.C., et al., *Selenium Modulates Oxidative Stress-Induced Cell Apoptosis in Human Myeloid HL-60 Cells Through Regulation of Calcium Release and Caspase-3 and -9 Activities.* Journal of Membrane Biology, 2009. **232**(1): p. 15.
110. Kessi, J. and K.W. Hanselmann, *Similarities between the Abiotic Reduction of Selenite with Glutathione and the Dissimilatory Reaction Mediated by Rhodospirillum rubrum and Escherichia coli.* Journal of Biological Chemistry, 2004. **279**(49): p. 50662-50669.
111. Anundi, I., J. Högberg, and A. Ståhl, *Involvement of glutathione reductase in selenite metabolism and toxicity, studied in isolated rat hepatocytes.* Archives of Toxicology, 1982. **50**(2): p. 113-123.
112. Suzuki, K., *Metabolomics of Selenium: Se Metabolites Based on Speciation Studies.* Journal of Health Science, 2005. **51**: p. 107-114.
113. Kajander, E.O., et al., *Effects of selenomethionine on cell growth and on S-adenosylmethionine metabolism in cultured malignant cells.* The Biochemical journal, 1990. **267**(3): p. 767-774.
114. Kajander, E.O., et al., *Metabolism, cellular actions, and cytotoxicity of selenomethionine in cultured cells.* Biological Trace Element Research, 1991. **28**(1): p. 57-68.
115. Kajander, E.O. and A.M. Raina, *Affinity-chromatographic purification of S-adenosyl-L-homocysteine hydrolase. Some properties of the enzyme from rat liver.* The Biochemical journal, 1981. **193**(2): p. 503-512.

116. Xu, X.-M., et al., *Biosynthesis of Selenocysteine on Its tRNA in Eukaryotes.* PLOS Biology, 2006. **5**(1): p. e4.
117. Carlson, B.A., et al., *Identification and characterization of phosphoseryl-tRNA[Ser]Sec kinase.* Proceedings of the National Academy of Sciences of the United States of America, 2004. **101**(35): p. 12848.
118. Allmang, C., L. Wurth, and A. Krol, *The selenium to selenoprotein pathway in eukaryotes: More molecular partners than anticipated.* Biochimica et Biophysica Acta (BBA) - General Subjects, 2009. **1790**(11): p. 1415-1423.
119. Kryukov, G.V., et al., *Characterization of mammalian selenoproteomes.* Science, 2003. **300**(5624): p. 1439-1443.
120. Papp, L.V., et al., *Functional characterization of alternatively spliced human SECISBP2 transcript variants.* Nucleic Acids Research, 2008. **36**(22): p. 7192-7206.
121. Fagegaltier, D., et al., *Characterization of mSelB, a novel mammalian elongation factor for selenoprotein translation.* EMBO Journal, 2000. **19**(17): p. 4796-4805.
122. Small-Howard, A., et al., *Supramolecular complexes mediate selenocysteine incorporation in vivo.* Molecular and Cellular Biology, 2006. **26**(6): p. 2337-2346.
123. Xu, X.M., et al., *Evidence for direct roles of two additional factors, SECp43 and soluble liver antigen, in the selenoprotein synthesis machinery.* Journal of Biological Chemistry, 2005. **280**(50): p. 41568-41575.
124. Chavatte, L., B.A. Brown, and D.M. Driscoll, *Ribosomal protein L30 is a component of the UGA-selenocysteine recoding machinery in eukaryotes.* Nature structural & molecular biology, 2005. **12**(5): p. 408-416.
125. Olson, G.E., et al., *Apolipoprotein E Receptor-2 (ApoER2) Mediates Selenium Uptake from Selenoprotein P by the Mouse Testis*.* Journal of Biological Chemistry, 2007. **282**(16): p. 12290-12297.
126. Herz, J., *LRP: a bright beacon at the blood-brain barrier.* The Journal of clinical investigation, 2003. **112**(10): p. 1483-1485.
127. Gammelgaard, B., S. Stürup, and M.V. Christensen, *Human urinary excretion and metabolism of 82Se-enriched selenite and selenate determined by LC-ICP-MS.* Metallomics, 2012. **4**(2): p. 149-155.
128. Kuehnelt, D., et al., *Selenium metabolites in human urine after ingestion of selenite, L-selenomethionine, or DL-selenomethionine: a quantitative case study by HPLC/ICPMS.* Analytical and Bioanalytical Chemistry, 2005. **383**(2): p. 235-246.
129. Kobayashi, Y., et al., *Selenosugars are key and urinary metabolites for selenium excretion within the required to low-toxic range.* Proceedings of the National Academy of Sciences, 2002. **99**(25): p. 15932.
130. Suzuki, K.T., K. Kurasaki, and N. Suzuki, *Selenocysteine β-lyase and methylselenol demethylase in the metabolism of Se-methylated selenocompounds into selenide.* Biochimica et Biophysica Acta (BBA) - General Subjects, 2007. **1770**(7): p. 1053-1061.
131. Ganther, H.E., *Pathways of Selenium Metabolism Including Respiratory Excretory Products.* Journal of the American College of Toxicology, 1986. **5**(1): p. 1-5.
132. Rao, R., *Endotoxemia and gut barrier dysfunction in alcoholic liver disease.* Hepatology, 2009. **50**(2): p. 638-644.
133. Mazalli, M.R. and N. Bragagnolo, *Increase of Cholesterol Oxidation and Decrease of PUFA as a Result of Thermal Processing and Storage in Eggs Enriched with n-3 Fatty Acids.* Journal of Agricultural and Food Chemistry, 2009. **57**(11): p. 5028-5034.
134. Parks, D.A., *Oxygen radicals: mediators of gastrointestinal pathophysiology.* Gut, 1989. **30**(3): p. 293-298.

135. Sánchez, S., et al., *Effects of Dipyrone on Inflammatory Infiltration and Oxidative Metabolism in Gastric Mucosa: Comparison with Acetaminophen and Diclofenac.* Digestive Diseases and Sciences, 2002. **47**(6): p. 1389-1398.
136. Parks, D.A., T.K. Williams, and J.S. Beckman, *Conversion of xanthine dehydrogenase to oxidase in ischemic rat intestine: a reevaluation.* American Journal of Physiology-Gastrointestinal and Liver Physiology, 1988. **254**(5): p. G768-G774.
137. Babbs, C.F., *Oxygen radicals in ulcerative colitis.* Free Radical Biology and Medicine, 1992. **13**(2): p. 169-181.
138. Kajino-Sakamoto, R., et al., *TGF-β–Activated Kinase 1 Signaling Maintains Intestinal Integrity by Preventing Accumulation of Reactive Oxygen Species in the Intestinal Epithelium.* The Journal of Immunology, 2010. **185**(8): p. 4729.
139. Pérez, S., et al., *Redox signaling in the gastrointestinal tract.* Free Radical Biology and Medicine, 2017. **104**: p. 75-103.
140. Bhattacharyya, A., et al., *Oxidative stress: an essential factor in the pathogenesis of gastrointestinal mucosal diseases.* Physiological reviews, 2014. **94**(2): p. 329-354.
141. Tian, T., Z. Wang, and J. Zhang, *Pathomechanisms of Oxidative Stress in Inflammatory Bowel Disease and Potential Antioxidant Therapies.* Oxidative medicine and cellular longevity, 2017. **2017**: p. 4535194-4535194.
142. Kim, Y.J., E.-H. Kim, and K.B. Hahm, *Oxidative stress in inflammation-based gastrointestinal tract diseases: Challenges and opportunities.* Journal of Gastroenterology and Hepatology, 2012. **27**(6): p. 1004-1010.
143. Hrdina, J., et al., *The gastrointestinal microbiota affects the selenium status and selenoprotein expression in mice.* The Journal of Nutritional Biochemistry, 2009. **20**(8): p. 638-648.
144. Kasaikina, M.V., et al., *Dietary selenium affects host selenoproteome expression by influencing the gut microbiota.* FASEB journal : official publication of the Federation of American Societies for Experimental Biology, 2011. **25**(7): p. 2492-2499.
145. de Souza, A.P., et al., *The role of selenium in intestinal motility and morphology in a murine model of Typanosoma cruzi infection.* Parasitology Research, 2010. **106**(6): p. 1293-1298.
146. Barrett, C.W., et al., *Tumor Suppressor Function of the Plasma Glutathione Peroxidase Gpx3 in Colitis-Associated Carcinoma.* Cancer Research, 2013. **73**(3): p. 1245.
147. Speckmann, B., et al., *Induction of glutathione peroxidase 4 expression during enterocytic cell differentiation.* The Journal of biological chemistry, 2011. **286**(12): p. 10764-10772.
148. Andoh, A., et al., *Serum selenoprotein-P levels in patients with inflammatory bowel disease.* Nutrition, 2005. **21**(5): p. 574-579.
149. Steinbrenner, H., B. Speckmann, and H. Sies, *Toward understanding success and failures in the use of selenium for cancer prevention.* Antioxidants & redox signaling, 2013. **19**(2): p. 181-191.
150. Kudva, A.K., A.E. Shay, and K.S. Prabhu, *Selenium and inflammatory bowel disease.* American Journal of Physiology-Gastrointestinal and Liver Physiology, 2015. **309**(2): p. G71-G77.
151. Shibata, Y., M. Morita, and K. Fuwa, *Selenium and arsenic in biology: Their chemical forms and biological functions.* Advances in Biophysics, 1992. **28**: p. 31-80.
152. Yang, K.-L. and S.-J. Jiang, *Determination of selenium compounds in urine samples by liquid chromatography-inductively coupled plasma mass spectrometry with an ultrasonic nebulizer.* Analytica Chimica Acta, 1995. **307**(1): p. 109-115.

153. Manuel Marchante-Gayón, J., et al., *Speciation of selenium in human urine by HPLC-ICP-MS with a collision and reaction cell.* Journal of Analytical Atomic Spectrometry, 2001. **16**(5): p. 457-463.
154. Kuehnelt, D., et al., *Selenium metabolism to the trimethylselenonium ion (TMSe) varies markedly because of polymorphisms in the indolethylamine N-methyltransferase gene.* The American Journal of Clinical Nutrition, 2015. **102**(6): p. 1406-1415.
155. Hadrup, N. and G. Ravn-Haren, *Acute human toxicity and mortality after selenium ingestion: A review.* Journal of Trace Elements in Medicine and Biology, 2020. **58**: p. 126435.
156. Pentel, P., D. Fletcher, and J. Jentzen, *Fatal acute selenium toxicity.* Journal of forensic sciences, 1985. **30**(2): p. 556-562.
157. Hunsaker, D.M., H.A. Spiller, and D. Williams, *Acute Selenium Poisoning: Suicide by Ingestion.* Journal of Forensic Sciences, 2005. **50**(4): p. JFS2004247-5.
158. Köppel, C., et al., *Fatal Poisoning with Selenium Dioxide.* Journal of Toxicology: Clinical Toxicology, 1986. **24**(1): p. 21-35.
159. Williams, R. and A. Ansford, *Acute selenium toxicity: Australia's second fatality.* Pathology, 2007. **39**(2): p. 289-290.
160. See, K.A., et al., *Accidental death from acute selenium poisoning.* Medical Journal of Australia, 2006. **185**(7): p. 388-389.
161. Painter, E.P., *The Chemistry and Toxicity of Selenium Compounds, with Special Reference to the Selenium Problem.* Chemical Reviews, 1941. **28**(2): p. 179-213.
162. Marschall, T.A., et al., *Differing cytotoxicity and bioavailability of selenite, methylselenocysteine, selenomethionine, selenosugar 1 and trimethylselenonium ion and their underlying metabolic transformations in human cells.* Molecular Nutrition & Food Research, 2016. **60**(12): p. 2622-2632.
163. Rohn, I., et al., *Side-Directed Transfer and Presystemic Metabolism of Selenoneine in a Human Intestinal Barrier Model.* Molecular Nutrition & Food Research, 2019. **63**(12): p. 1900080.
164. Selvaraj, V., et al., *Selenium (sodium selenite) causes cytotoxicity and apoptotic mediated cell death in PLHC-1 fish cell line through DNA and mitochondrial membrane potential damage.* Ecotoxicology and Environmental Safety, 2013. **87**: p. 80-88.
165. Yang, L., et al., *Sodium selenite induces apoptosis and inhibits autophagy in human synovial sarcoma cell line SW982 in vitro.* Mol Med Rep, 2018. **17**(5): p. 6560-6568.
166. Stewart, M.S., et al., *Induction of differentiation and apoptosis by sodium selenite in human colonic carcinoma cells (HT29).* Cancer Letters, 1997. **117**(1): p. 35-40.
167. Shen, H.-M., C.-F. Yang, and C.-N. Ong, *Sodium selenite-induced oxidative stress and apoptosis in human hepatoma HepG2 cells.* International Journal of Cancer, 1999. **81**(5): p. 820-828.
168. Zou, Y., et al., *The JNK signaling pathway is involved in sodium-selenite-induced apoptosis mediated by reactive oxygen in HepG2 cells.* Cancer Biology & Therapy, 2008. **7**(5): p. 689-696.
169. Xiang, N., R. Zhao, and W. Zhong, *Sodium selenite induces apoptosis by generation of superoxide via the mitochondrial-dependent pathway in human prostate cancer cells.* Cancer Chemotherapy and Pharmacology, 2009. **63**(2): p. 351-362.
170. Valdiglesias, V., et al., *In vitro evaluation of selenium genotoxic, cytotoxic, and protective effects: a review.* Archives of Toxicology, 2010. **84**(5): p. 337-351.
171. Biswas, S., G. Talukder, and A. Sharma, *Chromosome damage induced by selenium salts in human peripheral lymphocytes.* Toxicology in Vitro, 2000. **14**(5): p. 405-408.

172. Lo, L.W., J. Koropatnick, and H.F. Stich, *The mutagenecity and cytotoxicity of selenite, "activated" selenite and selenate for normal and DNA repair-deficient human fibroblasts.* Mutation Research/Fundamental and Molecular Mechanisms of Mutagenesis, 1978. **49**(3): p. 305-312.
173. Lu, J., et al., *Selenite induction of DNA strand breaks and apoptosis in mouse leukemic L1210 cells.* Biochemical Pharmacology, 1994. **47**(9): p. 1531-1535.
174. Bao, P., et al., *Selenite-Induced Toxicity in Cancer Cells Is Mediated by Metabolic Generation of Endogenous Selenium Nanoparticles.* Journal of Proteome Research, 2015. **14**(2): p. 1127-1136.
175. Wallenberg, M., S. Misra, and M. Björnstedt, *Selenium Cytotoxicity in Cancer.* Basic & Clinical Pharmacology & Toxicology, 2014. **114**(5): p. 377-386.
176. Rayman, M.P., *Food-chain selenium and human health: emphasis on intake.* British Journal of Nutrition, 2008. **100**(2): p. 254-268.
177. Ammar, E.M. and D. Couri, *Acute toxicity of sodium selenite and selenomethionine in mice after ICV or IV administration.* Neurotoxicology, 1981. **2**(2): p. 383-386.
178. Kim, Y.Y. and D.C. Mahan, *Comparative effects of high dietary levels of organic and inorganic selenium on selenium toxicity of growing-finishing pigs.* Journal of Animal Science, 2001. **79**(4): p. 942-948.
179. Müller, S., J. Heider, and A. Böck, *The path of unspecific incorporation of selenium in Escherichia coli.* Archives of Microbiology, 1997. **168**(5): p. 421-427.
180. Lazard, M., et al., *Recent advances in the mechanism of selenoamino acids toxicity in eukaryotic cells.* Biomolecular Concepts, 2017. **8**(2): p. 93-104.
181. Schrauzer, G.N., *Selenomethionine: A Review of Its Nutritional Significance, Metabolism and Toxicity.* The Journal of Nutrition, 2000. **130**(7): p. 1653-1656.
182. Plateau, P., et al., *Exposure to selenomethionine causes selenocysteine misincorporation and protein aggregation in Saccharomyces cerevisiae.* Scientific Reports, 2017. **7**(1): p. 44761.
183. Hoefig, C.S., et al., *Comparison of different selenocompounds with respect to nutritional value vs. toxicity using liver cells in culture.* The Journal of Nutritional Biochemistry, 2011. **22**(10): p. 945-955.
184. Spallholz, J.E., V.P. Palace, and T.W. Reid, *Methioninase and selenomethionine but not Se-methylselenocysteine generate methylselenol and superoxide in an in vitro chemiluminescent assay: implications for the nutritional carcinostatic activity of selenoamino acids.* Biochemical Pharmacology, 2004. **67**(3): p. 547-554.
185. Yang, H. and X. Jia, *Safety evaluation of Se-methylselenocysteine as nutritional selenium supplement: Acute toxicity, genotoxicity and subchronic toxicity.* Regulatory Toxicology and Pharmacology, 2014. **70**(3): p. 720-727.
186. Tan, J.a., et al., *Selenium in soil and endemic diseases in China.* Science of The Total Environment, 2002. **284**(1): p. 227-235.
187. Yamashita, Y. and M. Yamashita, *Identification of a Novel Selenium-containing Compound, Selenoneine, as the Predominant Chemical Form of Organic Selenium in the Blood of Bluefin Tuna.* Journal of Biological Chemistry, 2010. **285**(24): p. 18134-18138.
188. Achouba, A., et al., *Selenoneine is a major selenium species in beluga skin and red blood cells of Inuit from Nunavik.* Chemosphere, 2019. **229**: p. 549-558.
189. Yamashita, Y., M. Yamashita, and H. Iida, *Selenium content in seafood in Japan.* Nutrients, 2013. **5**(2): p. 388-395.
190. Yamashita, M., et al., *Identification and Determination of Selenoneine, 2-Selenyl-Nα, Nα, Nα-Trimethyl-l-Histidine, as the Major Organic Selenium in Blood Cells in a Fish-Eating*

Population on Remote Japanese Islands. Biological Trace Element Research, 2013. **156**(1): p. 36-44.
191. Yamashita, Y., T. Yabu, and M. Yamashita, *Discovery of the strong antioxidant selenoneine in tuna and selenium redox metabolism.* World journal of biological chemistry, 2010. **1**(5): p. 144-150.
192. Yamashita, Y., et al., *Selenoneine, total selenium, and total mercury content in the muscle of fishes.* Fisheries Science, 2011. **77**(4): p. 679-686.
193. Lajin, B., et al., *Investigating the intra-individual variability in the human metabolic profile of urinary selenium.* Journal of Trace Elements in Medicine and Biology, 2016. **37**: p. 31-36.
194. Achouba, A., et al., *Plasma levels of selenium-containing proteins in Inuit adults from Nunavik.* Environment International, 2016. **96**: p. 8-15.
195. Little, M., et al., *Determinants of selenoneine concentration in red blood cells of Inuit from Nunavik (Northern Québec, Canada).* Environment International, 2019. **127**: p. 243-252.
196. Klein, M., et al., *Identification in human urine and blood of a novel selenium metabolite, Se-methylselenoneine, a potential biomarker of metabolization in mammals of the naturally occurring selenoneine, by HPLC coupled to electrospray hybrid linear ion trap-orbital ion trap MS.* Metallomics, 2011. **3**(5): p. 513-520.
197. Turrini, N.G., et al., *Biosynthesis and isolation of selenoneine from genetically modified fission yeast.* Metallomics, 2018. **10**(10): p. 1532-1538.
198. Ey, J., E. Schömig, and D. Taubert, *Dietary Sources and Antioxidant Effects of Ergothioneine.* Journal of Agricultural and Food Chemistry, 2007. **55**(16): p. 6466-6474.
199. Kalaras, M.D., et al., *Mushrooms: A rich source of the antioxidants ergothioneine and glutathione.* Food Chemistry, 2017. **233**: p. 429-433.
200. Rathore, H., S. Prasad, and S. Sharma, *Mushroom nutraceuticals for improved nutrition and better human health: A review.* PharmaNutrition, 2017. **5**(2): p. 35-46.
201. Sheridan, K.J., et al., *Ergothioneine Biosynthesis and Functionality in the Opportunistic Fungal Pathogen, Aspergillus fumigatus.* Scientific Reports, 2016. **6**(1): p. 35306.
202. Genghof, D.S. and O.V. Damme, *Biosynthesis of Ergothioneine and Hercynine by Mycobacteria.* Journal of Bacteriology, 1964. **87**(4): p. 852.
203. Melville, D.B., et al., *Ergothioneine in Microorganisms.* Journal of Biological Chemistry, 1956. **223**(1): p. 9-17.
204. McMenamy, R.H., et al., *Studies of Unbound Amino Acid Distributions in Plasma, Erythrocytes, Leukocytes And Urine of Normal Human Subjects.* The Journal of clinical investigation, 1960. **39**(11): p. 1675-1687.
205. Weigand-Heller, A.J., P.M. Kris-Etherton, and R.B. Beelman, *The bioavailability of ergothioneine from mushrooms (Agaricus bisporus) and the acute effects on antioxidant capacity and biomarkers of inflammation.* Preventive Medicine, 2012. **54**: p. S75-S78.
206. Mitsuyama, H. and J. May, *Uptake and antioxidant effects of ergothioneine in human erythrocytes.* Clinical science, 1999. **97 4**: p. 407-11.
207. Kumosani, T.A., *L-ergothioneine level in red blood cells of healthy human males in the Western province of Saudi Arabia.* Experimental & Molecular Medicine, 2001. **33**(1): p. 20-22.
208. Nakamura, T., et al., *Functional Characterization of Ergothioneine Transport by Rat Organic Cation/Carnitine Transporter Octn1 (slc22a4).* Biological and Pharmaceutical Bulletin, 2008. **31**(8): p. 1580-1584.

209. Gründemann, D., et al., *Discovery of the ergothioneine transporter.* Proceedings of the National Academy of Sciences of the United States of America, 2005. **102**(14): p. 5256.
210. Bacher, P., et al., *Substrate discrimination by ergothioneine transporter SLC22A4 and carnitine transporter SLC22A5: Gain-of-function by interchange of selected amino acids.* Biochimica et Biophysica Acta (BBA) - Biomembranes, 2009. **1788**(12): p. 2594-2602.
211. Cheah, I.K., et al., *Administration of Pure Ergothioneine to Healthy Human Subjects: Uptake, Metabolism, and Effects on Biomarkers of Oxidative Damage and Inflammation.* Antioxidants & Redox Signaling, 2016. **26**(5): p. 193-206.
212. Yamashita, M., et al., *Selenoneine, a Novel Selenium-Containing Compound, Mediates Detoxification Mechanisms against Methylmercury Accumulation and Toxicity in Zebrafish Embryo.* Marine Biotechnology, 2013. **15**(5): p. 559-570.
213. Arduini, A., et al., *Possible mechanism of inhibition of nitrite-induced oxidation of oxyhemoglobin by ergothioneine and uric acid.* Archives of Biochemistry and Biophysics, 1992. **294**(2): p. 398-402.
214. Borodina, I., et al., *The biology of ergothioneine, an antioxidant nutraceutical.* Nutrition Research Reviews, 2020. **33**(2): p. 190-217.
215. Pedrero Zayas, Z., et al., *Hemoglobin as a major binding protein for methylmercury in white-sided dolphin liver.* Analytical and Bioanalytical Chemistry, 2014. **406**(4): p. 1121-1129.
216. Lim, D., D. Gründemann, and F.P. Seebeck, *Total Synthesis and Functional Characterization of Selenoneine.* Angewandte Chemie International Edition, 2019. **58**(42): p. 15026-15030.
217. Servillo, L., N. D'Onofrio, and M.L. Balestrieri, *Ergothioneine Antioxidant Function: From Chemistry to Cardiovascular Therapeutic Potential.* Journal of Cardiovascular Pharmacology, 2017. **69**(4).
218. Abbott, N.J., *Comparative Physiology of the Blood-Brain Barrier*, in *Physiology and Pharmacology of the Blood-Brain Barrier*, M.W.B. Bradbury, Editor. 1992, Springer Berlin Heidelberg: Berlin, Heidelberg. p. 371-396.
219. Brøchner, C.B., C.B. Holst, and K. Møllgård, *Outer brain barriers in rat and human development.* Frontiers in Neuroscience, 2015. **9**: p. 75.
220. O'Brown, N.M., S.J. Pfau, and C. Gu, *Bridging barriers: a comparative look at the blood-brain barrier across organisms.* Genes & development, 2018. **32**(7-8): p. 466-478.
221. Abbott, N.J., et al., *Structure and function of the blood–brain barrier.* Neurobiology of Disease, 2010. **37**(1): p. 13-25.
222. Erickson, M.A. and W.A. Banks, *Blood–Brain Barrier Dysfunction as a Cause and Consequence of Alzheimer's Disease.* Journal of Cerebral Blood Flow & Metabolism, 2013. **33**(10): p. 1500-1513.
223. Terasaki, T. and S. Ohtsuki, *Brain-to-blood transporters for endogenous substrates and xenobiotics at the blood-brain barrier: an overview of biology and methodology.* NeuroRx : the journal of the American Society for Experimental NeuroTherapeutics, 2005. **2**(1): p. 63-72.
224. Rhea, E.M. and W.A. Banks, *Role of the Blood-Brain Barrier in Central Nervous System Insulin Resistance.* Frontiers in Neuroscience, 2019. **13**: p. 521.
225. Mayhan, W.G., *Regulation of Blood—Brain Barrier Permeability.* Microcirculation, 2001. **8**(2): p. 89-104.
226. Muldoon, L.L., et al., *Immunologic privilege in the central nervous system and the blood-brain barrier.* Journal of cerebral blood flow and metabolism : official journal of the International Society of Cerebral Blood Flow and Metabolism, 2013. **33**(1): p. 13-21.

227. Lenz, K.M. and L.H. Nelson, *Microglia and Beyond: Innate Immune Cells As Regulators of Brain Development and Behavioral Function.* Frontiers in Immunology, 2018. **9**: p. 698.
228. Thapa, P. and D.L. Farber, *The Role of the Thymus in the Immune Response.* Thorac Surg Clin, 2019. **29**(2): p. 123-131.
229. Zhao, E., et al., *Bone marrow and the control of immunity.* Cellular & Molecular Immunology, 2012. **9**(1): p. 11-19.
230. Kniesel, U. and H. Wolburg, *Tight Junctions of the Blood–Brain Barrier.* Cellular and Molecular Neurobiology, 2000. **20**(1): p. 57-76.
231. Liu, W.-Y., et al., *Tight Junction in Blood-Brain Barrier: An Overview of Structure, Regulation, and Regulator Substances.* CNS Neuroscience & Therapeutics, 2012. **18**(8): p. 609-615.
232. Chen, F., et al., *Disruptions of occludin and claudin-5 in brain endothelial cells in vitro and in brains of mice with acute liver failure.* Hepatology, 2009. **50**(6): p. 1914-1923.
233. Steinemann, A., et al., *Claudin-1, -2 and -3 Are Selectively Expressed in the Epithelia of the Choroid Plexus of the Mouse from Early Development and into Adulthood While Claudin-5 is Restricted to Endothelial Cells.* Frontiers in Neuroanatomy, 2016. **10**: p. 16.
234. Bauer, H., et al., *The Dual Role of Zonula Occludens (ZO) Proteins.* Journal of Biomedicine and Biotechnology, 2010. **2010**: p. 402593.
235. Tang, V.W. and D.A. Goodenough, *Paracellular Ion Channel at the Tight Junction.* Biophysical Journal, 2003. **84**(3): p. 1660-1673.
236. Kawedia, J.D., et al., *Interaction between transcellular and paracellular water transport pathways through Aquaporin 5 and the tight junction complex.* Proceedings of the National Academy of Sciences, 2007. **104**(9): p. 3621.
237. Villabona-Rueda, A., et al., *The Evolving Concept of the Blood Brain Barrier (BBB): From a Single Static Barrier to a Heterogeneous and Dynamic Relay Center.* Frontiers in cellular neuroscience, 2019. **13**: p. 405-405.
238. Abbott, N.J., L. Rönnbäck, and E. Hansson, *Astrocyte–endothelial interactions at the blood–brain barrier.* Nature Reviews Neuroscience, 2006. **7**(1): p. 41-53.
239. Smalheiser, N.R., *Do Neural Cells Communicate with Endothelial Cells via Secretory Exosomes and Microvesicles?* Cardiovascular Psychiatry and Neurology, 2009. **2009**: p. 383086.
240. Wu, K.-W., et al., *Neurovascular Interaction Promotes the Morphological and Functional Maturation of Cortical Neurons.* Frontiers in Cellular Neuroscience, 2017. **11**: p. 290.
241. Hawkins, B.T. and T.P. Davis, *The Blood-Brain Barrier/Neurovascular Unit in Health and Disease.* Pharmacological Reviews, 2005. **57**(2): p. 173.
242. Janzer, R.C. and M.C. Raff, *Astrocytes induce blood–brain barrier properties in endothelial cells.* Nature, 1987. **325**(6101): p. 253-257.
243. Siddharthan, V., et al., *Human astrocytes/astrocyte-conditioned medium and shear stress enhance the barrier properties of human brain microvascular endothelial cells.* Brain Research, 2007. **1147**: p. 39-50.
244. Bergers, G. and S. Song, *The role of pericytes in blood-vessel formation and maintenance.* Neuro-oncology, 2005. **7**(4): p. 452-464.
245. Balabanov, R. and P. Dore-Duffy, *Role of the CNS microvascular pericyte in the blood-brain barrier.* Journal of Neuroscience Research, 1998. **53**(6): p. 637-644.
246. Hellström, M., et al., *Lack of Pericytes Leads to Endothelial Hyperplasia and Abnormal Vascular Morphogenesis.* Journal of Cell Biology, 2001. **153**(3): p. 543-554.
247. Kubotera, H., et al., *Astrocytic endfeet re-cover blood vessels after removal by laser ablation.* Scientific Reports, 2019. **9**(1): p. 1263.

248. Miller, F.N. and D.E. Sims, *Contractile elements in the regulation of macromolecular permeability.* Federation proceedings, 1986. **45**(2): p. 84-88.
249. Rucker, H.K., H.J. Wynder, and W.E. Thomas, *Cellular mechanisms of CNS pericytes.* Brain Research Bulletin, 2000. **51**(5): p. 363-369.
250. Thuringer, D., E. Solary, and C. Garrido, *The Microvascular Gap Junction Channel: A Route to Deliver MicroRNAs for Neurological Disease Treatment.* Frontiers in Molecular Neuroscience, 2017. **10**: p. 246.
251. Winkler, E.A., R.D. Bell, and B.V. Zlokovic, *Central nervous system pericytes in health and disease.* Nature Neuroscience, 2011. **14**(11): p. 1398-1405.
252. Gauthier, M.-K., et al., *Dysregulation of the neuregulin-1–ErbB network modulates endogenous oligodendrocyte differentiation and preservation after spinal cord injury.* European Journal of Neuroscience, 2013. **38**(5): p. 2693-2715.
253. Vazana, U., et al., *Glutamate-Mediated Blood–Brain Barrier Opening: Implications for Neuroprotection and Drug Delivery.* The Journal of Neuroscience, 2016. **36**(29): p. 7727.
254. Nishijima, T., et al., *Neuronal Activity Drives Localized Blood-Brain-Barrier Transport of Serum Insulin-like Growth Factor-I into the CNS.* Neuron, 2010. **67**(5): p. 834-846.
255. Fischer, H., R. Gottschlich, and A. Seelig, *Blood-Brain Barrier Permeation: Molecular Parameters Governing Passive Diffusion.* The Journal of Membrane Biology, 1998. **165**(3): p. 201-211.
256. Zhang, E.Y., et al., *Structural Biology and Function of Solute Transporters: Implications for Identifying and Designing Substrates.* Drug Metabolism Reviews, 2002. **34**(4): p. 709-750.
257. Liu, X., et al., *Development of a computational approach to predict blood-brain barrier permeability.* Drug Metab Dispos, 2004. **32**(1): p. 132-9.
258. Barar, J., et al., *Blood-brain barrier transport machineries and targeted therapy of brain diseases.* BioImpacts : BI, 2016. **6**(4): p. 225-248.
259. Pulgar, V.M., *Transcytosis to Cross the Blood Brain Barrier, New Advancements and Challenges.* Frontiers in Neuroscience, 2019. **12**: p. 1019.
260. Ohtsuki, S. and T. Terasaki, *Contribution of Carrier-Mediated Transport Systems to the Blood–Brain Barrier as a Supporting and Protecting Interface for the Brain; Importance for CNS Drug Discovery and Development.* Pharmaceutical Research, 2007. **24**(9): p. 1745-1758.
261. Roberts, L.M., et al., *Subcellular localization of transporters along the rat blood–brain barrier and blood–cerebral-spinal fluid barrier by in vivo biotinylation.* Neuroscience, 2008. **155**(2): p. 423-438.
262. Tsuji, A., *Small molecular drug transfer across the blood-brain barrier via carrier-mediated transport systems.* NeuroRx : the journal of the American Society for Experimental NeuroTherapeutics, 2005. **2**(1): p. 54-62.
263. Mahringer, A. and G. Fricker, *ABC transporters at the blood–brain barrier.* Expert Opinion on Drug Metabolism & Toxicology, 2016. **12**(5): p. 499-508.
264. Dallas, S., D.S. Miller, and R. Bendayan, *Multidrug resistance-associated proteins: expression and function in the central nervous system.* Pharmacological reviews, 2006. **58**(2): p. 140-161.
265. Herz, J. and P. Marschang, *Coaxing the LDL Receptor Family into the Fold.* Cell, 2003. **112**(3): p. 289-292.
266. Visser, C.C., et al., *Characterization and Modulation of the Transferrin Receptor on Brain Capillary Endothelial Cells.* Pharmaceutical Research, 2004. **21**(5): p. 761-769.

267. Pan, W. and A.J. Kastin, *TNFα Transport across the Blood–Brain Barrier Is Abolished in Receptor Knockout Mice.* Experimental Neurology, 2002. **174**(2): p. 193-200.
268. Zhang, W., et al., *Differential expression of receptors mediating receptor-mediated transcytosis (RMT) in brain microvessels, brain parenchyma and peripheral tissues of the mouse and the human.* Fluids and Barriers of the CNS, 2020. **17**(1): p. 47.
269. Sauer, I., et al., *An Apolipoprotein E-Derived Peptide Mediates Uptake of Sterically Stabilized Liposomes into Brain Capillary Endothelial Cells.* Biochemistry, 2005. **44**(6): p. 2021-2029.
270. Claudio, L., et al., *Increased vesicular transport and decreased mitochondrial content in blood-brain barrier endothelial cells during experimental autoimmune encephalomyelitis.* The American journal of pathology, 1989. **135**(6): p. 1157-1168.
271. Scholz, M., et al., *Neutrophils and the blood–brain barrier dysfunction after trauma.* Medicinal Research Reviews, 2007. **27**(3): p. 401-416.
272. Konsman, Jan P., B. Drukarch, and A.-M. Van Dam, *(Peri)vascular production and action of pro-inflammatory cytokines in brain pathology.* Clinical Science, 2006. **112**(1): p. 1-25.
273. Helms, H.C., et al., *In vitro models of the blood-brain barrier: An overview of commonly used brain endothelial cell culture models and guidelines for their use.* Journal of cerebral blood flow and metabolism : official journal of the International Society of Cerebral Blood Flow and Metabolism, 2016. **36**(5): p. 862-890.
274. Czupalla, C.J., S. Liebner, and K. Devraj, *In Vitro Models of the Blood–Brain Barrier*, in *Cerebral Angiogenesis: Methods and Protocols*, R. Milner, Editor. 2014, Springer New York: New York, NY. p. 415-437.
275. Stone, N.L., T.J. England, and S.E. O'Sullivan, *A Novel Transwell Blood Brain Barrier Model Using Primary Human Cells.* Frontiers in Cellular Neuroscience, 2019. **13**: p. 230.
276. Wolff, A., et al., *In Vitro Blood-Brain Barrier Models - An Overview of Established Models and New Microfluidic Approaches.* Journal of Pharmaceutical Sciences, 2015. **104**(9): p. 2727-2746.
277. Garberg, P., et al., *In vitro models for the blood–brain barrier.* Toxicology in Vitro, 2005. **19**(3): p. 299-334.
278. Bagchi, S., et al., *In-vitro blood-brain barrier models for drug screening and permeation studies: an overview.* Drug design, development and therapy, 2019. **13**: p. 3591-3605.
279. He, Y., et al., *Cell-culture models of the blood-brain barrier.* Stroke, 2014. **45**(8): p. 2514-2526.
280. Cucullo, L., et al., *Development of a Humanized In Vitro Blood–Brain Barrier Model to Screen for Brain Penetration of Antiepileptic Drugs.* Epilepsia, 2007. **48**(3): p. 505-516.
281. Cucullo, L., et al., *Immortalized Human Brain Endothelial Cells and Flow-Based Vascular Modeling: A Marriage of Convenience for Rational Neurovascular Studies.* Journal of Cerebral Blood Flow & Metabolism, 2007. **28**(2): p. 312-328.
282. Cucullo, L., et al., *A new dynamic in vitro model for the multidimensional study of astrocyte–endothelial cell interactions at the blood–brain barrier.* Brain Research, 2002. **951**(2): p. 243-254.
283. Cucullo, L., et al., *A dynamic in vitro BBB model for the study of immune cell trafficking into the central nervous system.* Journal of cerebral blood flow and metabolism : official journal of the International Society of Cerebral Blood Flow and Metabolism, 2011. **31**(2): p. 767-777.
284. Prabhakarpandian, B., et al., *SyM-BBB: a microfluidic Blood Brain Barrier model.* Lab on a chip, 2013. **13**(6): p. 1093-1101.

285. Booth, R. and H. Kim, *Characterization of a microfluidic in vitro model of the blood-brain barrier (μBBB).* Lab on a Chip, 2012. **12**(10): p. 1784-1792.
286. Jeong, S., et al., *A Three-Dimensional Arrayed Microfluidic Blood–Brain Barrier Model With Integrated Electrical Sensor Array.* IEEE Transactions on Biomedical Engineering, 2018. **65**(2): p. 431-439.
287. Adriani, G., et al., *A 3D neurovascular microfluidic model consisting of neurons, astrocytes and cerebral endothelial cells as a blood–brain barrier.* Lab on a Chip, 2017. **17**(3): p. 448-459.
288. Bhalerao, A., et al., *In vitro modeling of the neurovascular unit: advances in the field.* Fluids and Barriers of the CNS, 2020. **17**(1): p. 22.
289. Urich, E., et al., *Multicellular Self-Assembled Spheroidal Model of the Blood Brain Barrier.* Scientific Reports, 2013. **3**(1): p. 1500.
290. Gastfriend, B.D., S.P. Palecek, and E.V. Shusta, *Modeling the blood-brain barrier: Beyond the endothelial cells.* Current opinion in biomedical engineering, 2018. **5**: p. 6-12.
291. Cho, C.-F., et al., *Blood-brain-barrier spheroids as an in vitro screening platform for brain-penetrating agents.* Nature Communications, 2017. **8**(1): p. 15623.
292. Burk, R.F. and K.E. Hill, *Regulation of Selenium Metabolism and Transport.* Annual Review of Nutrition, 2015. **35**(1): p. 109-134.
293. Burk, R.F., K.E. Hill, and A.K. Motley, *Selenoprotein Metabolism and Function: Evidence for More than One Function for Selenoprotein P.* The Journal of Nutrition, 2003. **133**(5): p. 1517S-1520S.
294. Shetty, S.P. and P.R. Copeland, *The Selenium Transport Protein, Selenoprotein P, Requires Coding Sequence Determinants to Promote Efficient Selenocysteine Incorporation.* Journal of Molecular Biology, 2018. **430**(24): p. 5217-5232.
295. Pillai, R., J.H. Uyehara-Lock, and F.P. Bellinger, *Selenium and selenoprotein function in brain disorders.* IUBMB Life, 2014. **66**(4): p. 229-39.
296. Short, S.P., J.M. Pilat, and C.S. Williams, *Roles for selenium and selenoprotein P in the development, progression, and prevention of intestinal disease.* Free Radical Biology and Medicine, 2018. **127**: p. 26-35.
297. Scharpf, M., et al., *Neuronal and ependymal expression of selenoprotein P in the human brain.* J Neural Transm, 2007. **114**(7): p. 877-84.
298. Yang, X.G., et al., *Synthesis and secretion of selenoprotein P by cultured rat astrocytes.* Biochimica Et Biophysica Acta-General Subjects, 2000. **1474**(3): p. 390-396.
299. Steinbrenner, H., et al., *Involvement of selenoprotein P in protection of human astrocytes from oxidative damage.* Free Radical Biology and Medicine, 2006. **40**(9): p. 1513-1523.
300. Loef, M., G.N. Schrauzer, and H. Walach, *Selenium and Alzheimer's disease: a systematic review.* J Alzheimers Dis, 2011. **26**(1): p. 81-104.
301. Burk, R.F., et al., *Selenoprotein P and apolipoprotein E receptor-2 interact at the blood-brain barrier and also within the brain to maintain an essential selenium pool that protects against neurodegeneration.* The FASEB Journal, 2014. **28**(8): p. 3579-3588.
302. Sasuclark, A.R., V.S. Khadka, and M.W. Pitts, *Cell-Type Specific Analysis of Selenium-Related Genes in Brain.* Antioxidants (Basel, Switzerland), 2019. **8**(5): p. 120.
303. Hill, K.E., et al., *Deletion of selenoprotein P alters distribution of selenium in the mouse.* Journal of Biological Chemistry, 2003. **278**(16): p. 13640-13646.
304. Schomburg, L., et al., *Gene disruption discloses role of selenoprotein P in selenium delivery to target tissues.* Biochemical Journal, 2003. **370**: p. 397-402.

305. Hoffmann, P.R., et al., *The selenoproteome exhibits widely varying, tissue-specific dependence on selenoprotein P for selenium supply.* Nucleic Acids Res, 2007. **35**(12): p. 3963-73.
306. Valentine, W.M., et al., *Neurodegeneration in mice resulting from loss of functional selenoprotein P or its receptor apolipoprotein E receptor 2.* Journal of Neuropathology and Experimental Neurology, 2008. **67**(1): p. 68-77.
307. Hill, K.E., et al., *Neurological Dysfunction Occurs in Mice with Targeted Deletion of the Selenoprotein P Gene.* The Journal of Nutrition, 2004. **134**(1): p. 157-161.
308. Kurokawa, S., et al., *Mammalian Selenocysteine Lyase Is Involved in Selenoprotein Biosynthesis.* Journal of Nutritional Science and Vitaminology, 2011. **57**(4): p. 298-305.
309. Solovyev, N., A. Berthele, and B. Michalke, *Selenium speciation in paired serum and cerebrospinal fluid samples.* Anal Bioanal Chem, 2013. **405**(6): p. 1875-84.
310. Campos-Bedolla, P., et al., *Role of the Blood–Brain Barrier in the Nutrition of the Central Nervous System.* Archives of Medical Research, 2014. **45**(8): p. 610-638.
311. Seale, L.A., *Selenocysteine β-Lyase: Biochemistry, Regulation and Physiological Role of the Selenocysteine Decomposition Enzyme.* Antioxidants (Basel, Switzerland), 2019. **8**(9): p. 357.
312. Seale, L.A., et al., *Relationship between selenoprotein P and selenocysteine lyase: Insights into selenium metabolism.* Free radical biology & medicine, 2018. **127**: p. 182-189.
313. Aden, D.P., et al., *Controlled synthesis of HBsAg in a differentiated human liver carcinoma-derived cell line.* Nature, 1979. **282**(5739): p. 615-616.
314. Mersch-Sundermann, V., et al., *Use of a human-derived liver cell line for the detection of cytoprotective, antigenotoxic and cogenotoxic agents.* Toxicology, 2004. **198**(1): p. 329-340.
315. Franke, H., H.-J. Galla, and C.T. Beuckmann, *Primary cultures of brain microvessel endothelial cells: a valid and flexible model to study drug transport through the blood–brain barrier in vitro.* Brain Research Protocols, 2000. **5**(3): p. 248-256.
316. Kröll, S., et al., *Control of the Blood–Brain Barrier by Glucocorticoids and the Cells of the Neurovascular Unit.* Annals of the New York Academy of Sciences, 2009. **1165**(1): p. 228-239.
317. Bornhorst, J., et al., *Impact of manganese on and transfer across blood-brain and blood-cerebrospinal fluid barrier in vitro.* The Journal of biological chemistry, 2012. **287**(21): p. 17140-17151.
318. Srinivasan, B., et al., *TEER measurement techniques for in vitro barrier model systems.* Journal of laboratory automation, 2015. **20**(2): p. 107-126.
319. Benson, K., S. Cramer, and H.-J. Galla, *Impedance-based cell monitoring: barrier properties and beyond.* Fluids and Barriers of the CNS, 2013. **10**(1): p. 5.
320. Sambuy, Y., et al., *The Caco-2 cell line as a model of the intestinal barrier: influence of cell and culture-related factors on Caco-2 cell functional characteristics.* Cell Biology and Toxicology, 2005. **21**(1): p. 1-26.
321. Sun, H., et al., *The Caco-2 cell monolayer: usefulness and limitations.* Expert Opinion on Drug Metabolism & Toxicology, 2008. **4**(4): p. 395-411.
322. LennernÄS, H., *Human Jejunal Effective Permeability and Its Correlation with Preclinical Drug Absorption Models.* Journal of Pharmacy and Pharmacology, 1997. **49**(7): p. 627-638.

323. Yee, S., *In Vitro Permeability Across Caco-2 Cells (Colonic) Can Predict In Vivo (Small Intestinal) Absorption in Man—Fact or Myth.* Pharmaceutical Research, 1997. **14**(6): p. 763-766.
324. Zhu, S.-y., et al., *Lysosomal quality control of cell fate: a novel therapeutic target for human diseases.* Cell Death & Disease, 2020. **11**(9): p. 817.
325. Aits, S. and M. Jäättelä, *Lysosomal cell death at a glance.* Journal of Cell Science, 2013. **126**(9): p. 1905.
326. Repetto, G., A. del Peso, and J.L. Zurita, *Neutral red uptake assay for the estimation of cell viability/cytotoxicity.* Nature Protocols, 2008. **3**(7): p. 1125-1131.
327. Kurz, T., et al., *Lysosomes and oxidative stress in aging and apoptosis.* Biochimica et Biophysica Acta (BBA) - General Subjects, 2008. **1780**(11): p. 1291-1303.
328. Kurz, T., et al., *Lysosomes in iron metabolism, ageing and apoptosis.* Histochemistry and Cell Biology, 2008. **129**(4): p. 389-406.
329. Borra, R.C., et al., *A simple method to measure cell viability in proliferation and cytotoxicity assays.* Braz Oral Res, 2009. **23**(3): p. 255-62.
330. Wu, D. and P. Yotnda, *Production and detection of reactive oxygen species (ROS) in cancers.* Journal of visualized experiments : JoVE, 2011(57): p. 3357.
331. Halliwell, B. and M. Whiteman, *Measuring reactive species and oxidative damage in vivo and in cell culture: how should you do it and what do the results mean?* British journal of pharmacology, 2004. **142**(2): p. 231-255.
332. Kalyanaraman, B., et al., *Measuring reactive oxygen and nitrogen species with fluorescent probes: challenges and limitations.* Free Radical Biology and Medicine, 2012. **52**(1): p. 1-6.
333. Weydert, C.J. and J.J. Cullen, *Measurement of superoxide dismutase, catalase and glutathione peroxidase in cultured cells and tissue.* Nature Protocols, 2010. **5**(1): p. 51-66.
334. Rodushkin, I., et al., *Determination of 60 elements in whole blood by sector field inductively coupled plasma mass spectrometry.* Journal of Analytical Atomic Spectrometry, 2000. **15**(8): p. 937-944.
335. Michalke, B., *The coupling of LC to ICP-MS in element speciation - Part II: Recent trends in application.* Trac-Trends in Analytical Chemistry, 2002. **21**(3): p. 154-165.
336. Michalke, B., *The coupling of LC to ICP-MS in element speciation: I. General aspects.* Trac-Trends in Analytical Chemistry, 2002. **21**(2): p. 142-153.
337. Becker, J.S., *Fields of Application in Trace, Ultratrace and Surface Analysis*, in *Inorganic Mass Spectrometry: Principles and Applications*, J.S. Becker, Editor. 2007, John Wiley & Sons: Chichester. p. 255-458.
338. Rodríguez-González, P., et al., *Isotope dilution analysis for elemental speciation: a tutorial review.* Spectrochimica Acta Part B: Atomic Spectroscopy, 2005. **60**(2): p. 151-207.
339. Brenner, I., *Inductively Coupled Plasma Mass Spectrometry Applications*, in *Encyclopedia of Spectroscopy and Spectrometry (Third Edition)*, J.C. Lindon, G.E. Tranter, and D.W. Koppenaal, Editors. 2017, Academic Press: Oxford. p. 229-235.
340. Wang, H., et al., *Selenocystine against methyl mercury cytotoxicity in HepG2 cells.* Scientific Reports, 2017. **7**(1): p. 147.
341. Pan, X., et al., *H2Se Induces Reductive Stress in HepG2 Cells and Activates Cell Autophagy by Regulating the Redox of HMGB1 Protein under Hypoxia.* Theranostics, 2019. **9**(6): p. 1794-1808.

342. Cuello, S., et al., *Selenium methylselenocysteine protects human hepatoma HepG2 cells against oxidative stress induced by tert-butyl hydroperoxide.* Analytical and Bioanalytical Chemistry, 2007. **389**(7): p. 2167-2178.
343. Shamberger, R.J., *Metabolism of Selenium*, in *Biochemistry of Selenium*, R.J. Shamberger, Editor. 1983, Springer US: Boston, MA. p. 59-75.
344. Simmons, T.W., I.S. Jamall, and R.A. Lockshin, *Accumulation, distribution and toxicity of selenium in the adult house fly, Musca domestica.* Comparative Biochemistry and Physiology Part C: Comparative Pharmacology, 1988. **91**(2): p. 559-563.
345. Zwolak, I. and H. Zaporowska, *Selenium interactions and toxicity: a review.* Cell Biology and Toxicology, 2012. **28**(1): p. 31-46.
346. Wang, F., R. Gómez-Sintes, and P. Boya, *Lysosomal membrane permeabilization and cell death.* Traffic, 2018. **19**(12): p. 918-931.
347. O'Brien, J., et al., *Investigation of the Alamar Blue (resazurin) fluorescent dye for the assessment of mammalian cell cytotoxicity.* European Journal of Biochemistry, 2000. **267**(17): p. 5421-5426.
348. Hinrichsen, S. and B. Planer-Friedrich, *Cytotoxic activity of selenosulfate versus selenite in tumor cells depends on cell line and presence of amino acids.* Environmental Science and Pollution Research, 2016. **23**(9): p. 8349-8357.
349. Zou, Y., et al., *Relationship between reactive oxygen species and sodium-selenite-induced DNA damage in HepG2 cells.* Frontiers of Medicine in China, 2007. **1**(3): p. 327-332.
350. Rudzok, S., et al., *Toxicity profiles of four metals and 17 xenobiotics in the human hepatoma cell line HepG2 and the protozoa Tetrahymena pyriformis—A comparison.* Environmental Toxicology, 2011. **26**(2): p. 171-186.
351. Lammel, T., et al., *Internalization and cytotoxicity of graphene oxide and carboxyl graphene nanoplatelets in the human hepatocellular carcinoma cell line Hep G2.* Particle and Fibre Toxicology, 2013. **10**(1): p. 27.
352. Forceville, X., et al., *Elements of margin of safety, toxicity and action of sodium selenite in a lipopolysaccharide rat model.* Journal of Trace Elements in Medicine and Biology, 2014. **28**(3): p. 303-310.
353. Kim, J.H. and D.Y. Kil, *Comparison of toxic effects of dietary organic or inorganic selenium and prediction of selenium intake and tissue selenium concentrations in broiler chickens using feather selenium concentrations.* Poultry Science, 2020. **99**(12): p. 6462-6473.
354. Berntssen, M.H.G., et al., *Sensitivity and toxic mode of action of dietary organic and inorganic selenium in Atlantic salmon (Salmo salar).* Aquatic Toxicology, 2017. **192**: p. 116-126.
355. Spallholz, J.E. and D.J. Hoffman, *Selenium toxicity: cause and effects in aquatic birds.* Aquatic Toxicology, 2002. **57**(1): p. 27-37.
356. Spallholz, J.E., *On the nature of selenium toxicity and carcinostatic activity.* Free Radical Biology and Medicine, 1994. **17**(1): p. 45-64.
357. Drake, E.N., *Cancer chemoprevention: Selenium as a prooxidant, not an antioxidant.* Medical Hypotheses, 2006. **67**(2): p. 318-322.
358. Marschall, T.A., et al., *Tracing cytotoxic effects of small organic Se species in human liver cells back to total cellular Se and Se metabolites.* Metallomics, 2017. **9**(3): p. 268-277.
359. Chen, C., et al., *Microcalorimetric study of the toxic effect of selenium on the mitochondrial metabolism of cyprinus carpio liver.* Biological Trace Element Research, 1997. **60**(1): p. 115-122.

360. Lee, K.H. and D. Jeong, *Bimodal actions of selenium essential for antioxidant and toxic pro-oxidant activities: The selenium paradox (Review).* Mol Med Rep, 2012. **5**(2): p. 299-304.
361. Drobyshev, E., et al., *Capabilities of selenoneine to cross the in vitro blood–brain barrier model.* Metallomics, 2021. **13**(1).
362. Wiśniewski, J.R., et al., *In-depth quantitative analysis and comparison of the human hepatocyte and hepatoma cell line HepG2 proteomes.* Journal of Proteomics, 2016. **136**: p. 234-247.
363. Oldendorf, W.H., M.E. Cornford, and W.J. Brown, *The large apparent work capability of the blood-brain barrier: A study of the mitochondrial content of capillary endothelial cells in brain and other tissues of the rat.* Annals of Neurology, 1977. **1**(5): p. 409-417.
364. Kroepfl, N., et al., *Selenoneine and ergothioneine in human blood cells determined simultaneously by HPLC/ICP-QQQ-MS.* Journal of Analytical Atomic Spectrometry, 2019. **34**: p. 127-134.
365. Franke, H., H.-J. Galla, and C.T. Beuckmann, *An improved low-permeability in vitro-model of the blood–brain barrier: transport studies on retinoids, sucrose, haloperidol, caffeine and mannitol.* Brain Research, 1999. **818**(1): p. 65-71.
366. Smith, Q.R., H. Mandula, and J. Parepally. *Amino Acid Transport Across the Blood Brain Barrier*. 2006.
367. Mayumi, T., et al., *Studies on Ergothioneine. V. Determination by High Performance Liquid Chromatography and Application to Metabolic Research.* CHEMICAL & PHARMACEUTICAL BULLETIN, 1978. **26**(12): p. 3772-3778.
368. Pochini, L., et al., *OCTN: A Small Transporter Subfamily with Great Relevance to Human Pathophysiology, Drug Discovery, and Diagnostics.* SLAS DISCOVERY: Advancing the Science of Drug Discovery, 2018. **24**(2): p. 89-110.
369. Akahoshi, N., et al., *Dietary selenium deficiency or selenomethionine excess drastically alters organ selenium contents without altering the expression of most selenoproteins in mice.* The Journal of nutritional biochemistry, 2019. **69**: p. 120-129.
370. Cheah, I.K. and B. Halliwell, *Ergothioneine; antioxidant potential, physiological function and role in disease.* Biochimica et Biophysica Acta (BBA) - Molecular Basis of Disease, 2012. **1822**(5): p. 784-793.
371. Speckmann, B., et al., *Intestinal selenoprotein P in epithelial cells and in plasma cells.* Archives of Biochemistry and Biophysics, 2014. **541**: p. 30-36.
372. Rohn, I., et al., *Selenoneine ameliorates peroxide-induced oxidative stress in C. elegans.* Journal of Trace Elements in Medicine and Biology, 2019. **55**: p. 78-81.
373. Alhasan, R., et al., *Selenoneine: a Unique Reactive Selenium Species From the Blood of Tuna With Implications for Human Diseases.* Current Pharmacology Reports, 2019. **5**(3): p. 163-173.